

Supporting Information

Intramolecular Base-Free Catalytic Wittig Reaction: Synthesis of Benzoxepinones

Aiga Grandane^{†‡}, Lars Longwitz[‡], Catrin Roolf[§], Anke Spannenberg[‡], Hugo
Murua Escobar[§], Christian Junghans[§], Edgars Suna[†], Thomas Werner^{*‡}

[†]Latvian Institute of Organic Synthesis, Aizkraukles 21, LV-1006, Riga, Latvia

[‡]Leibniz Institute for Catalysis at the University of Rostock, Albert-Einstein-Straße 29a, 18059 Rostock

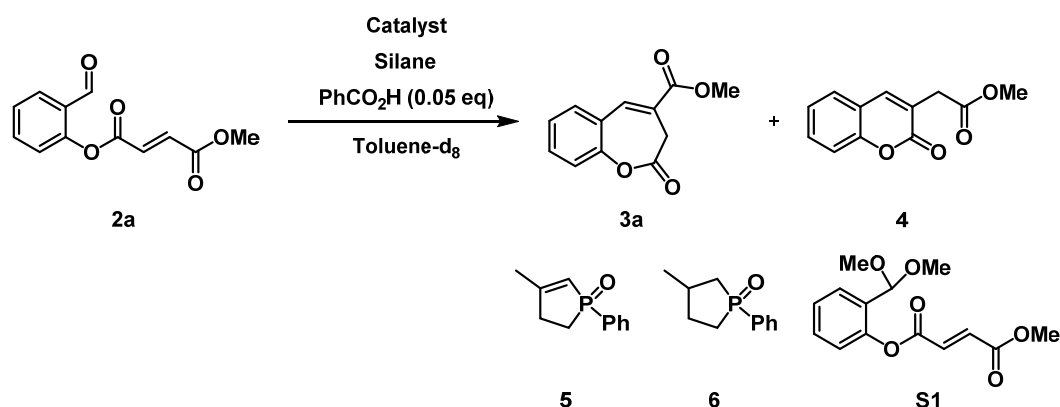
[§]Department of Internal Medicine, Medical Clinic III, Clinic for Hematology, Oncology and Palliative Care,
University Medical Center Rostock, Ernst-Heydemann-Straße 6, 18057 Rostock, Germany

Contents

Screening of Wittig reaction conditions	S2
Control experiments and mechanistic studies	S3
Additional information for the metabolic activity tests	S6
X-ray crystal structure analysis of 3a	S7
Spectral data	S8
References in the Supporting Information	S76

Screening of Wittig reaction conditions

Table S1. Screening of the Wittig reaction conditions

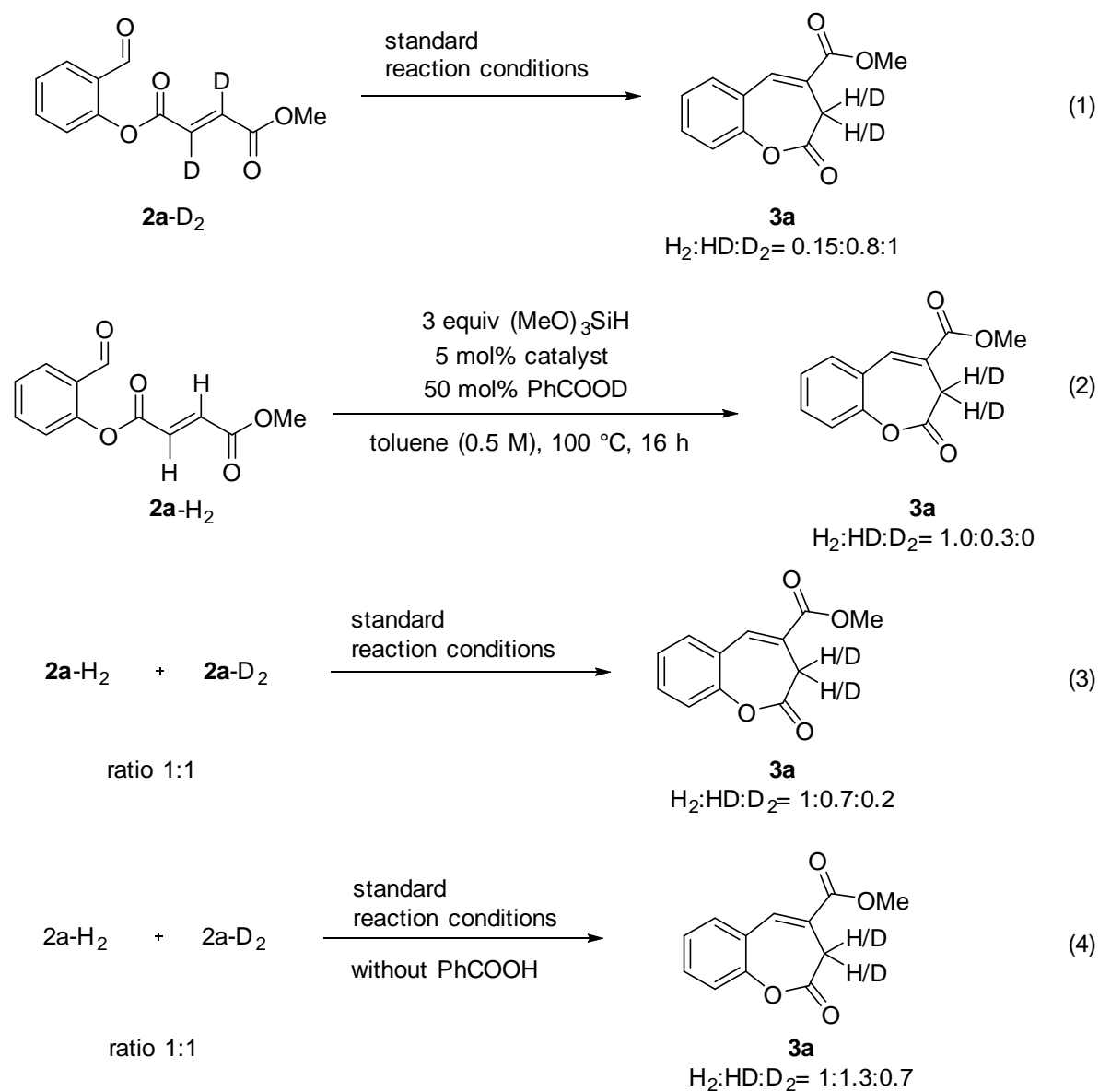


Entry	Catalyst (mol%)	Silane (equiv.)	Solvent	T, °C	t, h	Yield 3a , % ^a
1^b	PBu ₃ (5)	PhSiH ₃ (1)	Toluene- <i>d</i> ₈	125	24	27
2^c	PBu ₃ (5)	PhSiH ₃ (1)	Toluene- <i>d</i> ₈	125	24	34
3	5 (5)	(MeO) ₃ SiH (3)	Toluene- <i>d</i> ₈	100	16	41
4	6 (5)	(MeO) ₃ SiH (3)	Toluene- <i>d</i> ₈	100	16	38
5	5 (1)	(MeO) ₃ SiH (3)	Toluene- <i>d</i> ₈	100	16	18
6	5 (2.5)	(MeO) ₃ SiH (3)	Toluene- <i>d</i> ₈	100	16	39
7	5 (10)	(MeO) ₃ SiH (3)	Toluene- <i>d</i> ₈	100	16	38
8	5 (5)	(MeO) ₃ SiH (2)	Toluene- <i>d</i> ₈	100	16	33
9	5 (5)	(MeO) ₃ SiH (4)	Toluene- <i>d</i> ₈	100	16	22
10	5 (5)	PhSiH ₃ (3)	Toluene- <i>d</i> ₈	100	16	19
11	5 (5)	HexylSiH ₃ (3)	Toluene- <i>d</i> ₈	100	16	33
12	5 (5)	(MeO) ₃ SiH (3)	Toluene- <i>d</i> ₈	100	5	10
13	5 (5)	(MeO) ₃ SiH (3)	Toluene- <i>d</i> ₈	100	48	33
14	5 (5)	(MeO) ₃ SiH (3)	Toluene- <i>d</i> ₈	80	20	25
15	5 (5)	(MeO) ₃ SiH (3)	Toluene- <i>d</i> ₈	120	20	33
16^d	5 (5)	(MeO) ₃ SiH (3)	Toluene- <i>d</i> ₈	100	3	38
17^e	5 (5)	(MeO) ₃ SiH (3)	1,4-Dioxane	100	16	16
18	5 (5)	(MeO) ₃ SiH (3)	THF	100	16	14
19^f	5 (5)	(MeO) ₃ SiH (3)	MeOH	100	16	0

^aYield was determined by NMR with mesitylene as an internal standard. ^b6-membered lactone **4** (10 %) was formed as a side product. ^c additive PhCO₂H was not used; 6-membered lactone **4** (9 %) was formed. ^d microwave heating was used. ^e mixture contained 35% of unreacted starting material. ^f **S1** was the major product.

Control experiments and mechanistic studies

A complete list of the control experiments conducted with deuterated substrates **2a-D₂** is shown in the Scheme S1 below. The ratio of products was determined by ¹H NMR for the isolated products. As an example, the spectrum of the product obtained from reaction (eq 3, Scheme S1) is shown below.



Scheme S1. Control experiments utilizing deuterated substrates.

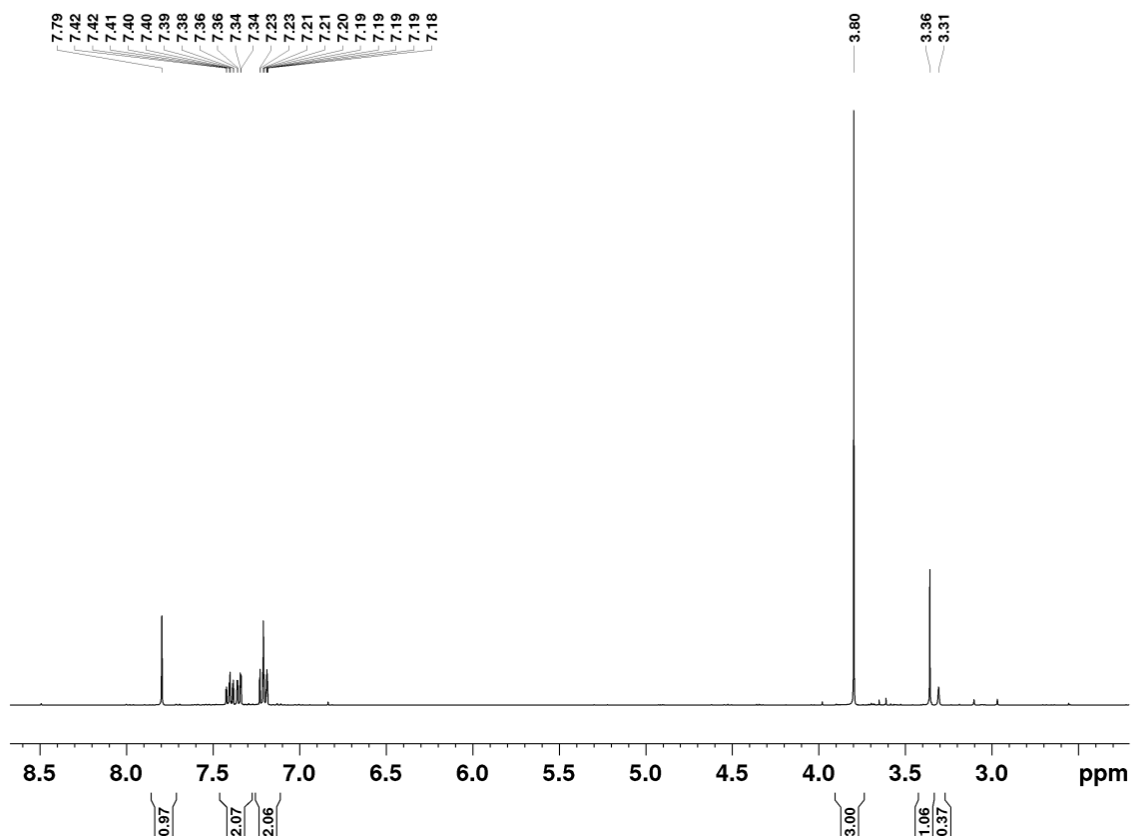
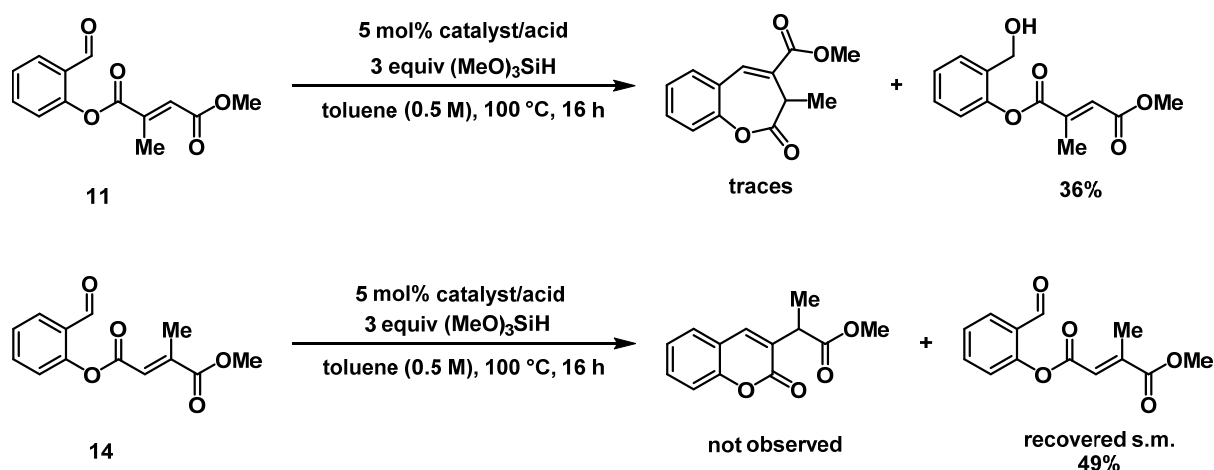


Figure S1. ¹H NMR of the isolated benzoxepinone from reaction (3).

The ratio H₂:HD:D₂ is obtained from the signals at 3.36 ppm and 3.31 ppm and calibrated on the three hydrogens of the methoxy group. The resulting ratio is 53:37:10 or approximately 1:0.7:0.2.

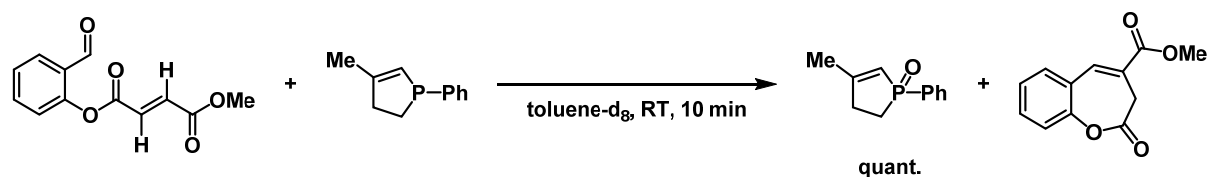
The results obtained with trisubstituted alkenes as precursors are shown below.



Scheme S2. Reaction with substrates blocked at the alkene functionality.

When compound **11** was employed as the substrate, only traces of the product could be obtained under standard reaction conditions. Interestingly, for this substrate a significant amount of benzyl alcohol was isolated as a side product. When the reactions were carried out with stoichiometric amounts of phosphane, no significant amount of product was formed either. The expected coumarin was not detected when compound **14** was used. Instead, around half of the starting material was recovered. We believe that the use of trisubstituted alkenes in the catalytic base-free Wittig reaction requires different conditions and is not necessarily a problem of the intramolecular variant.

Furthermore, we used stoichiometric amounts of phosphane to run the reaction and observed similar reactivity. Interestingly, the observed side products seemed to be partially unrelated to the Wittig reaction, while full conversion to the phosphane oxide was observed.



Scheme S3. Stoichiometric base-free Wittig reaction.

Potential intermediates of the reaction (Michael adduct or ylid) were investigated by *in situ* NMR experiments, but unfortunately we could not observe such species even when starting the reaction at -80 °C.

Additional information for the metabolic activity tests

The human acute lymphoblastic leukemia cell line SEM was purchased from DSMZ (Braunschweig, Germany) and cultured according to the manufacturer's protocol. Media was supplemented with 10 % heat-inactivated fetal bovine serum (Biochrom, Berlin, Germany) and 100 µg/ml penicillin and streptomycin (Biochrom). Cells were maintained in a 5% CO₂ humidified atmosphere at 37 °C.

All compounds were evaluated for their anti-metabolic activities in SEM cells using WST-1 assay (Roche, Mannheim, Germany) as previously described.¹ The novel arylindolylmaleimide PDA-66 displays pronounced antiproliferative effects in acute lymphoblastic leukemia cells.¹ Briefly, compounds were dissolved in DMSO (dimethyl sulfoxide) at 10 mM and stored in aliquots at -20°C. Working solutions were prepared freshly for experimental use. Cells were seeded in triplicates in a 96 well plate at a density of 5×10^4 cells/well in 150 µl medium and compounds were added with a final concentration of 5 µM or 10 µM. Control cells were cultured in their medium containing DMSO in the same concentration as present in the treated cells. Metabolic activity was assessed after 72 h by WST-1 assay. Metabolic activity of treated cells was expressed as a percentage of DMSO-treated controls (=100 %).

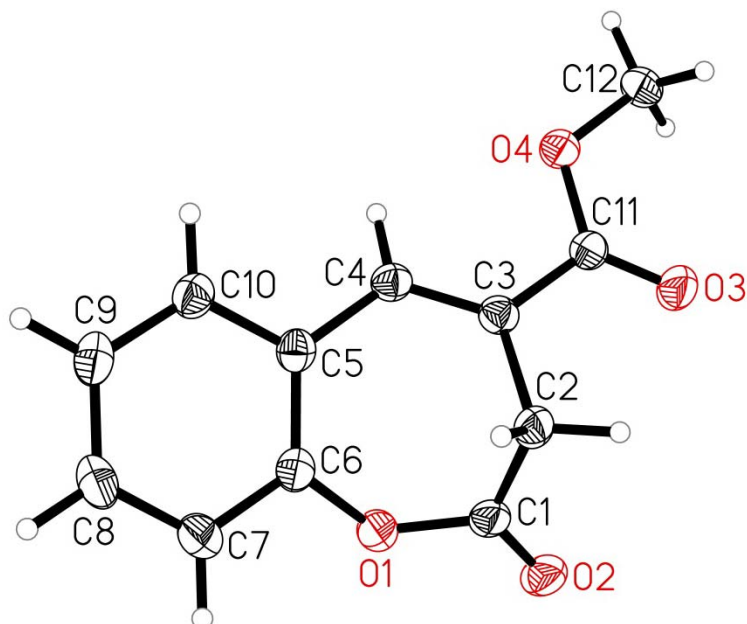
Table S2. Effects of compounds on SEM cells.

ID	C1	MA [%]	SD [%]	C2	MA [%]	SD [%]
DMSO	0.10%	100.0	2.6	0.10%	100.0	1.7
3a	5 µM	99.6	2.9	10 µM	105.9	2.0
3d	5 µM	101.6	4.4	10 µM	108.5	2.7
3b	5 µM	106.1	0.3	10 µM	99.7	2.4
3e	5 µM	108.5	0.6	10 µM	99.2	1.7
3f	5 µM	98.9	4.0	10 µM	108.2	3.1
3k	5 µM	98.2	2.0	10 µM	99.3	5.1
3j	5 µM	106.3	3.0	10 µM	101.0	3.0
3l	5 µM	99.4	1.7	10 µM	97.7	3.5
3h	5 µM	94.9	1.3	10 µM	97.6	1.6
3g	5 µM	99.4	2.2	10 µM	94.1	2.2
3m	5 µM	95.1	3.1	10 µM	91.0	1.1
3i	5 µM	96.1	0.3	10 µM	99.0	1.6

MA: metabolic activity SD: standard deviation

X-ray crystal structure analysis of 3a

Data were collected on a Bruker Kappa APEX II Duo diffractometer. The structure was solved by direct methods (SHELXS-97)² and refined by full-matrix least-squares procedures on F^2 (SHELXL-2014).³ XP (Bruker AXS) was used for graphical representation. CCDC 1869607 contains the supplementary crystallographic data for this paper. These data are provided free of charge by The Cambridge Crystallographic Data Centre.

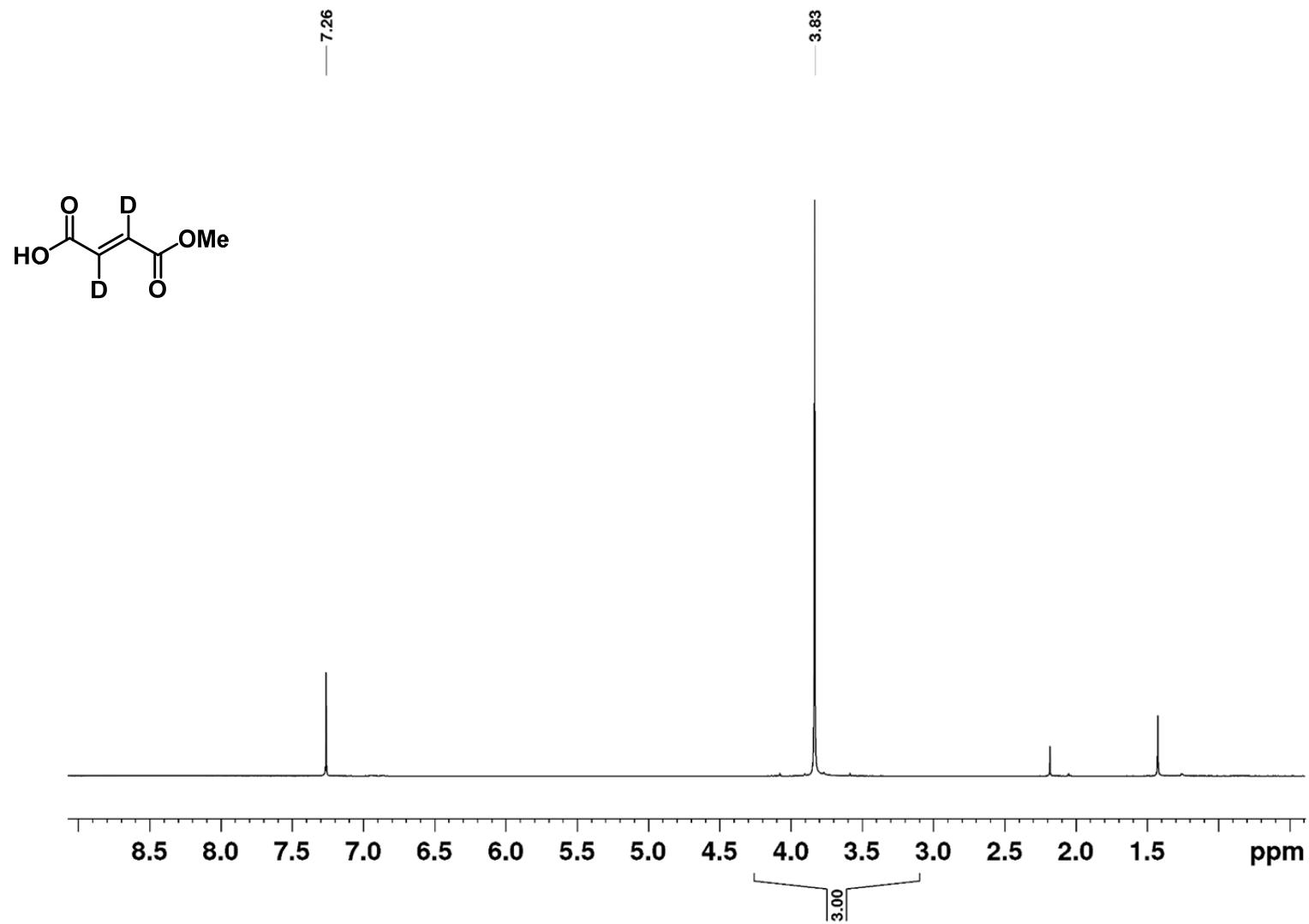


ORTEP representation of **3a**. Displacement ellipsoids correspond to 50% probability.

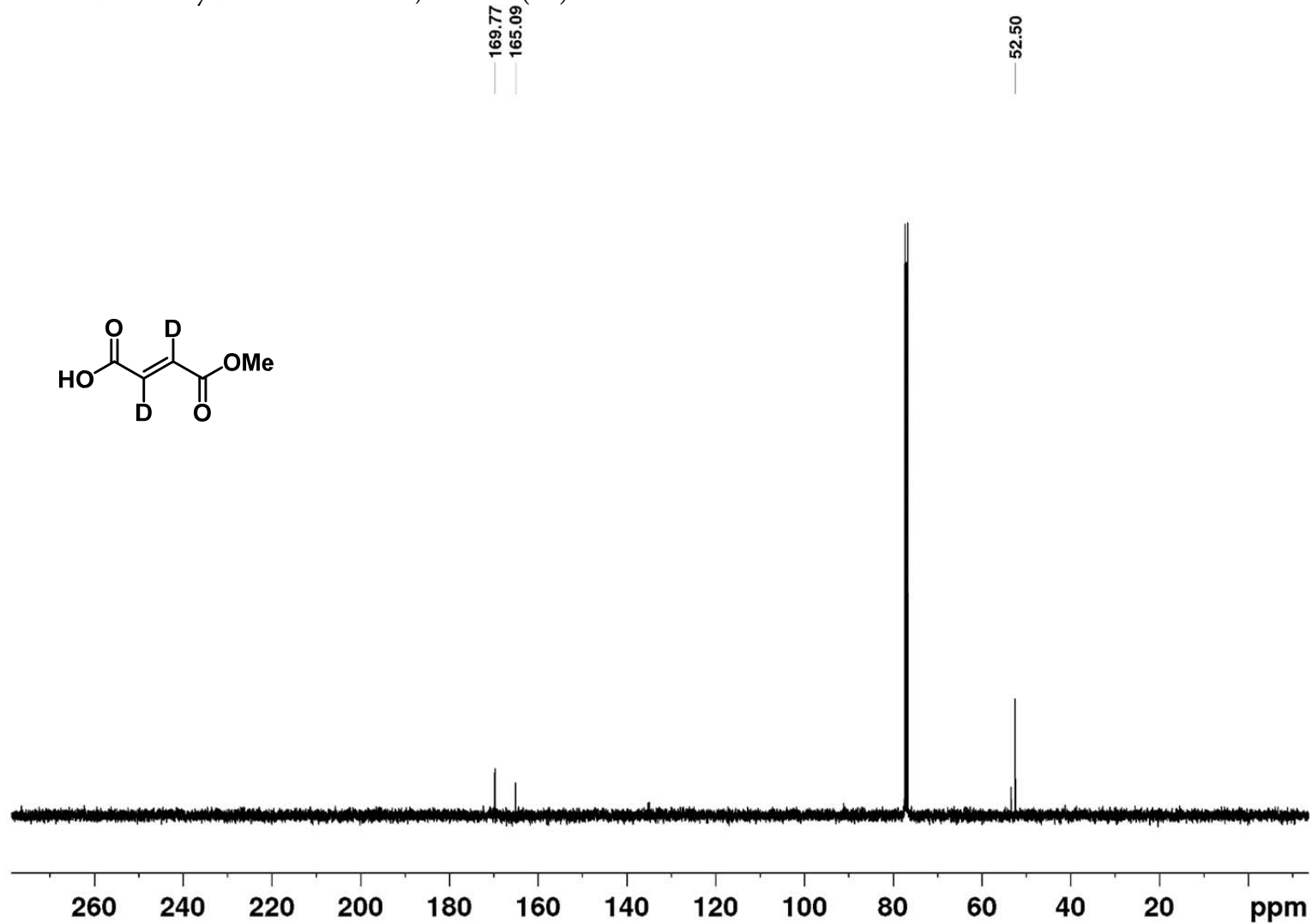
Empirical formula	C ₁₂ H ₁₀ O ₄
Formula weight	218.20
Temperature	150(2) K
Wavelength	1.54178 Å
Crystal system, space group	monoclinic, $P2_1/c$
Unit cell dimensions	$a = 11.7219(3)$ Å $\alpha = 90^\circ$ $b = 11.6068(3)$ Å $\beta = 108.6298(16)^\circ$ $c = 7.8791(2)$ Å $\gamma = 90^\circ$
Volume	1015.81(5) Å ³
Z, Density (calculated)	4, 1.427 g/cm ³
Absorption coefficient	0.906 mm ⁻¹
F(000)	456
Crystal size	0.13 x 0.11 x 0.05 mm
Reflections collected / unique	7628 / 1795 ($R_{\text{int}} = 0.0293$)
Max. and min. transmission	0.95 and 0.89
Data / restraints / parameters	1795 / 0 / 146
Goodness-of-fit on F^2	1.07
Final R indices [$I > 2\sigma(I)$]	$R_1 = 0.0360$, $wR_2 = 0.0932$
R indices (all data)	$R_1 = 0.0411$, $wR_2 = 0.0990$
Largest diff. peak and hole	0.203 and -0.251 e/Å ³

Spectral data

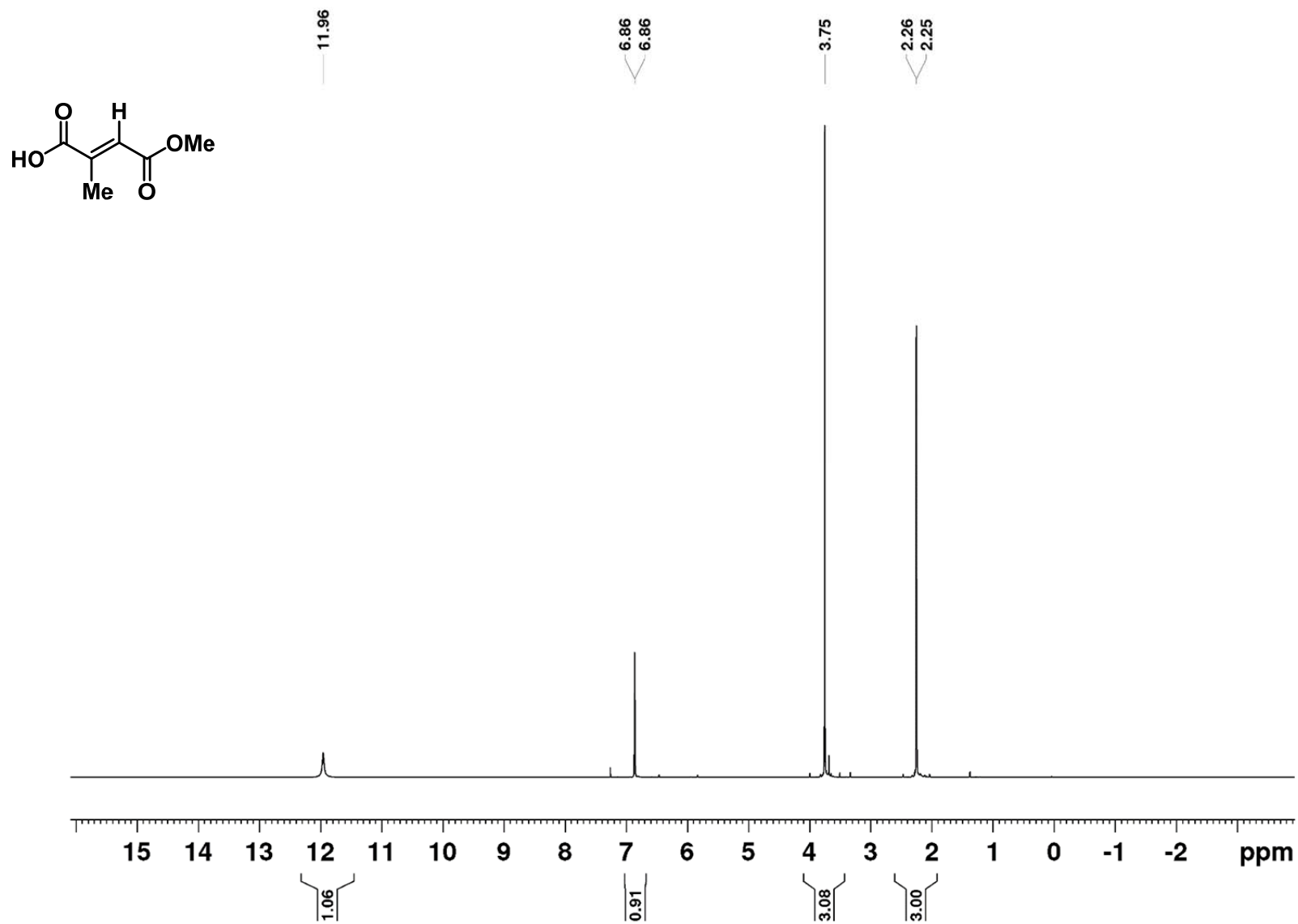
^1H NMR *E*-4-Methoxy-4-oxobut-2-enoic-2,3-d₂ acid (**15**)⁴



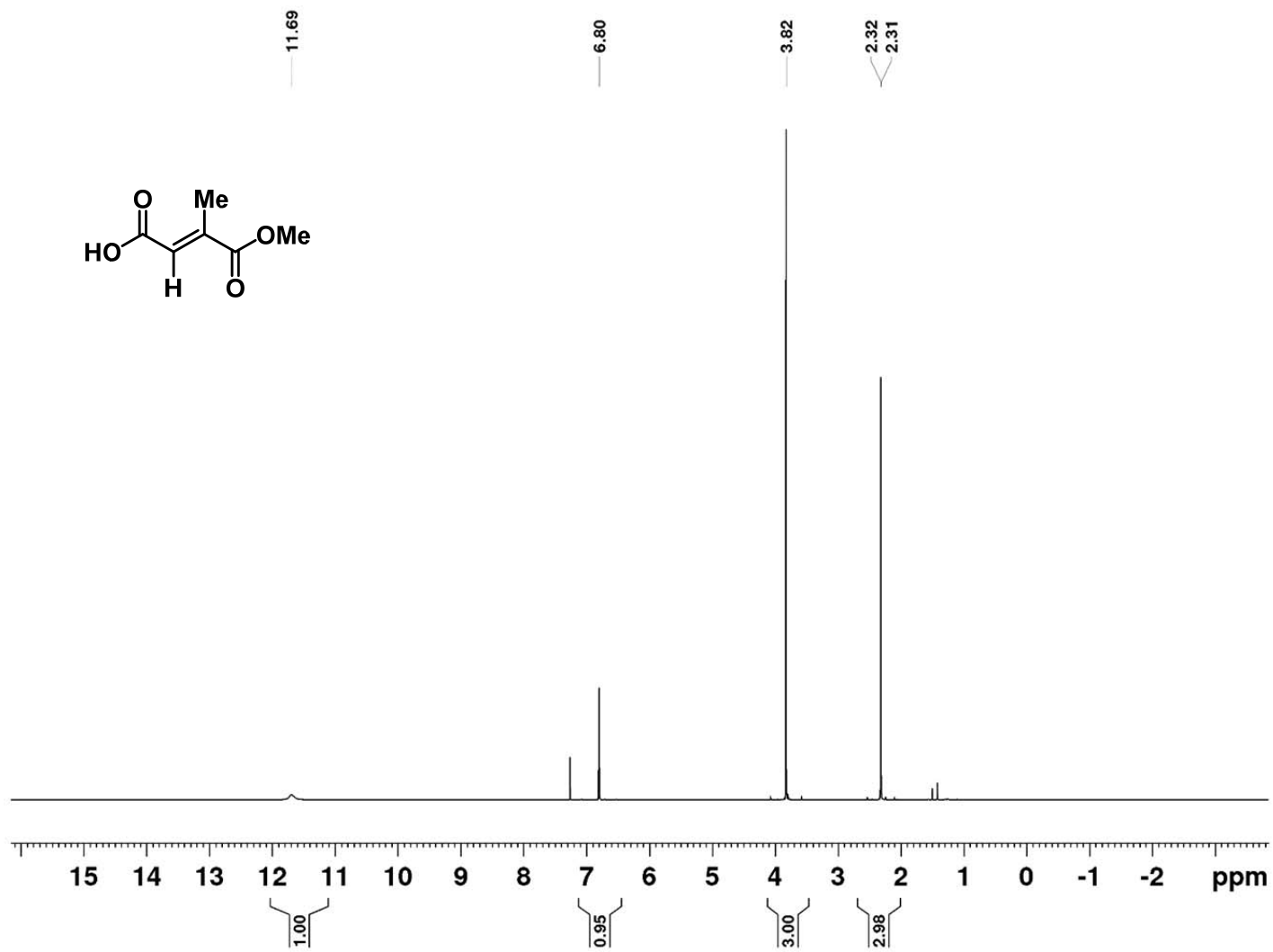
^{13}C NMR *E*-4-Methoxy-4-oxobut-2-enoic-2,3-d₂ acid (**15**)⁴



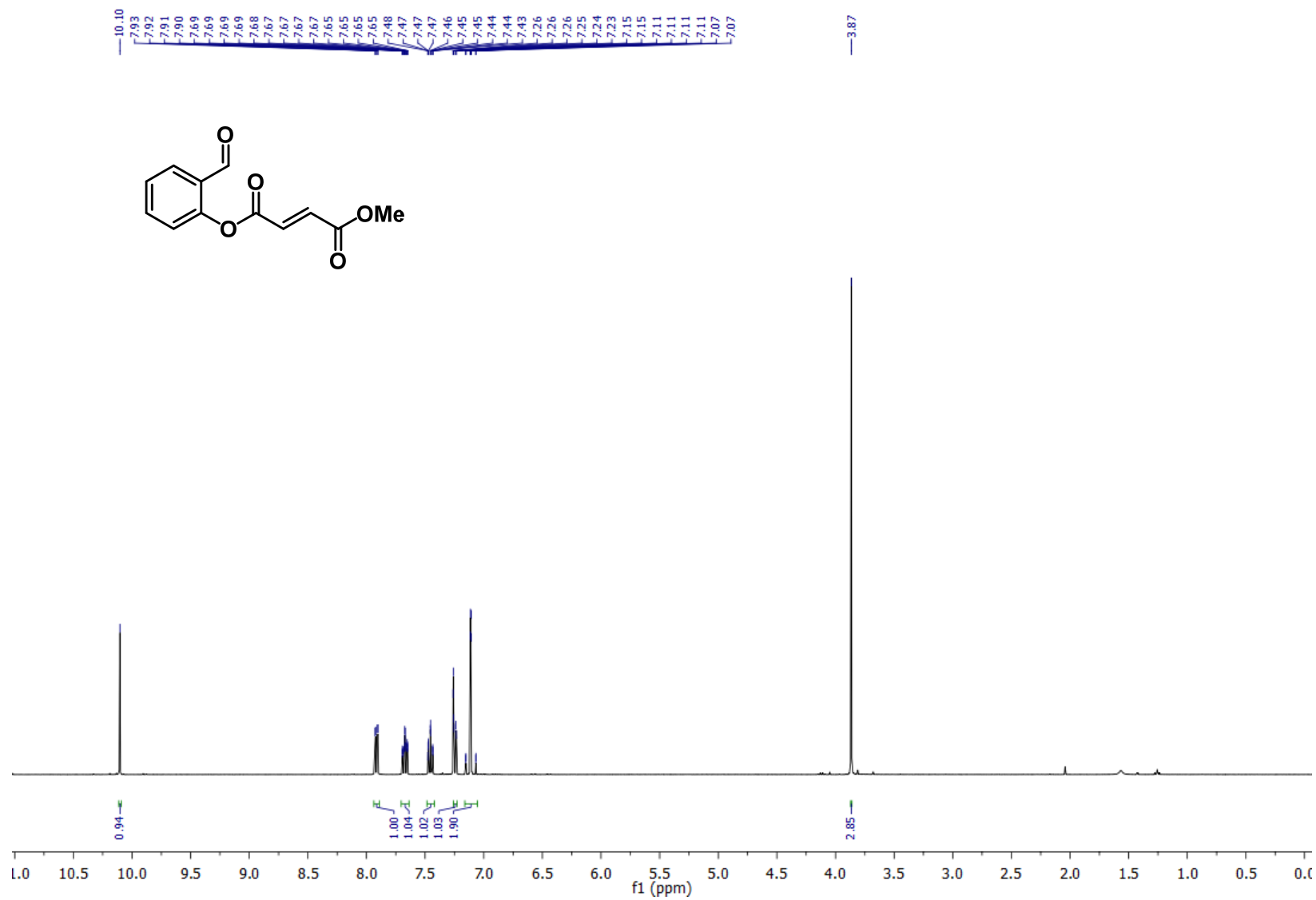
^1H NMR *E*-4-Methoxy-2-methyl-4-oxobut-2-enoic acid (**9**)^s



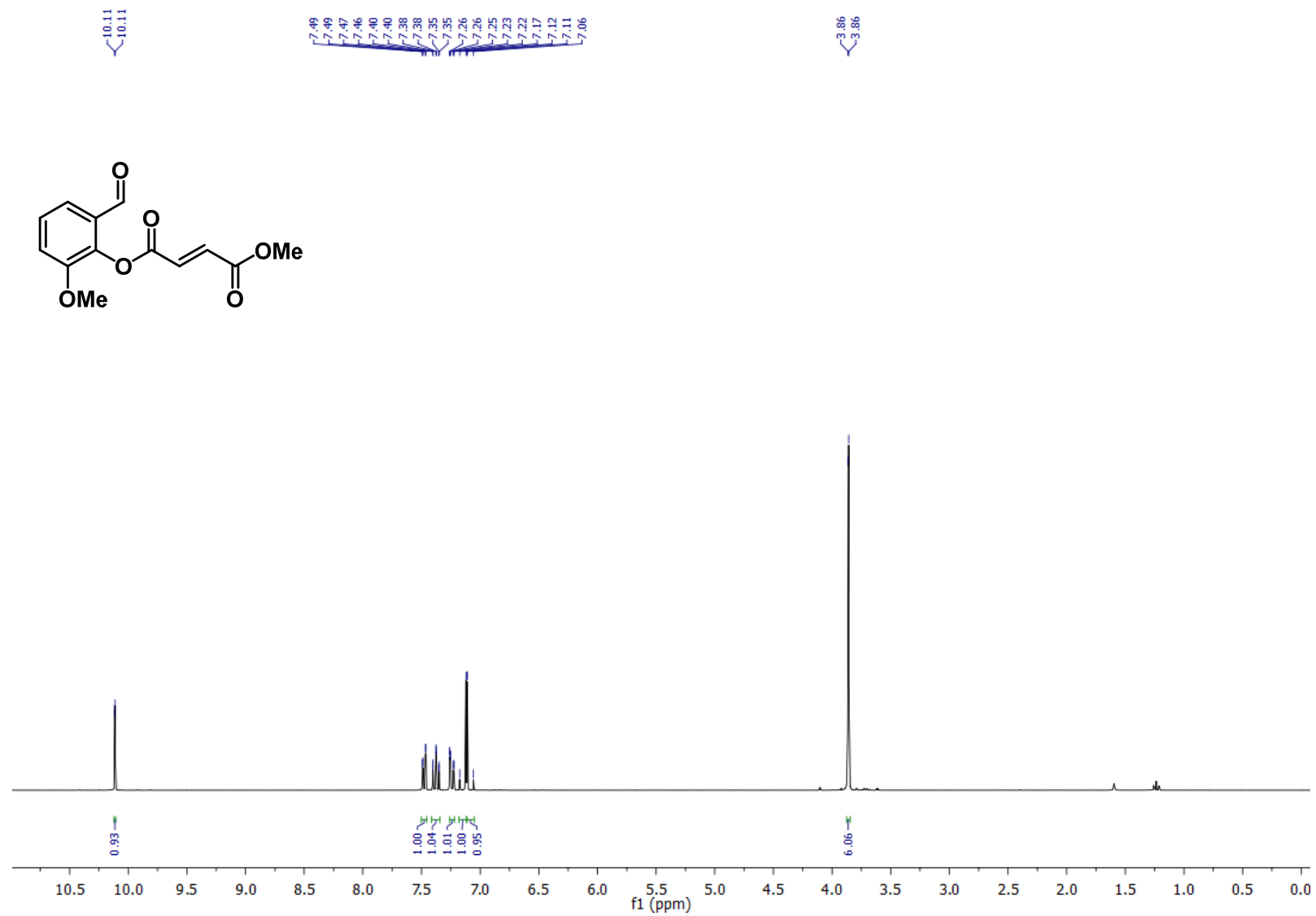
^1H NMR 4-Methoxy-3-methyl-4-oxobut-2-enoic acid (**12**)⁶



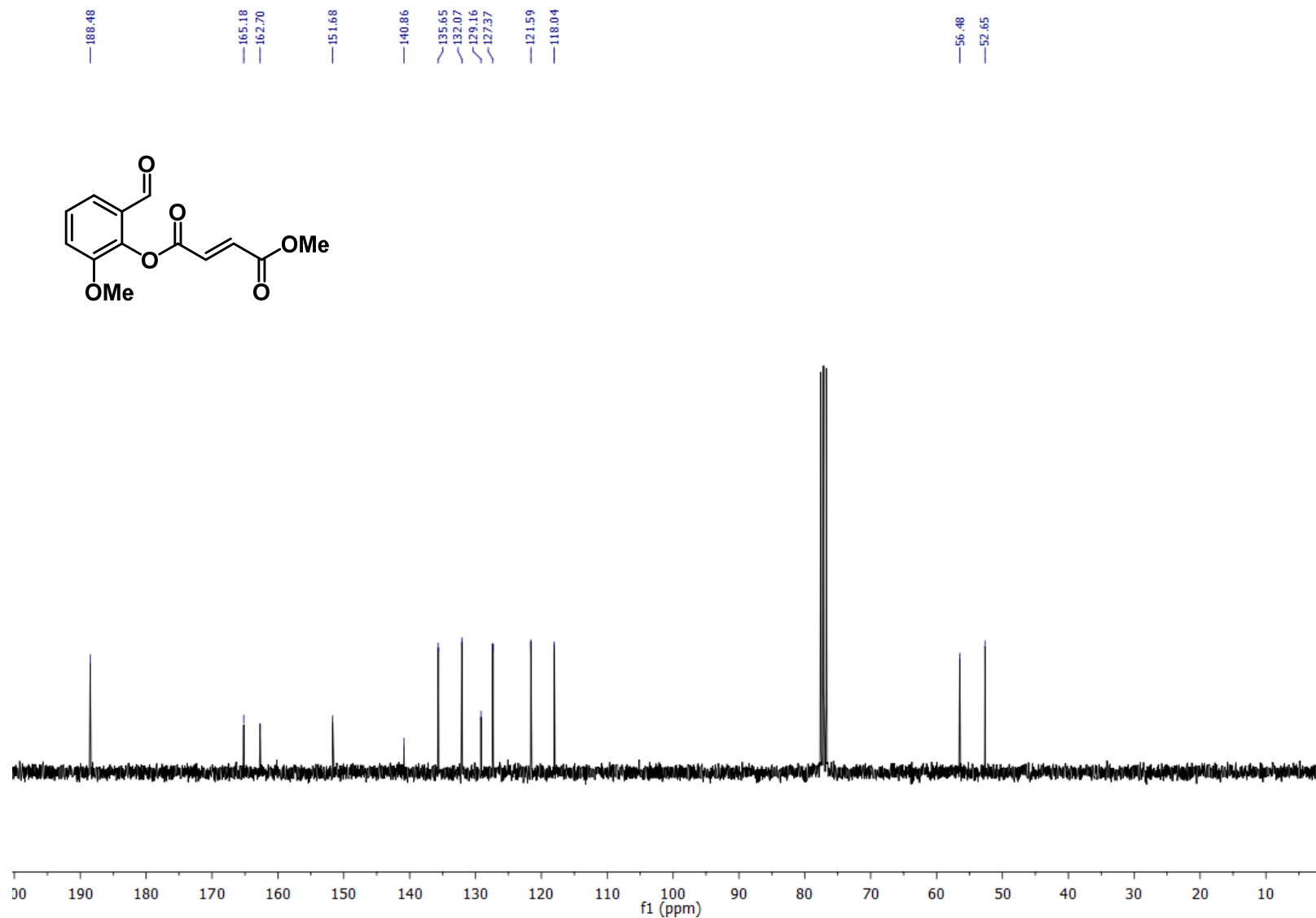
¹H NMR 2-Formylphenyl methyl fumarate (**2a**)



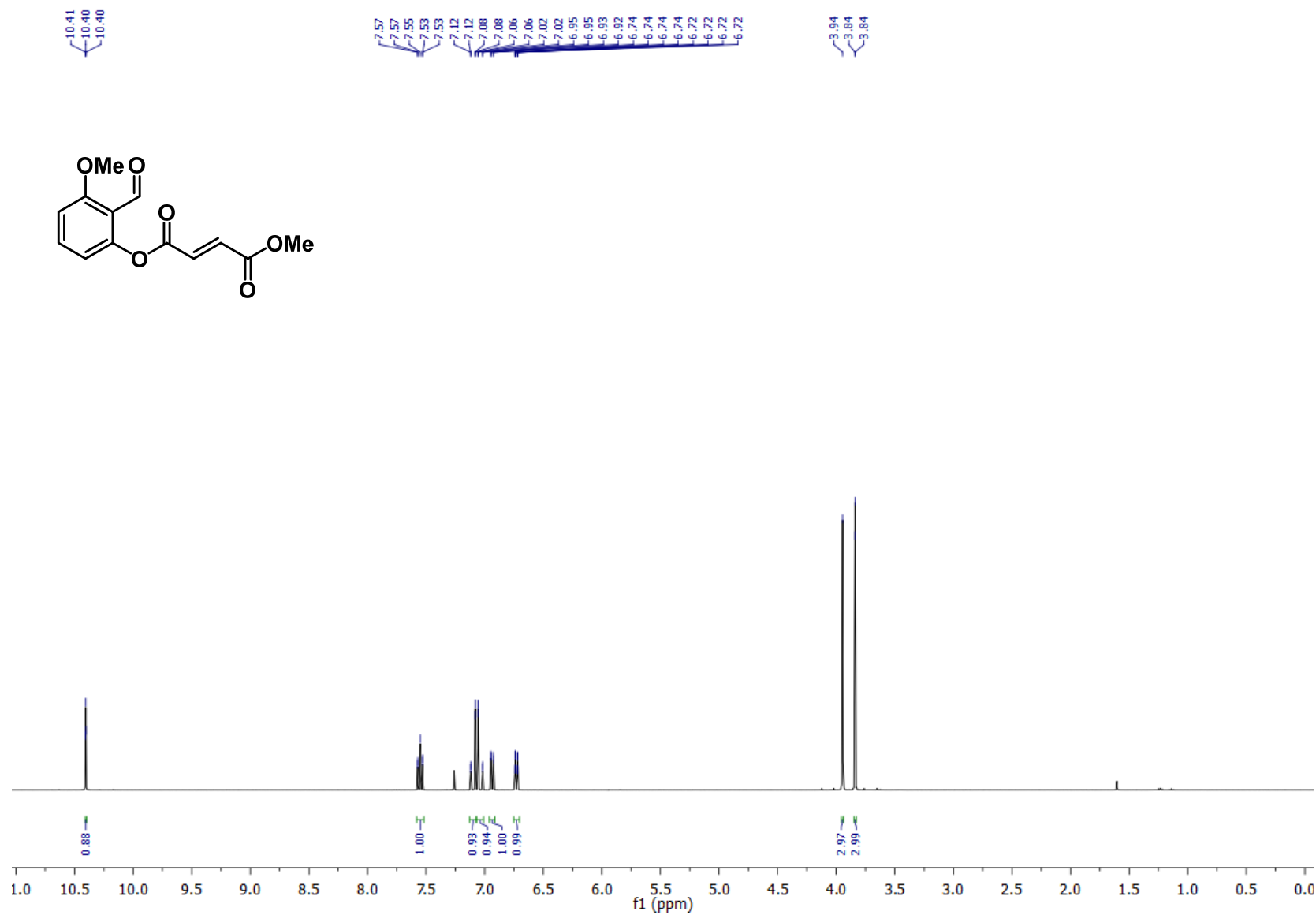
¹H NMR 2-Formyl-6-methoxyphenyl methyl fumarate (**2b**)



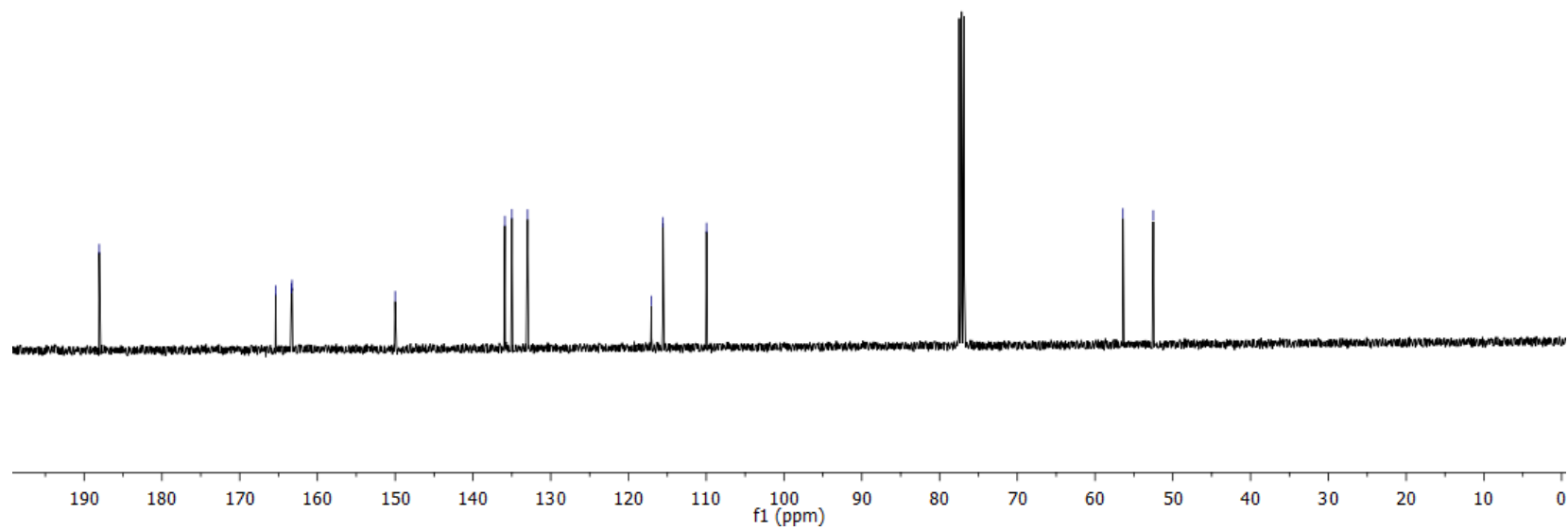
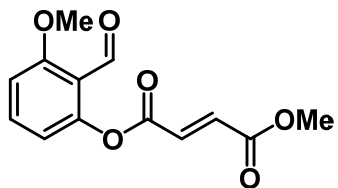
¹³C NMR 2-Formyl-6-methoxyphenyl methyl fumarate (**2b**)



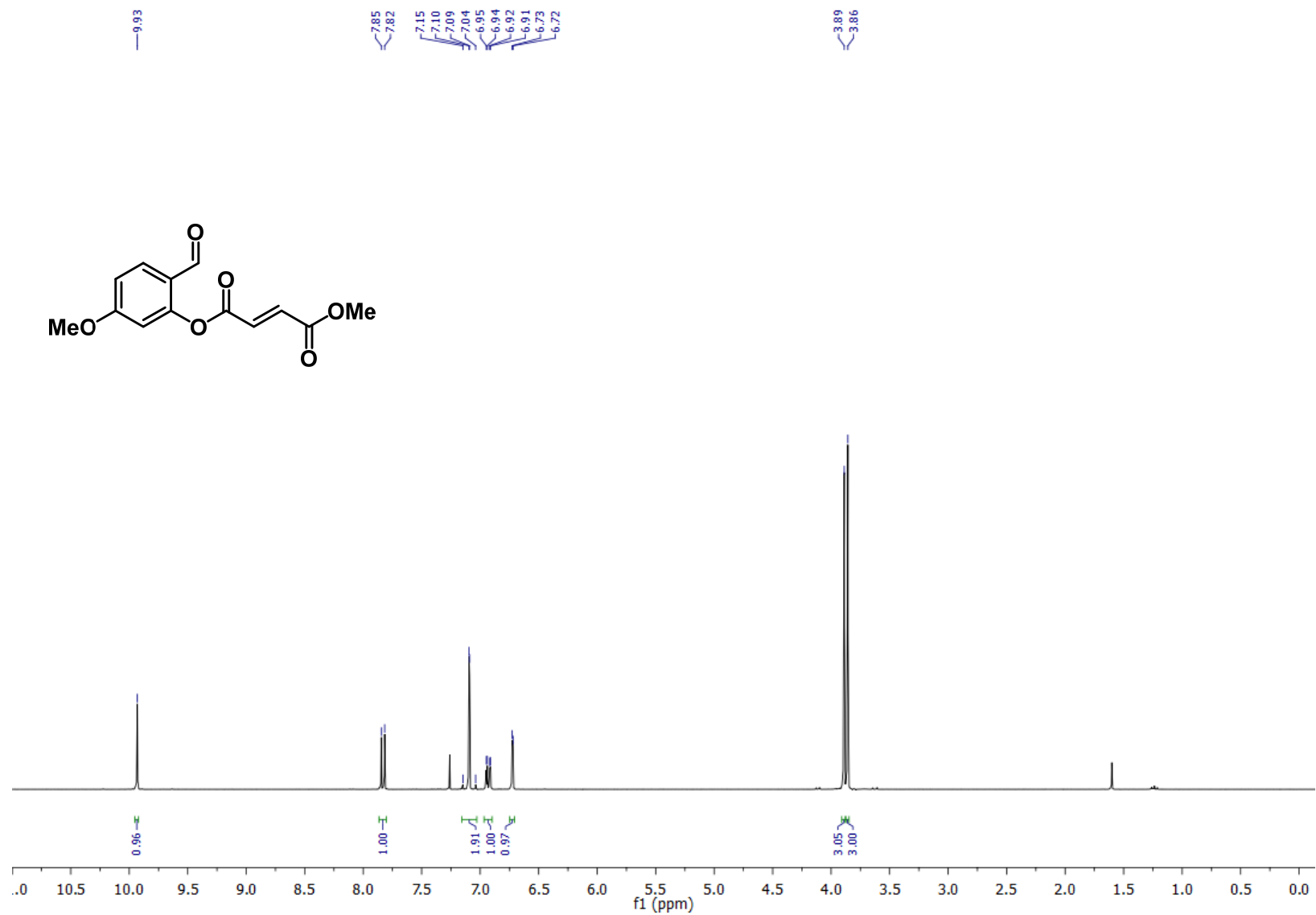
¹H NMR 2-Formyl-3-methoxyphenyl methyl fumarate (**2c**)



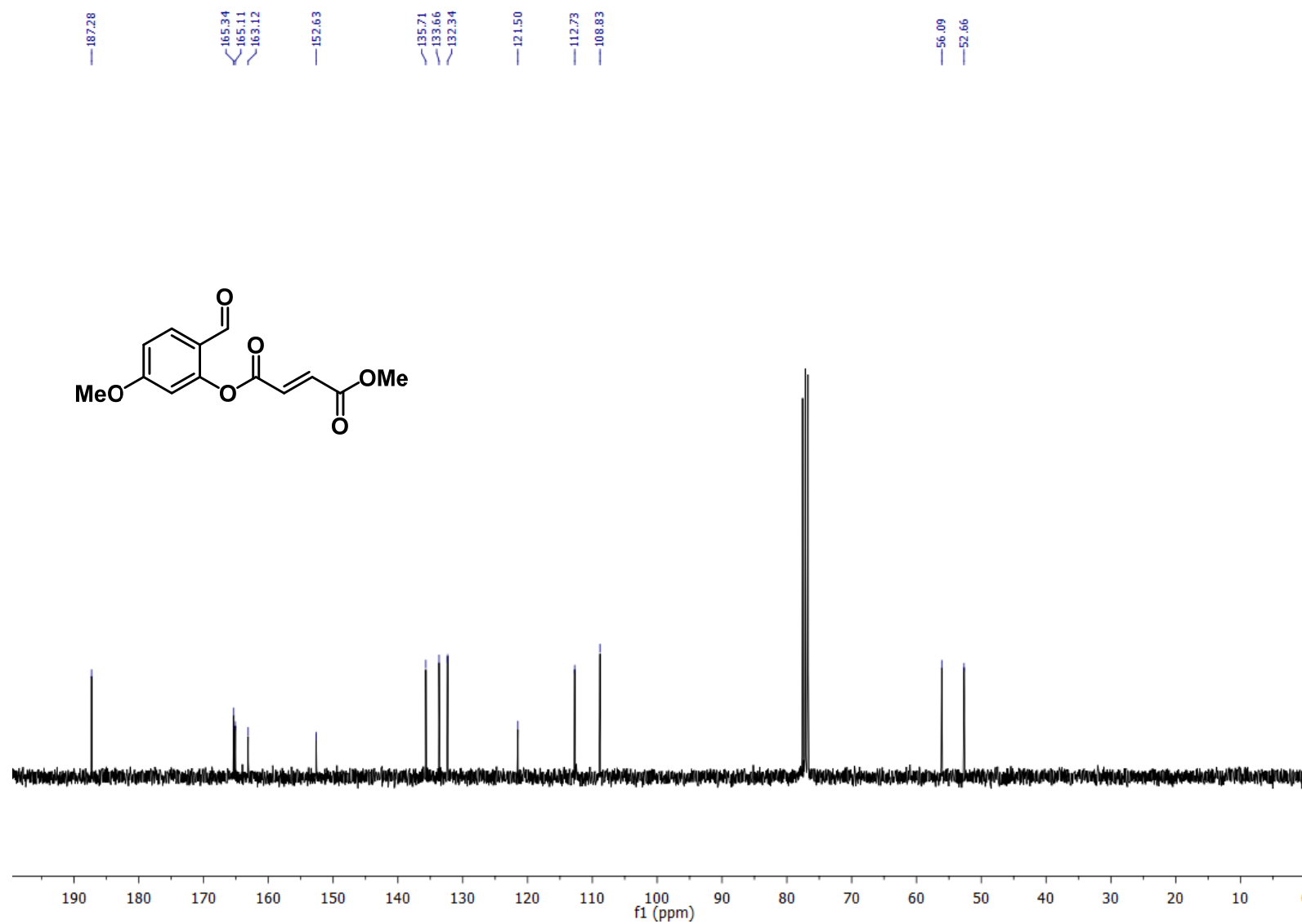
¹³C NMR 2-Formyl-3-methoxyphenyl methyl fumarate (**2c**)



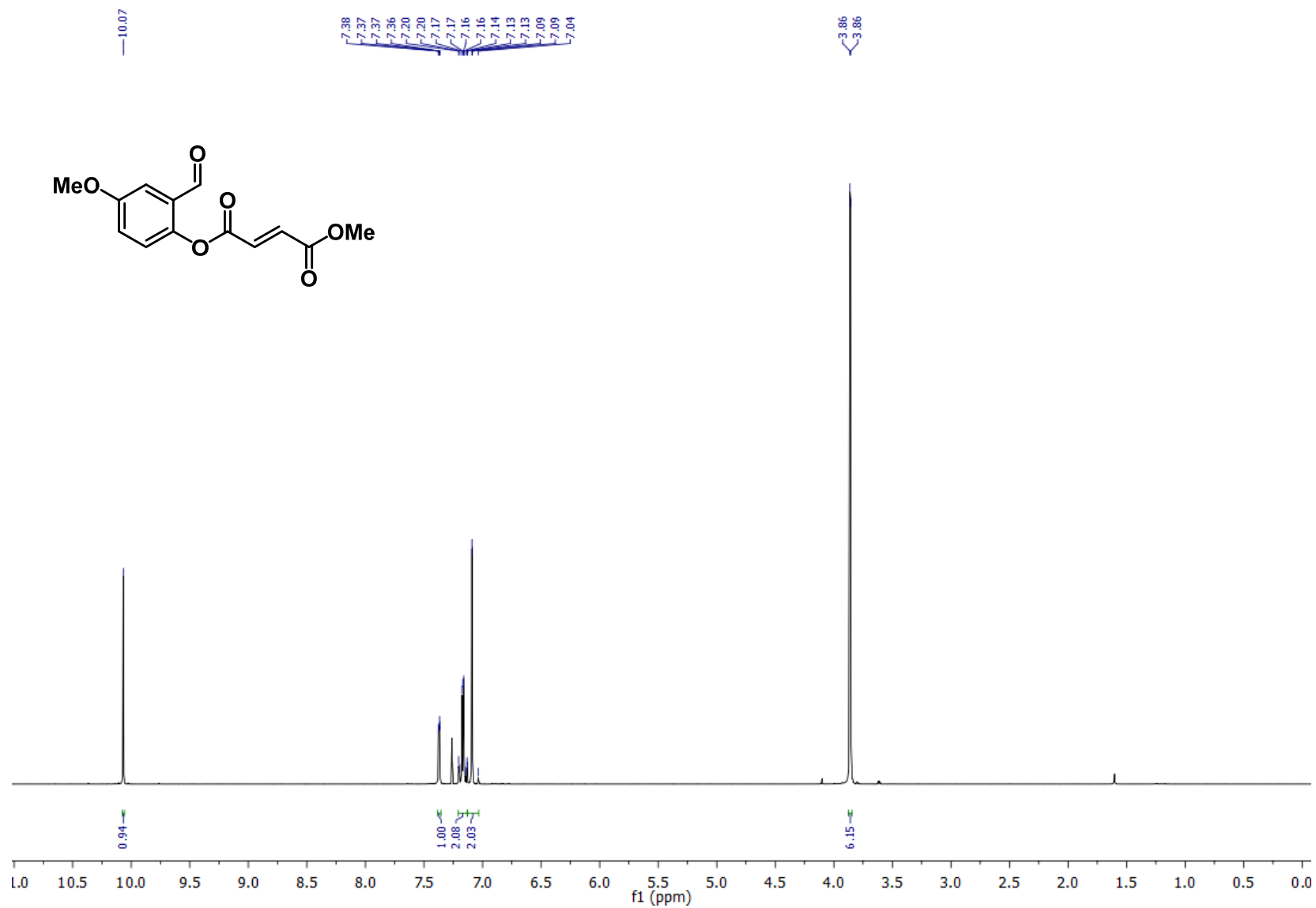
^1H NMR 2-Formyl-5-methoxyphenyl methyl fumarate (**2d**)



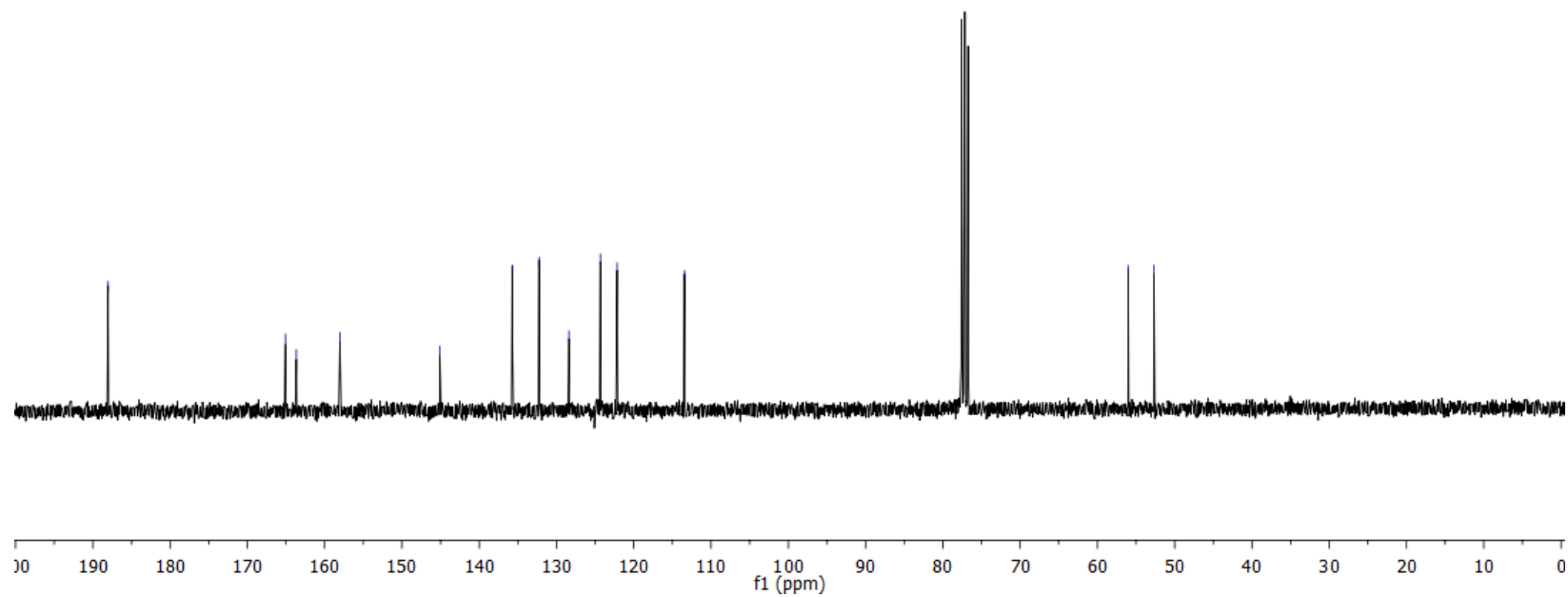
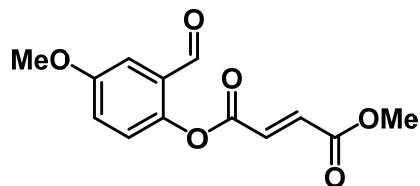
¹³C NMR 2-Formyl-5-methoxyphenyl methyl fumarate (**2d**)



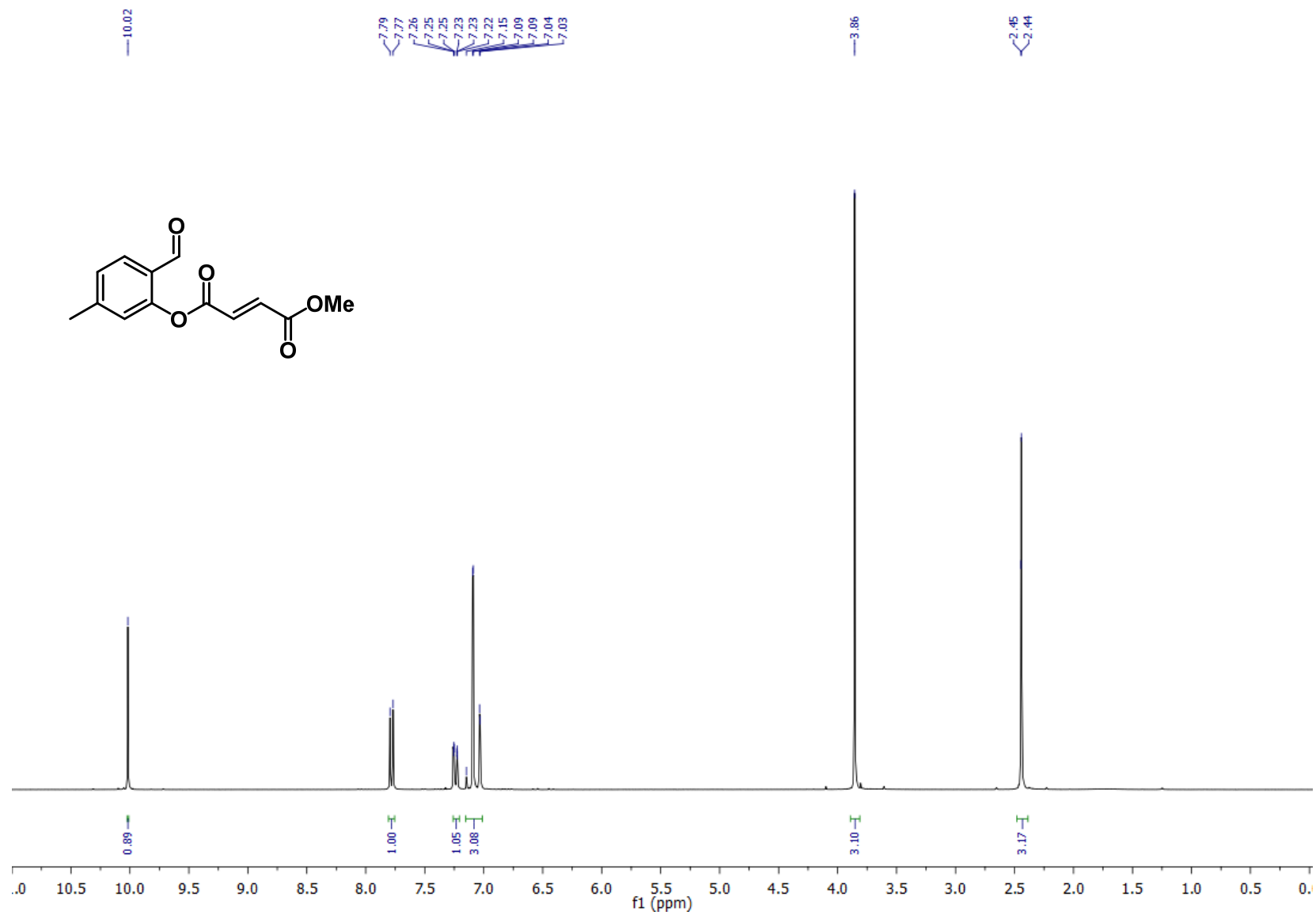
¹H NMR 2-Formyl-4-methoxyphenyl methyl fumarate (**2e**)



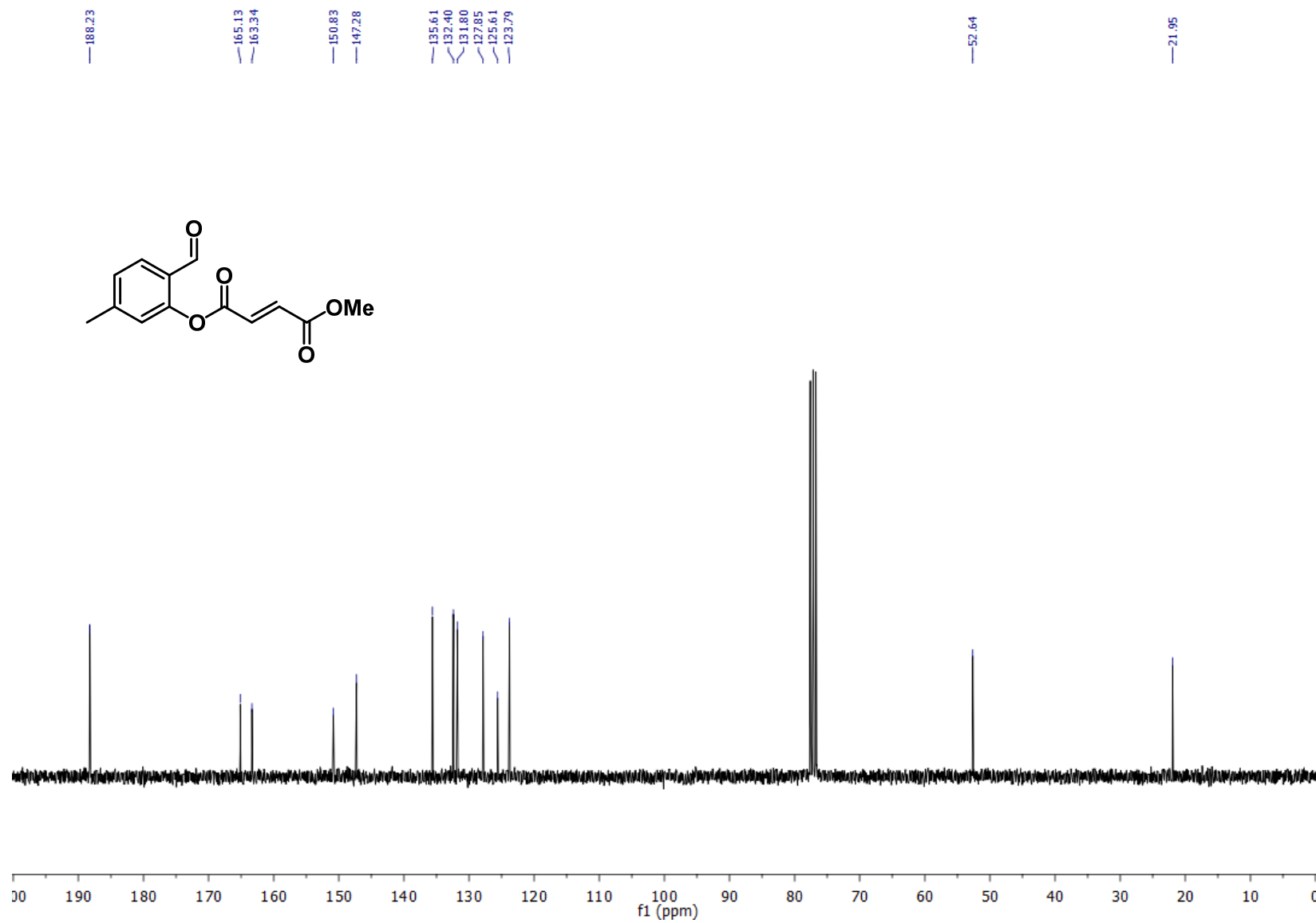
¹³C NMR 2-Formyl-4-methoxyphenyl methyl fumarate (**2e**)



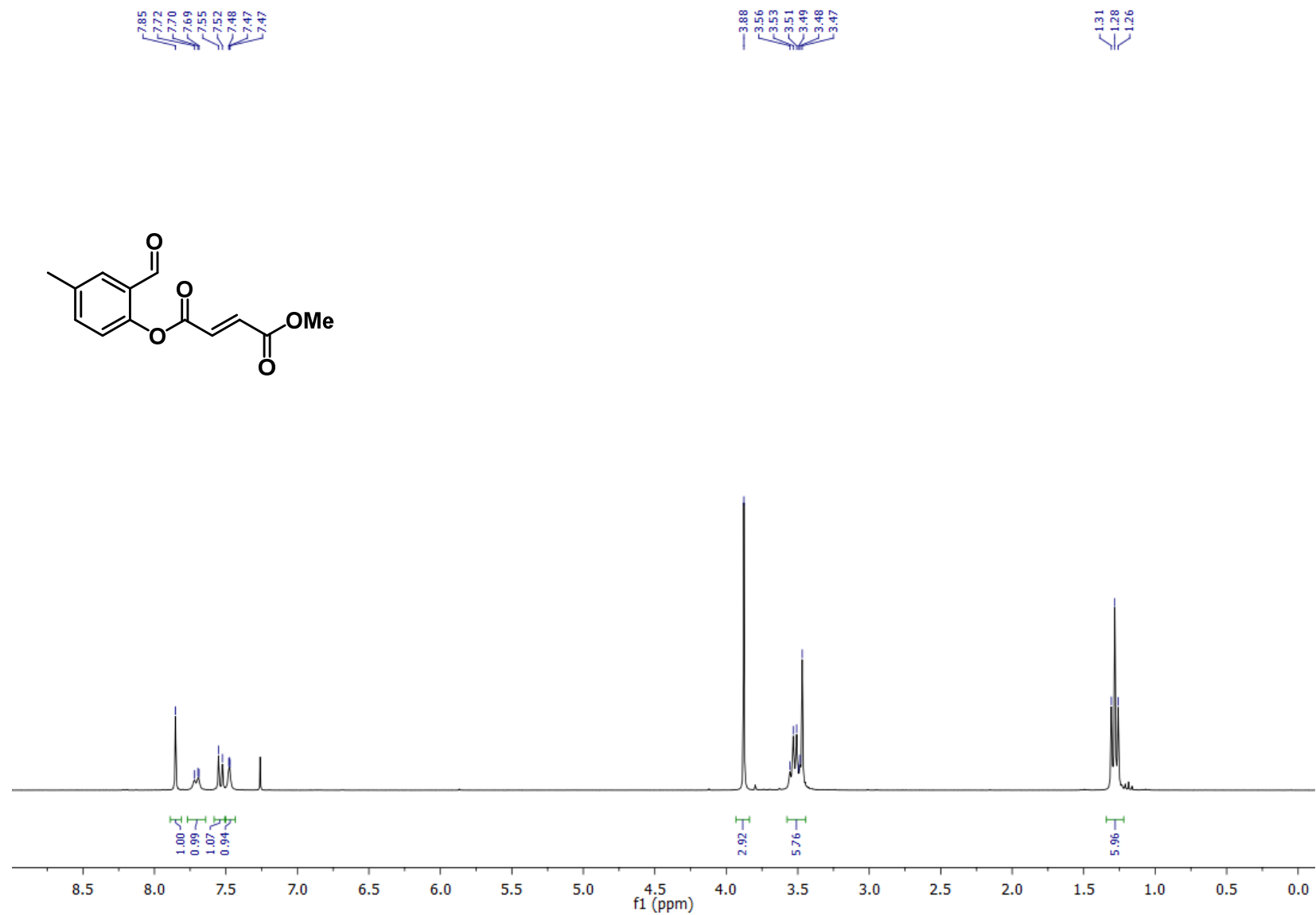
¹H NMR 2-Formyl-5-methylphenyl methyl fumarate (**2f**)



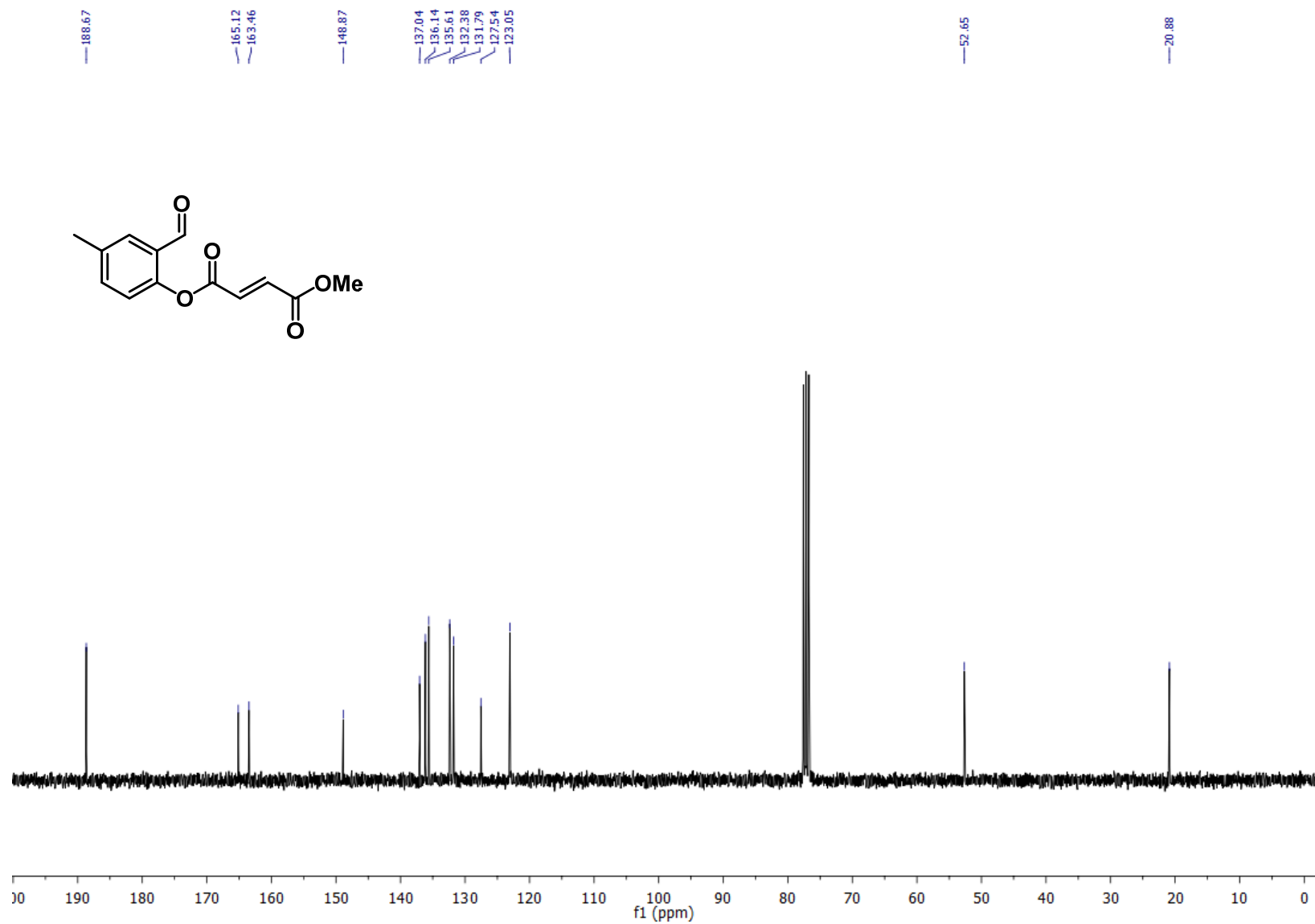
¹³C NMR 2-Formyl-5-methylphenyl methyl fumarate (**2f**)



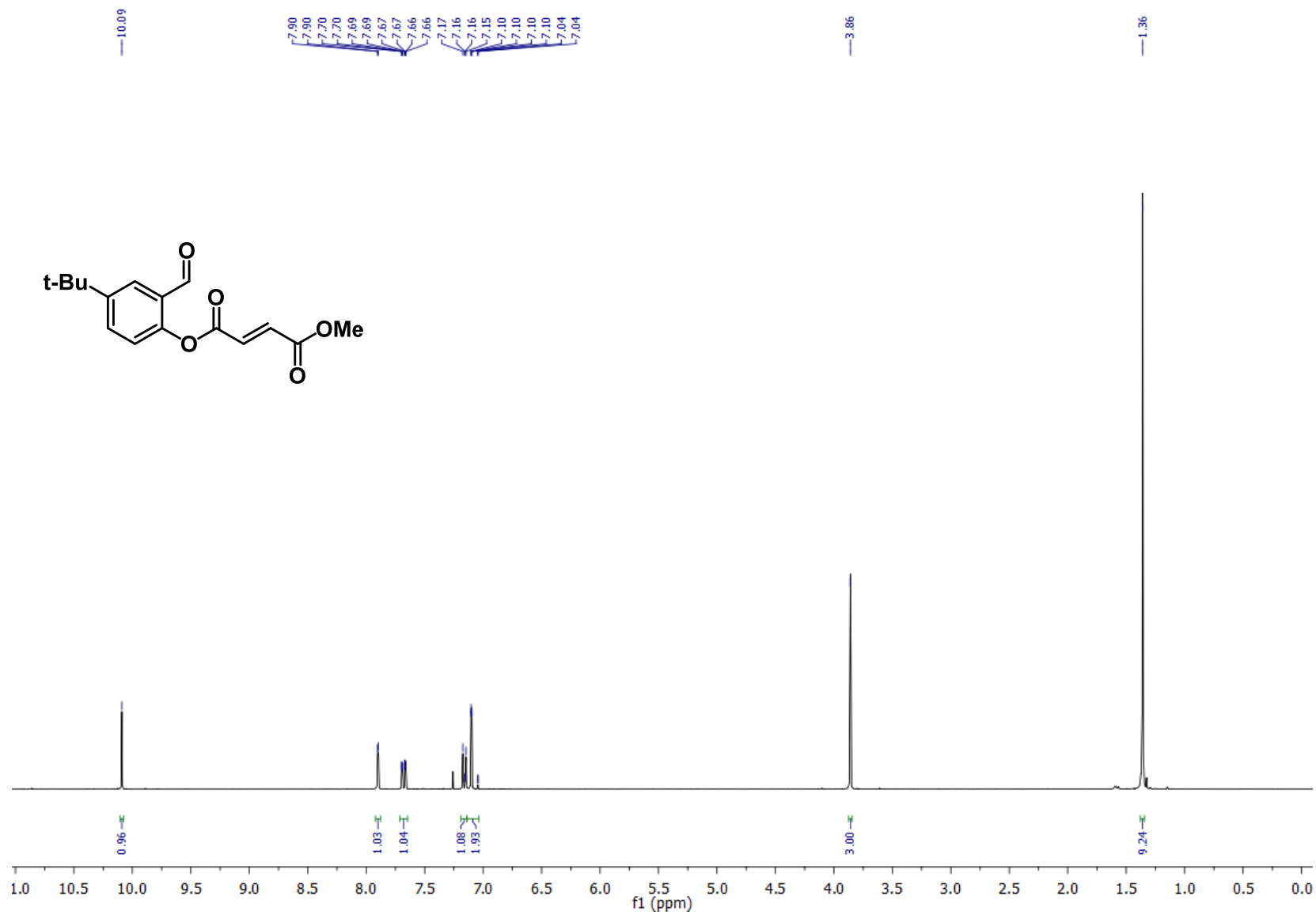
¹H NMR 2-Formyl-4-methylphenyl methyl fumarate (**2g**)



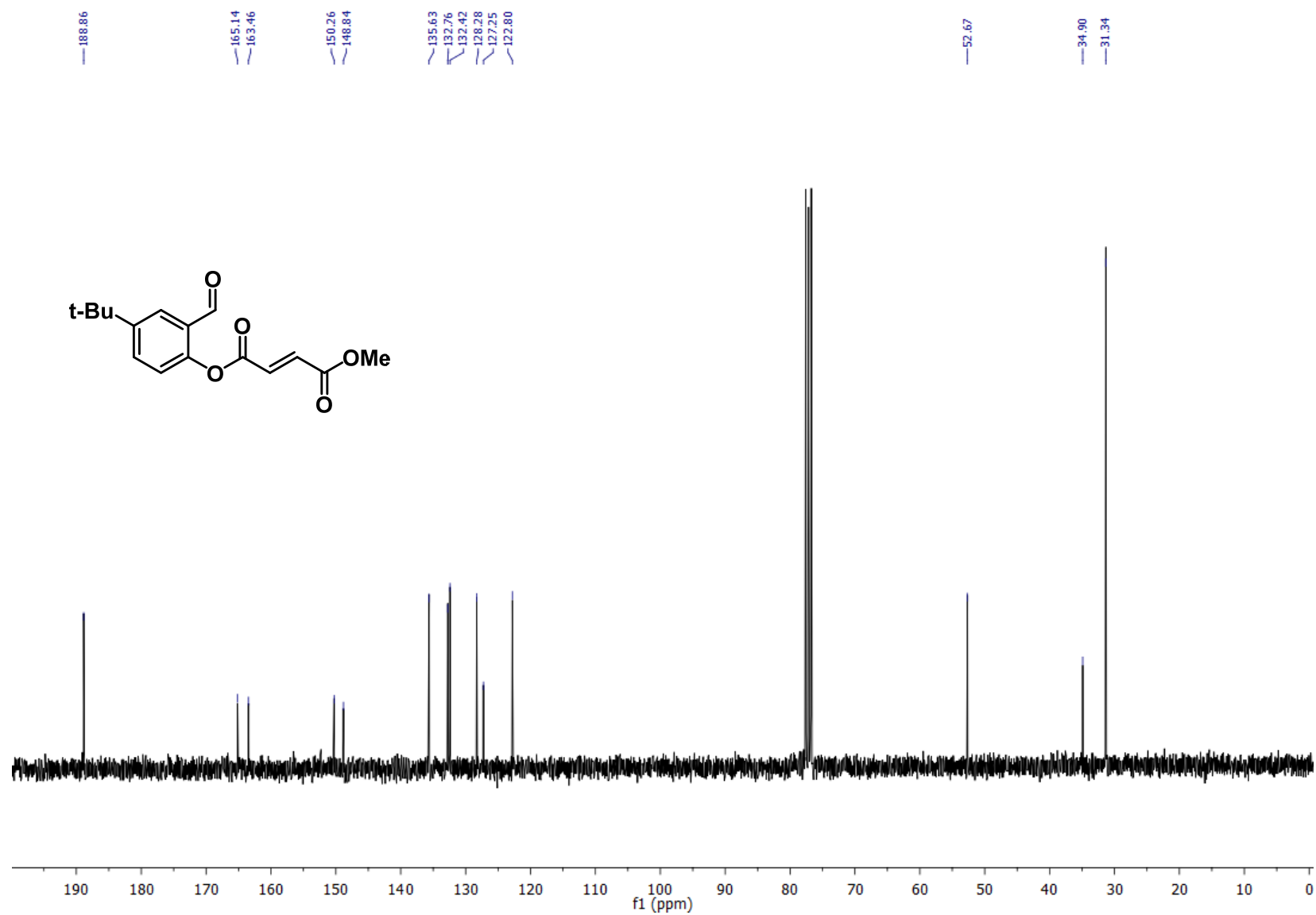
¹³C NMR 2-Formyl-4-methylphenyl methyl fumarate (**2g**)



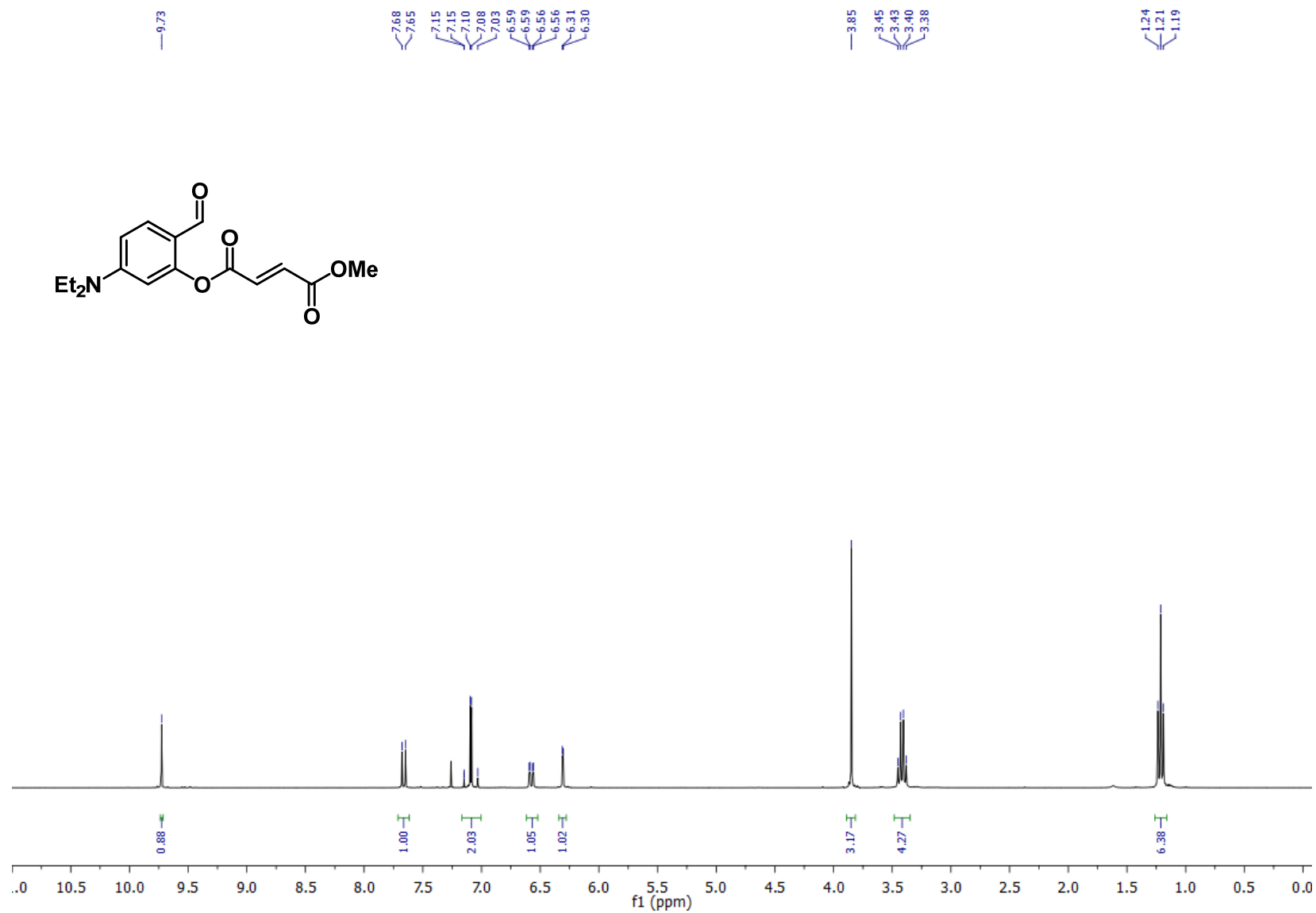
^1H NMR 4-(*tert*-Butyl)-2-formylphenyl methyl fumarate (**2h**)



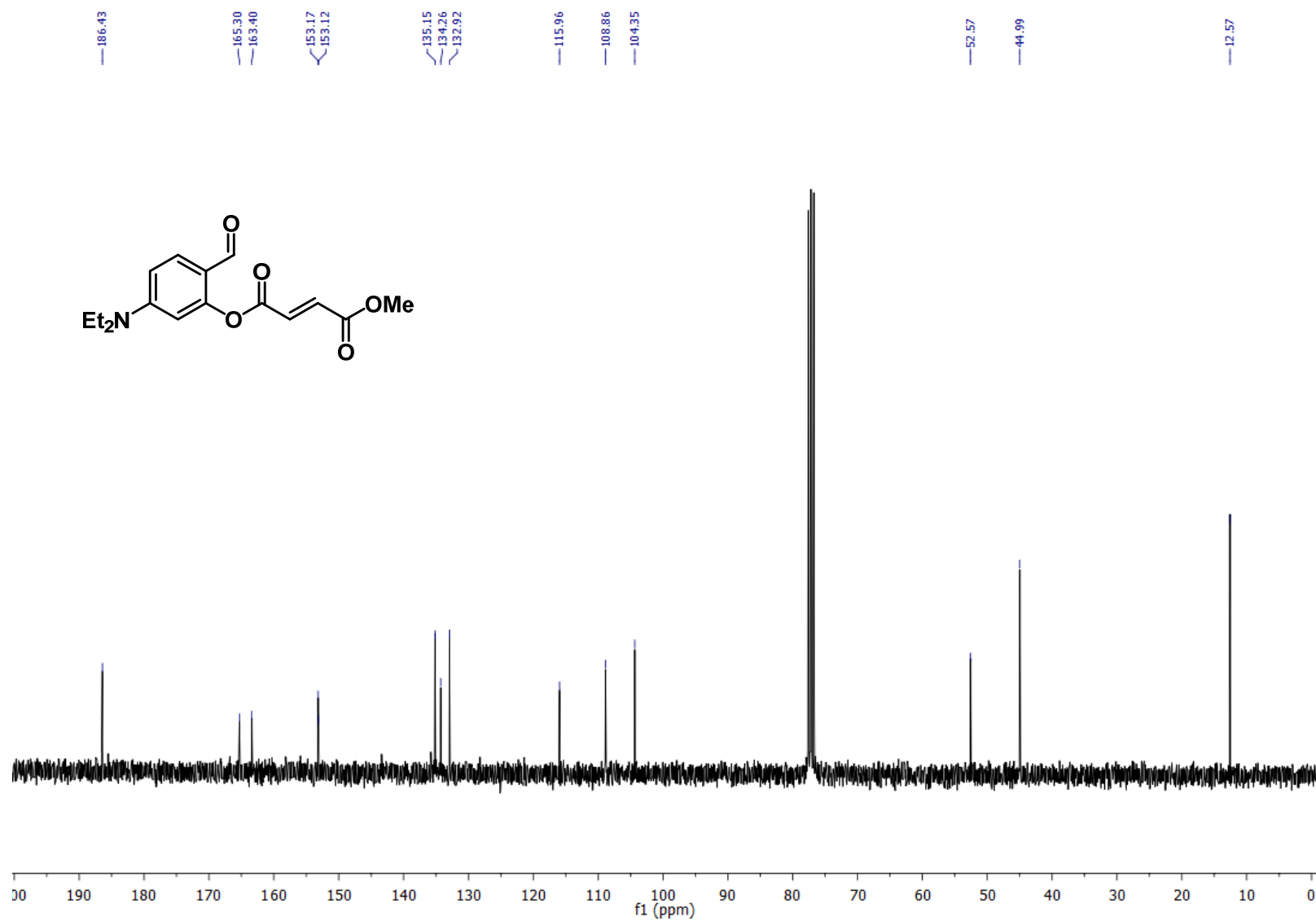
¹³C NMR 4-(*tert*-Butyl)-2-formylphenyl methyl fumarate (**2h**)



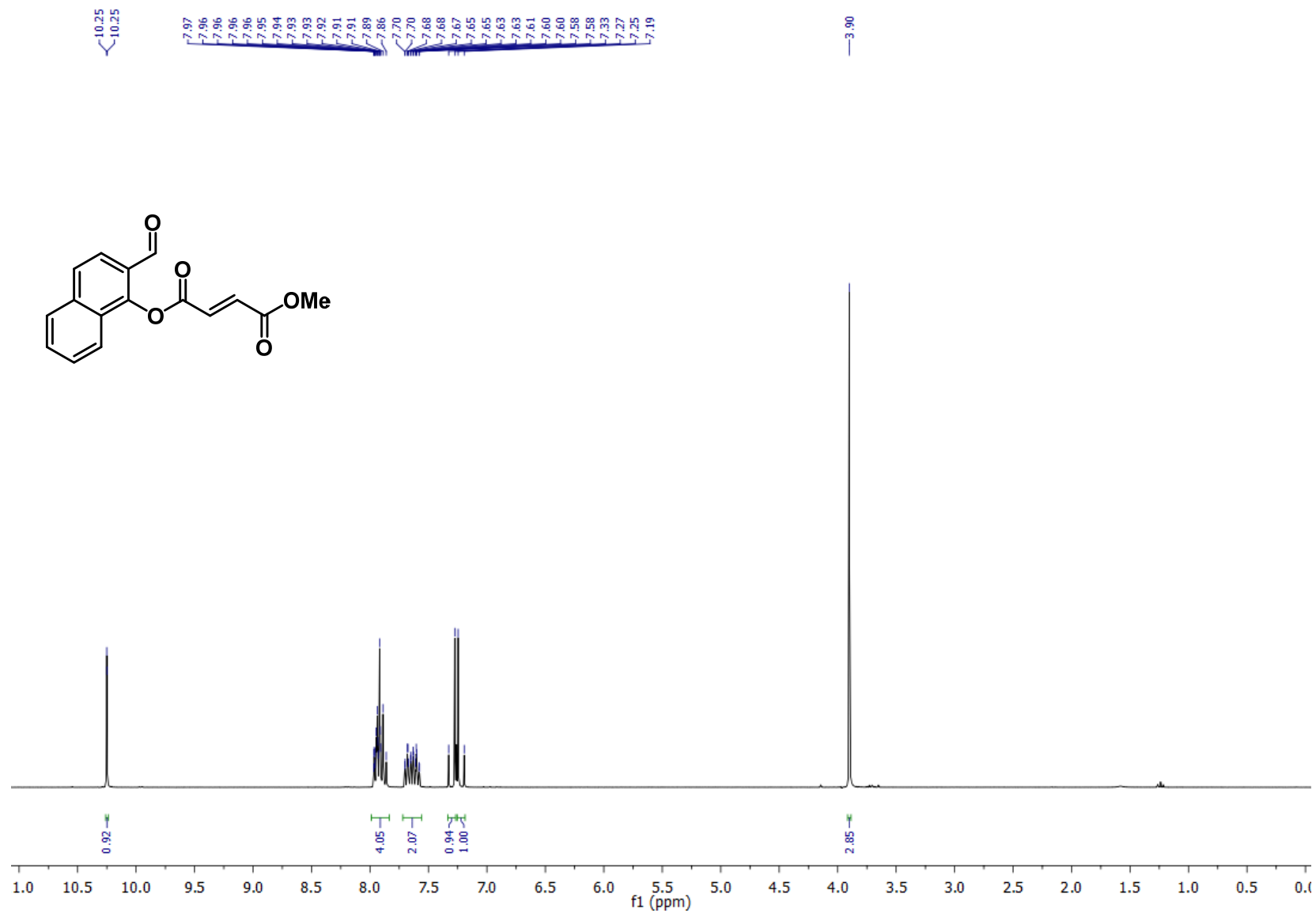
¹H NMR 5-(Diethylamino)-2-formylphenyl methyl fumarate (**2i**)



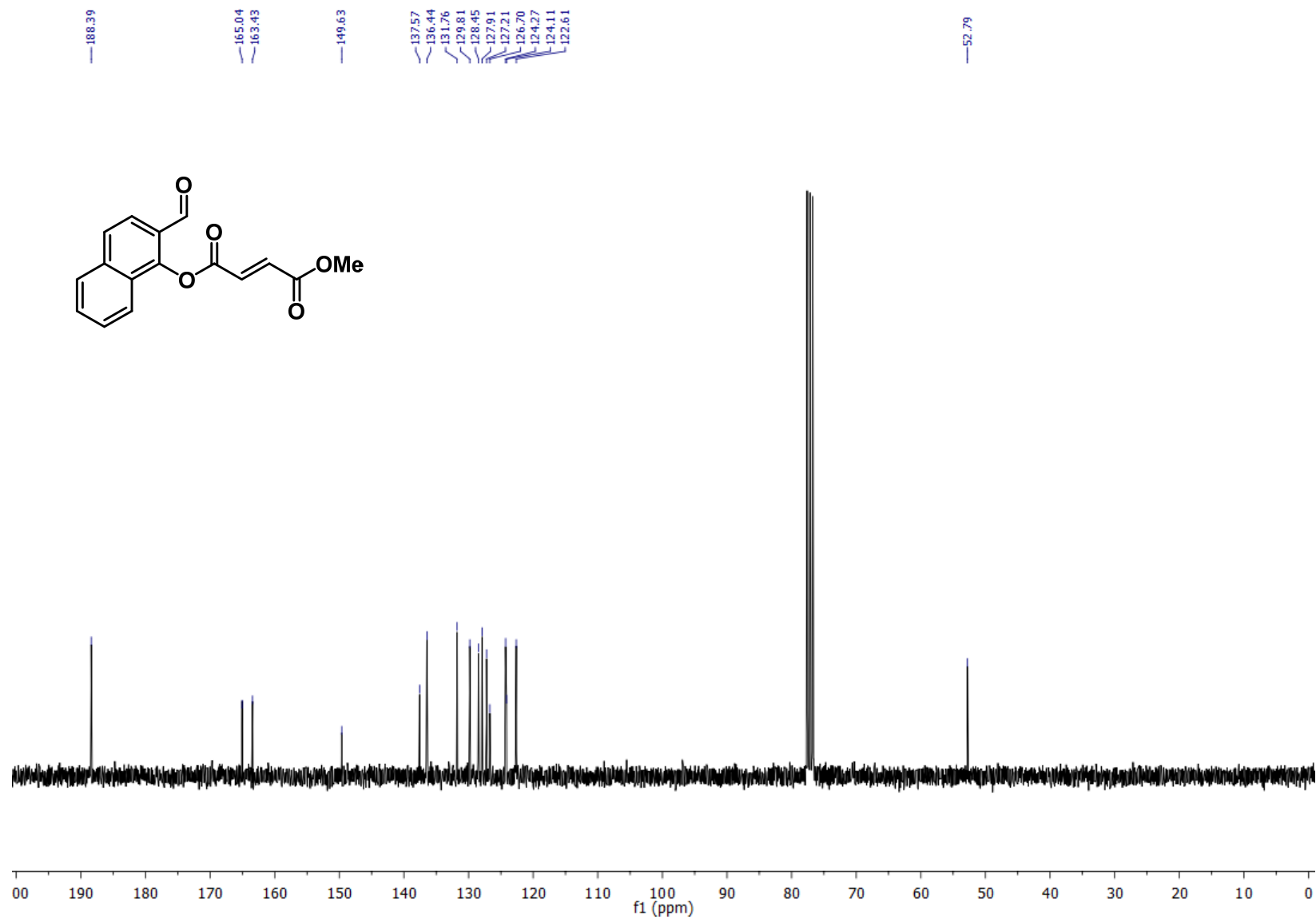
¹³C NMR 5-(Diethylamino)-2-formylphenyl methyl fumarate (**2i**)



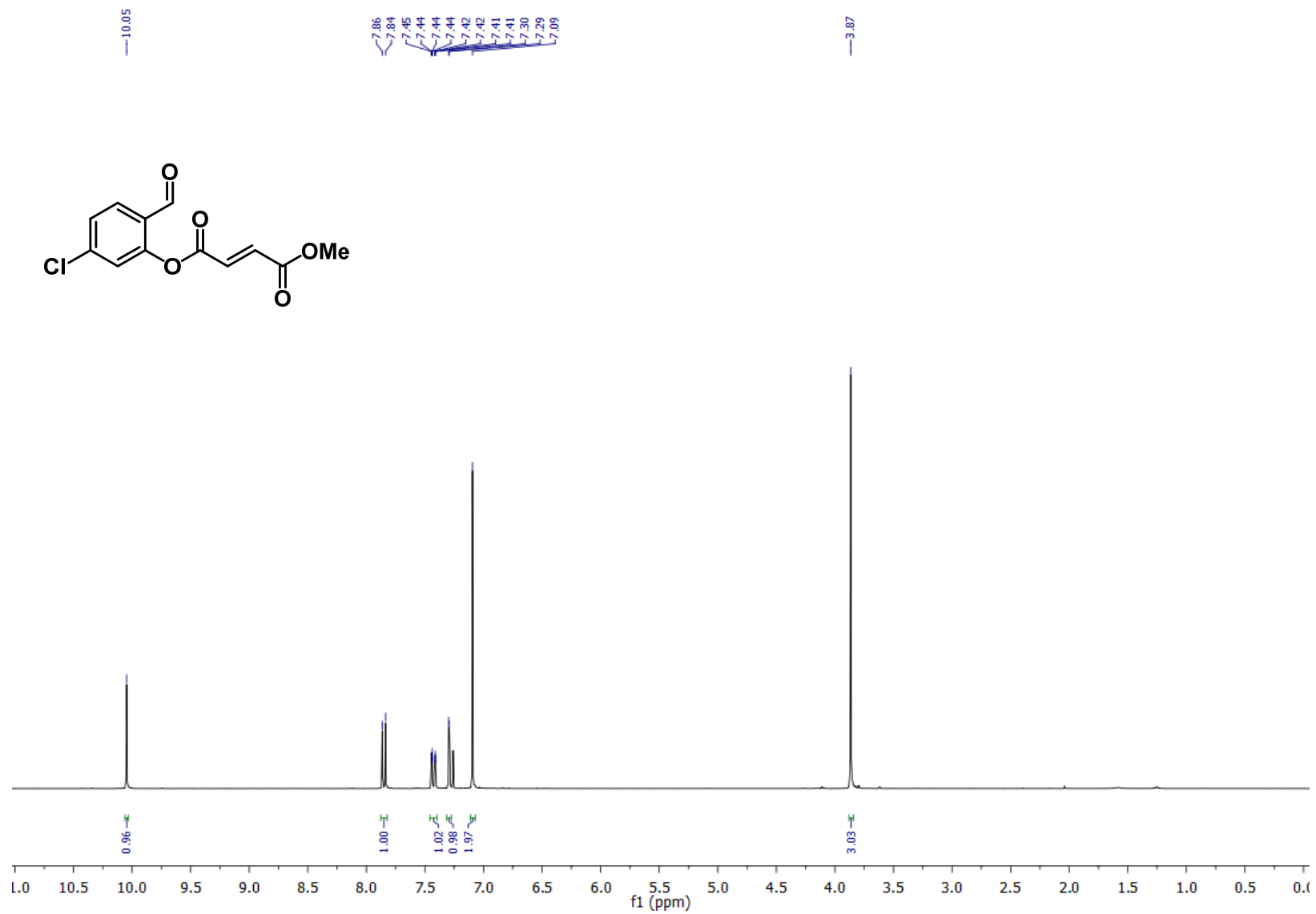
¹H NMR 2-Formylnaphthalen-1-yl methyl fumarate (**2j**)



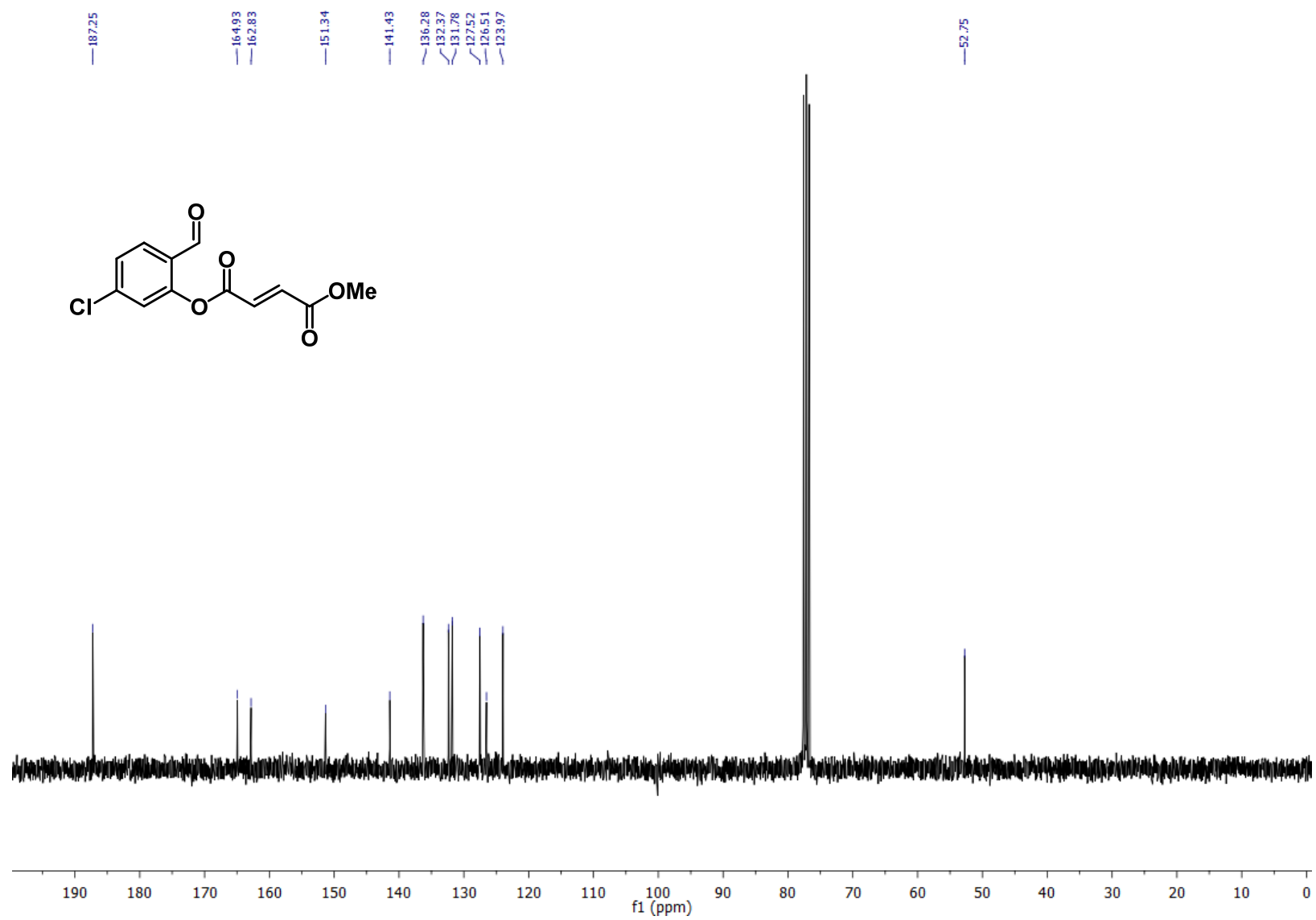
¹³C NMR 2-Formylnaphthalen-1-yl methyl fumarate (**2j**)



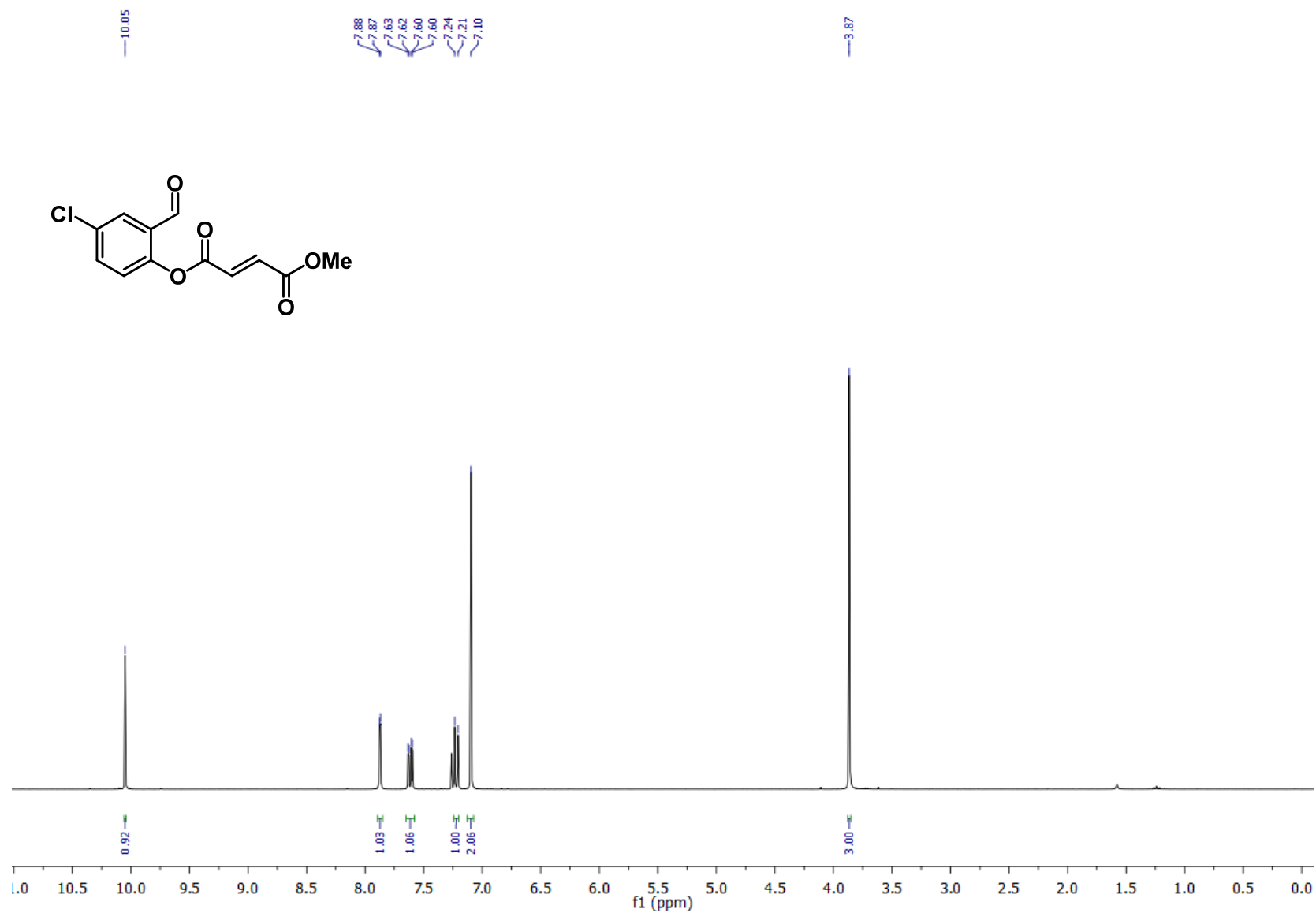
¹H NMR 5-Chloro-2-formylphenyl methyl fumarate (**2k**)



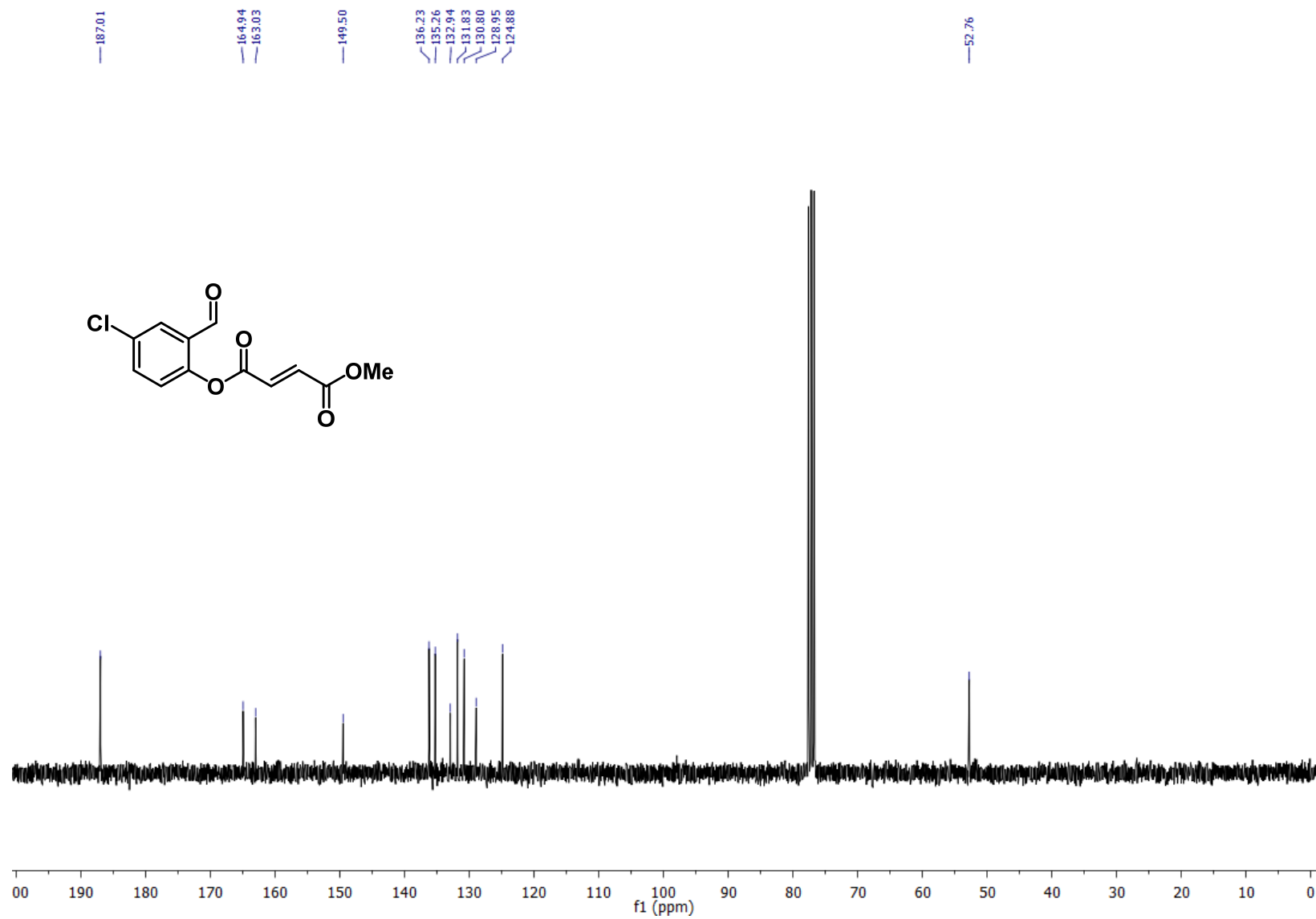
^{13}C NMR 5-Chloro-2-formylphenyl methyl fumarate (**2k**)



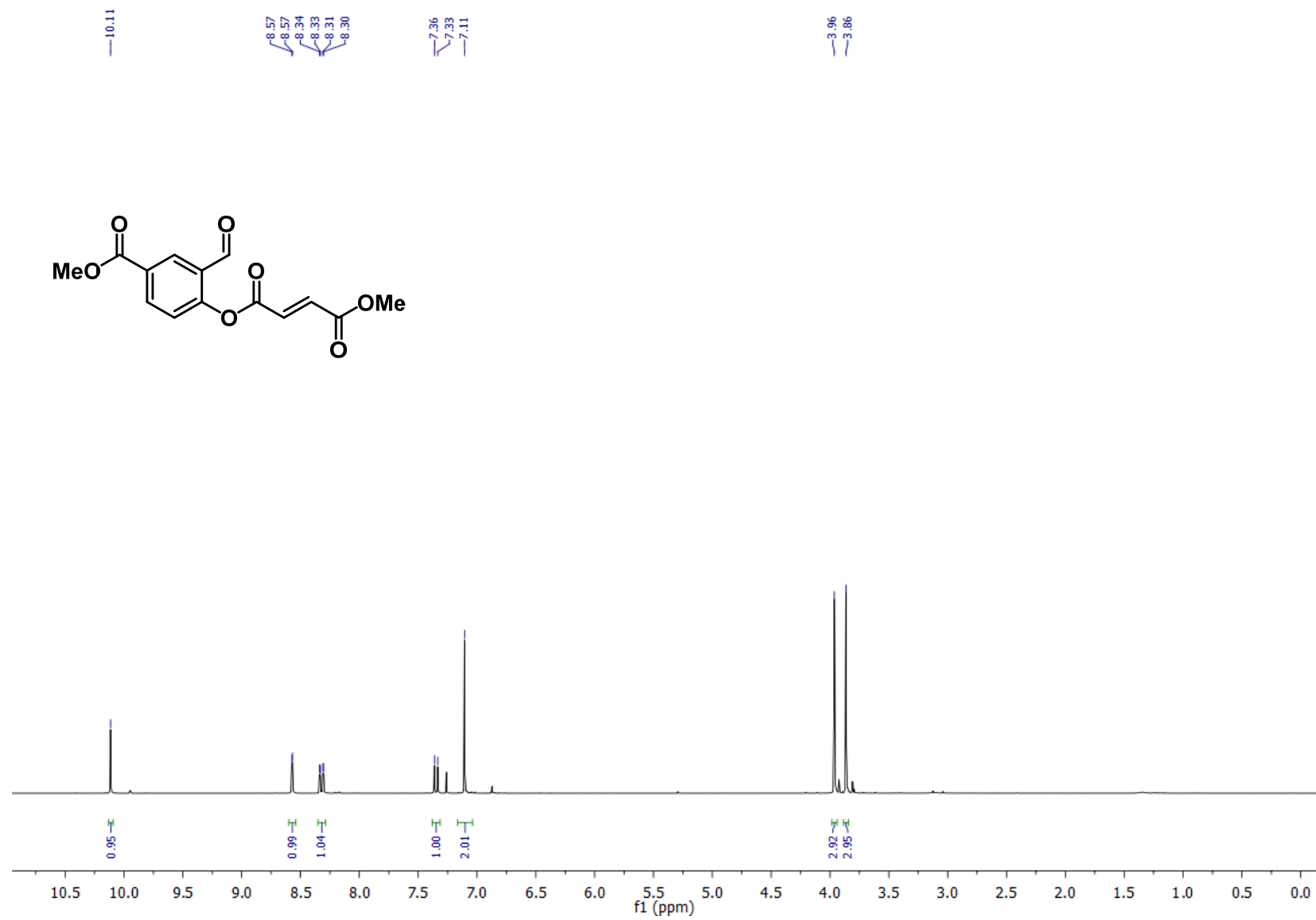
^1H NMR 4-Chloro-2-formylphenyl methyl fumarate (**21**)



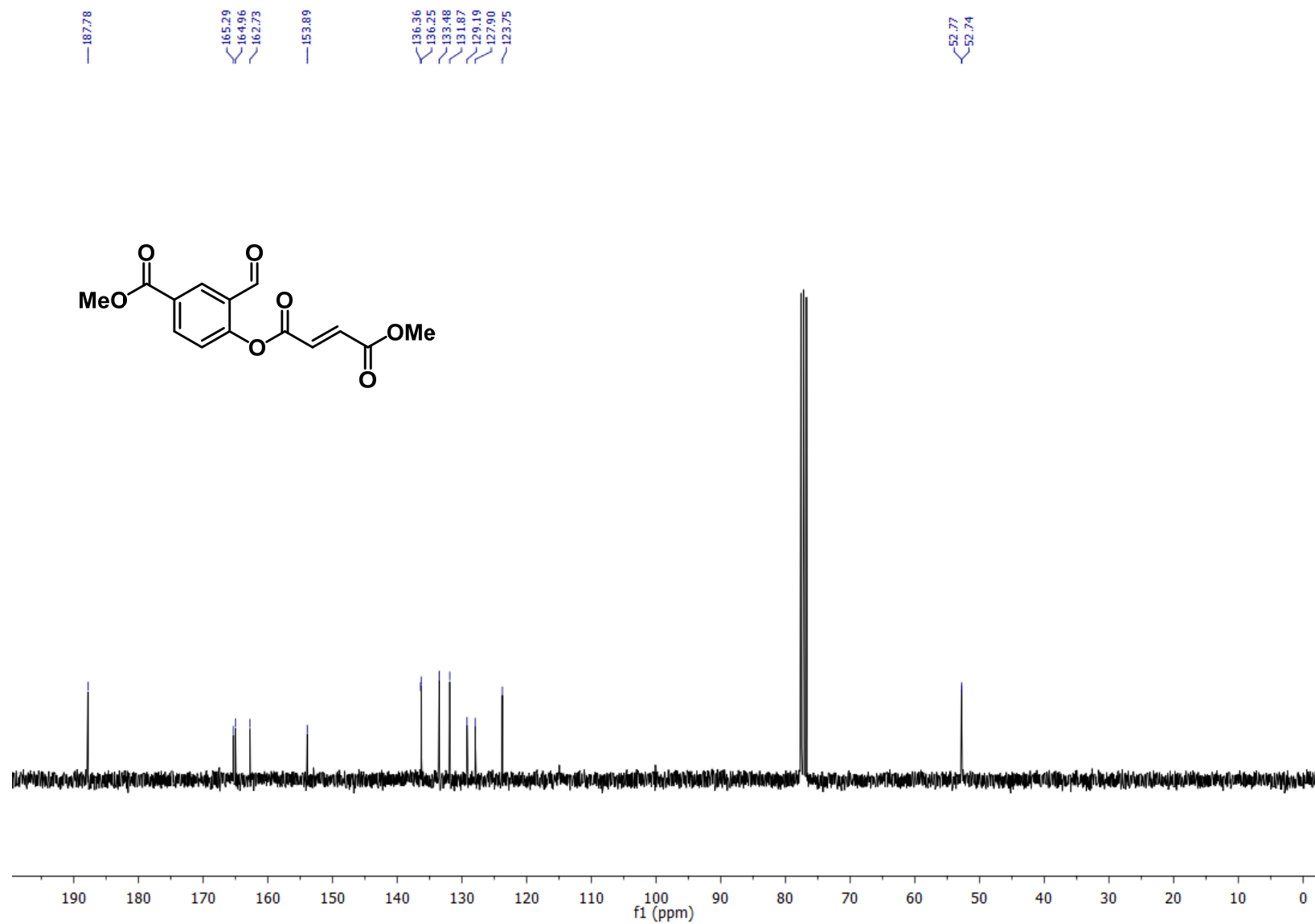
¹³C NMR 4-Chloro-2-formylphenyl methyl fumarate (**21**)



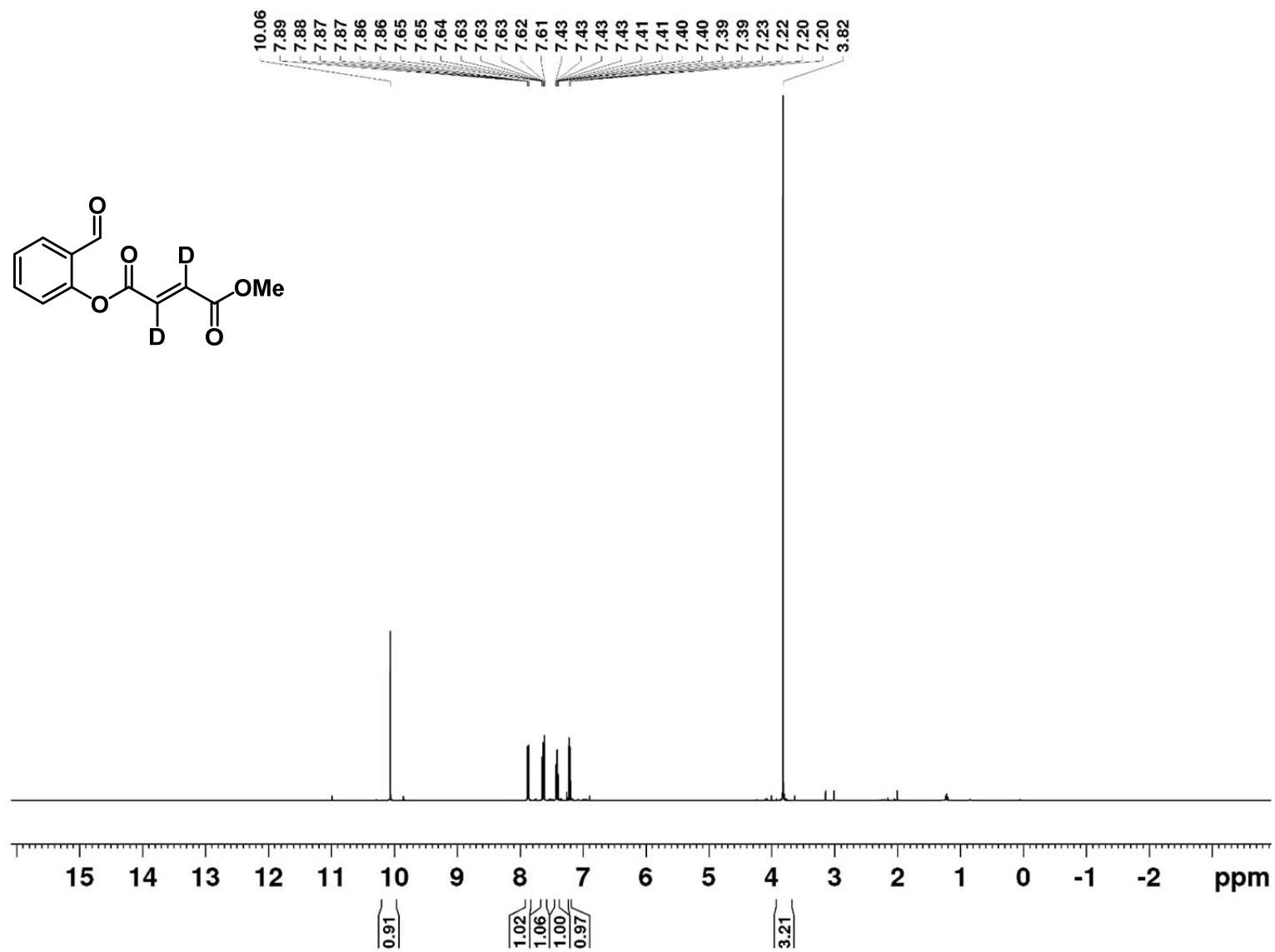
^1H NMR 2-Formyl-4-(methoxycarbonyl)phenyl methyl fumarate (**2m**)



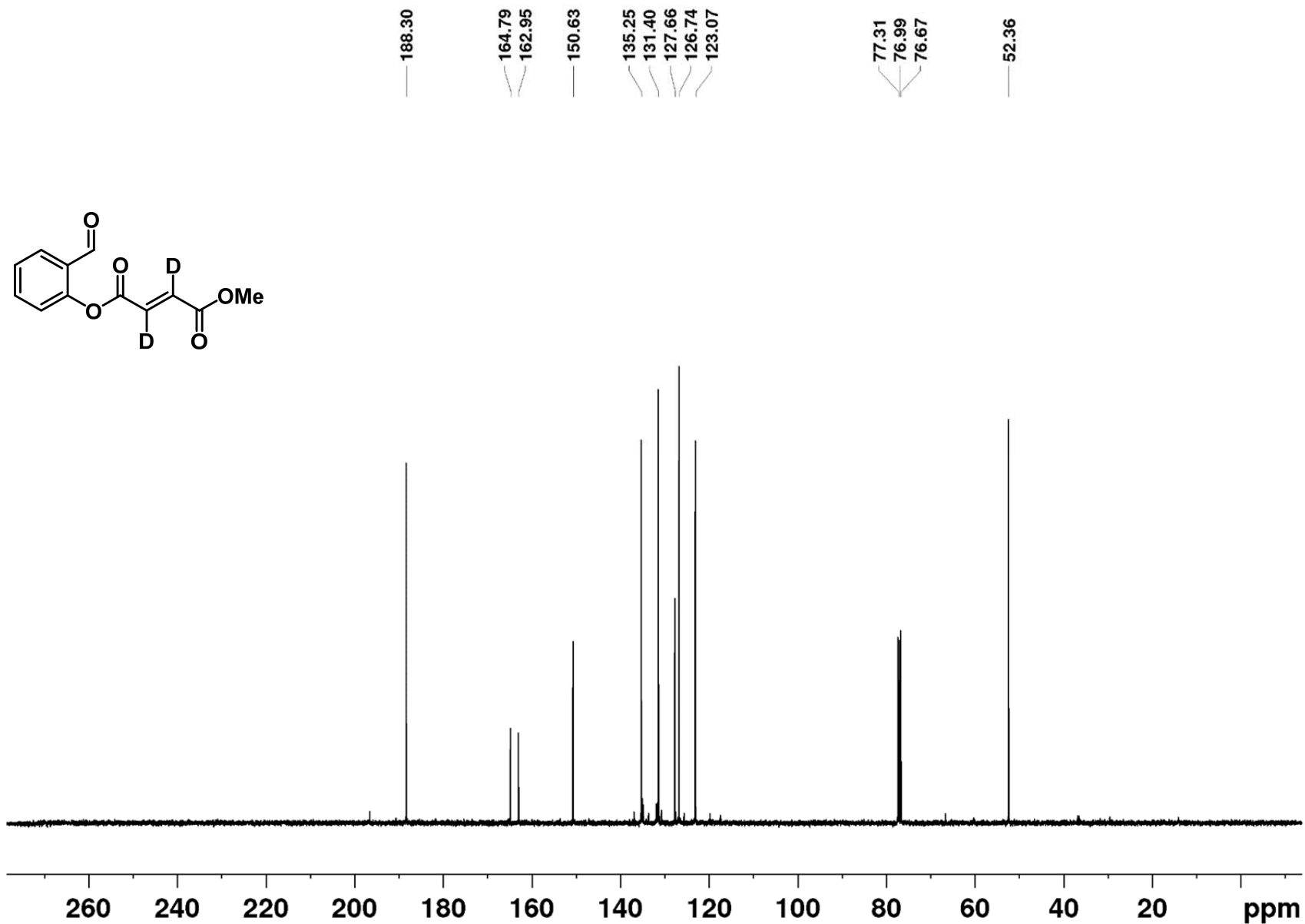
¹³C NMR 2-Formyl-4-(methoxycarbonyl)phenyl methyl fumarate (**2m**)



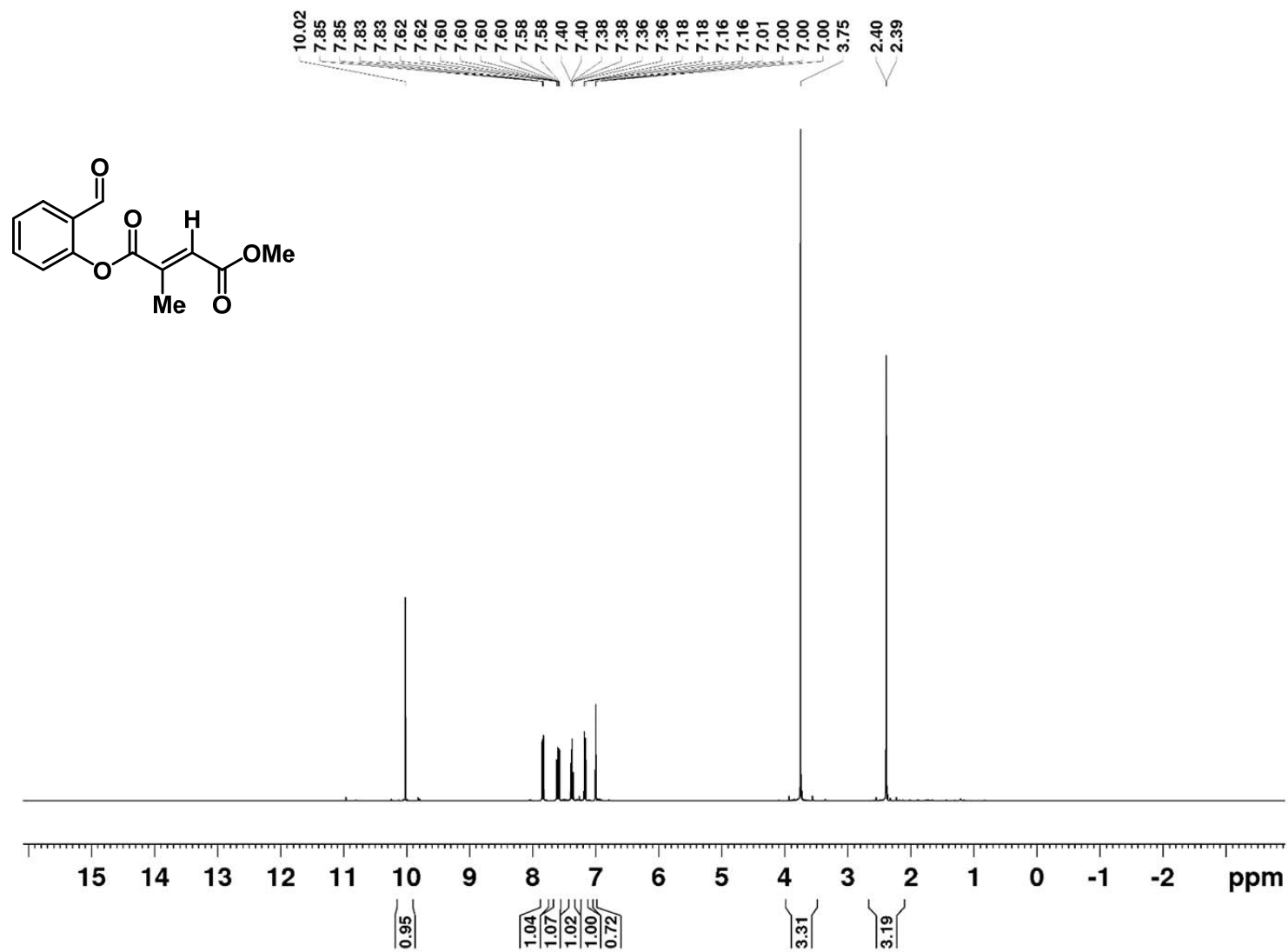
^1H NMR 2-Formylphenyl methyl fumarate-d₂ (**2a-D₂**)



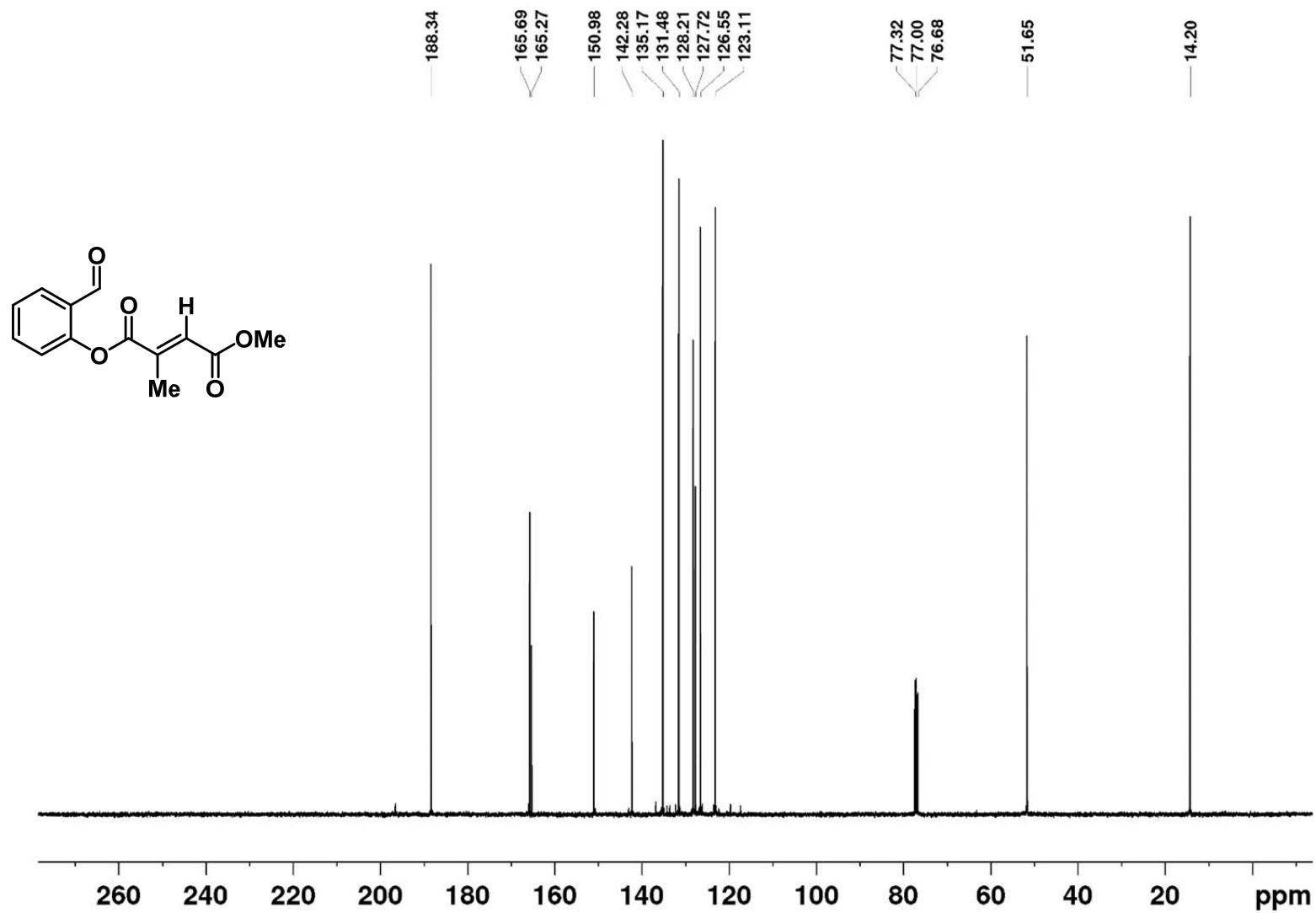
¹³C NMR 2-Formylphenyl methyl fumarate-d₂ (**2a-D₂**)



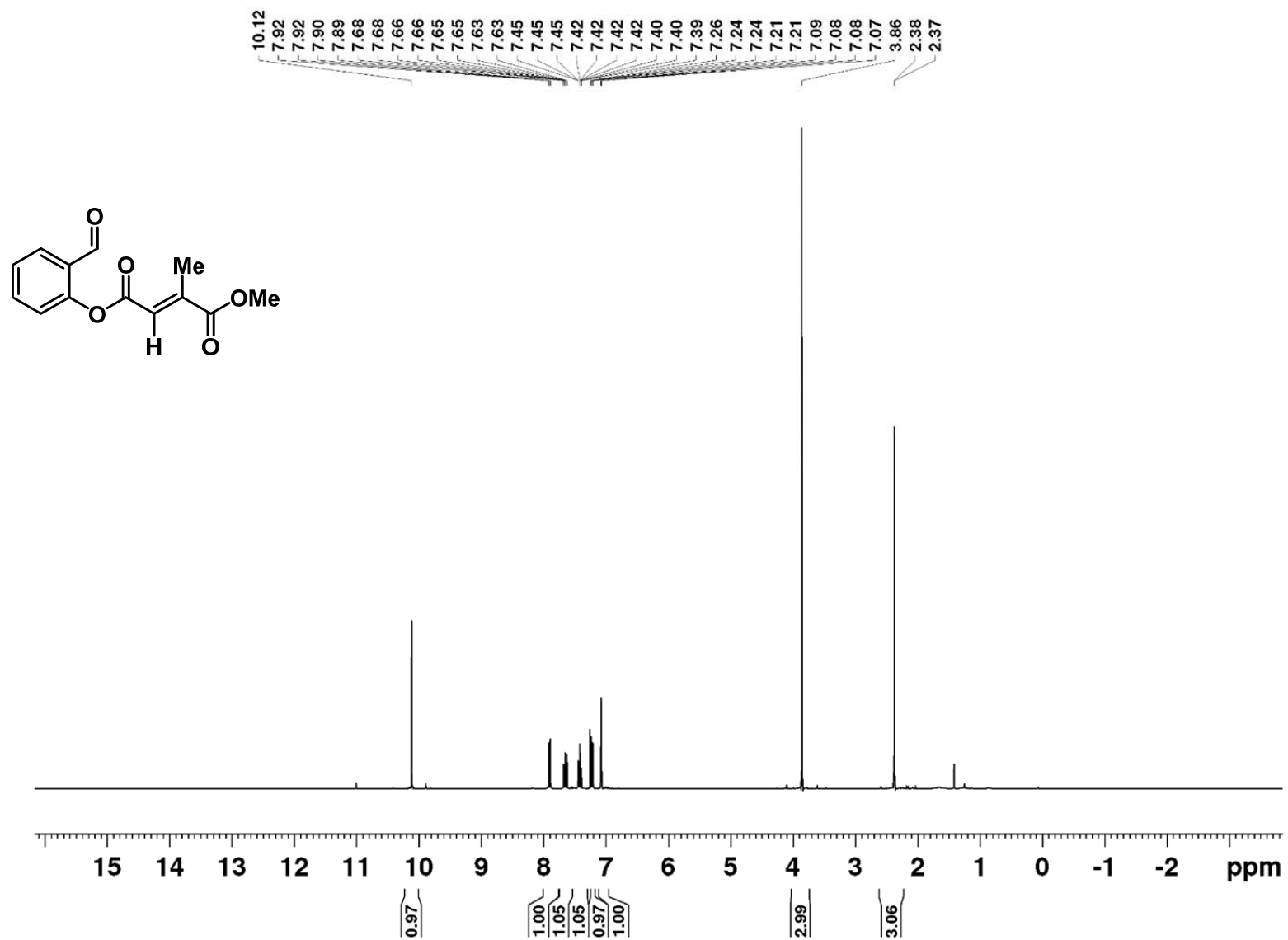
¹H NMR 1-(2-Formylphenyl) 4-methyl 2-methylfumarate (**11**)



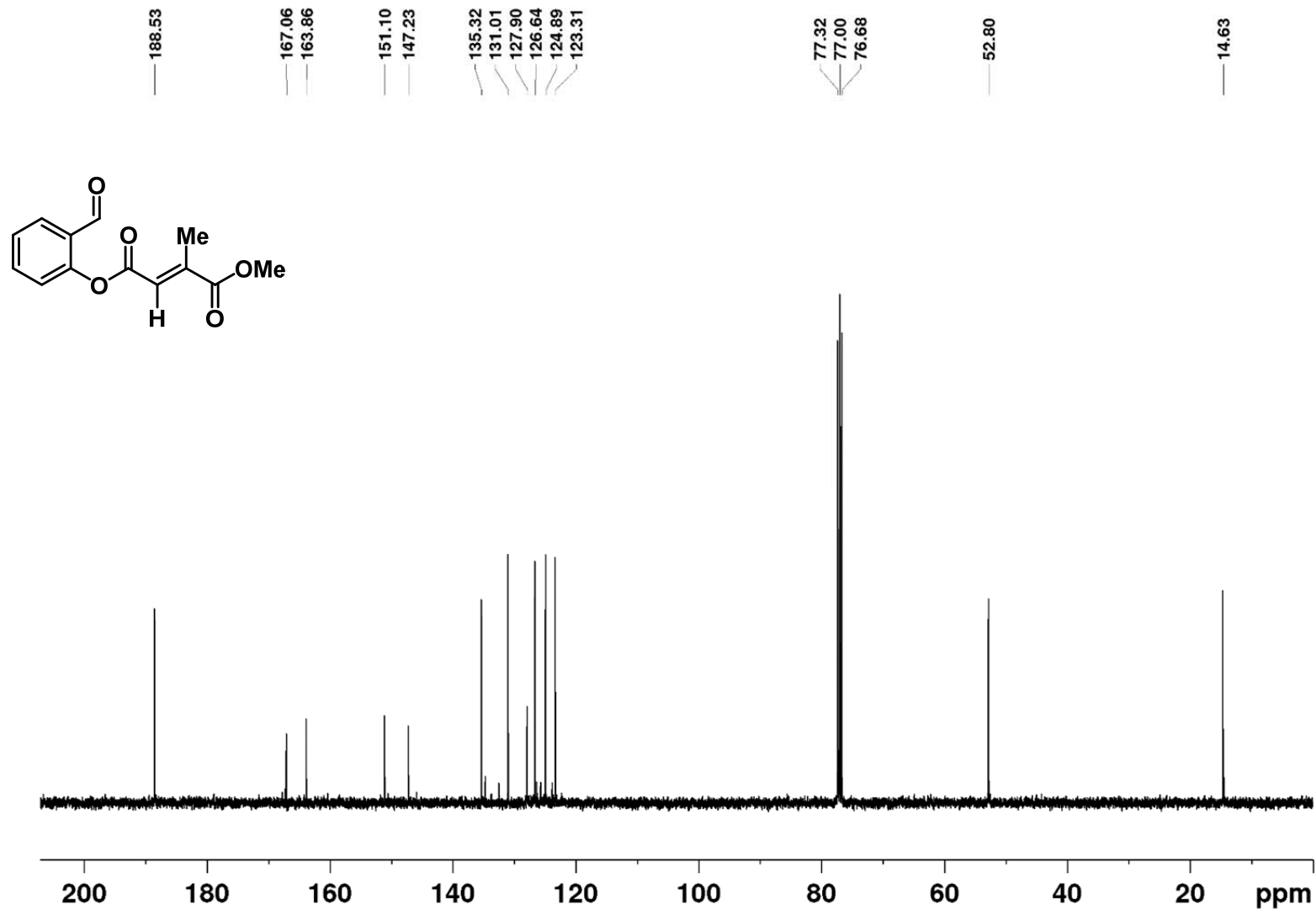
¹³C NMR 1-(2-Formylphenyl) 4-methyl 2-methylfumarate (**11**)



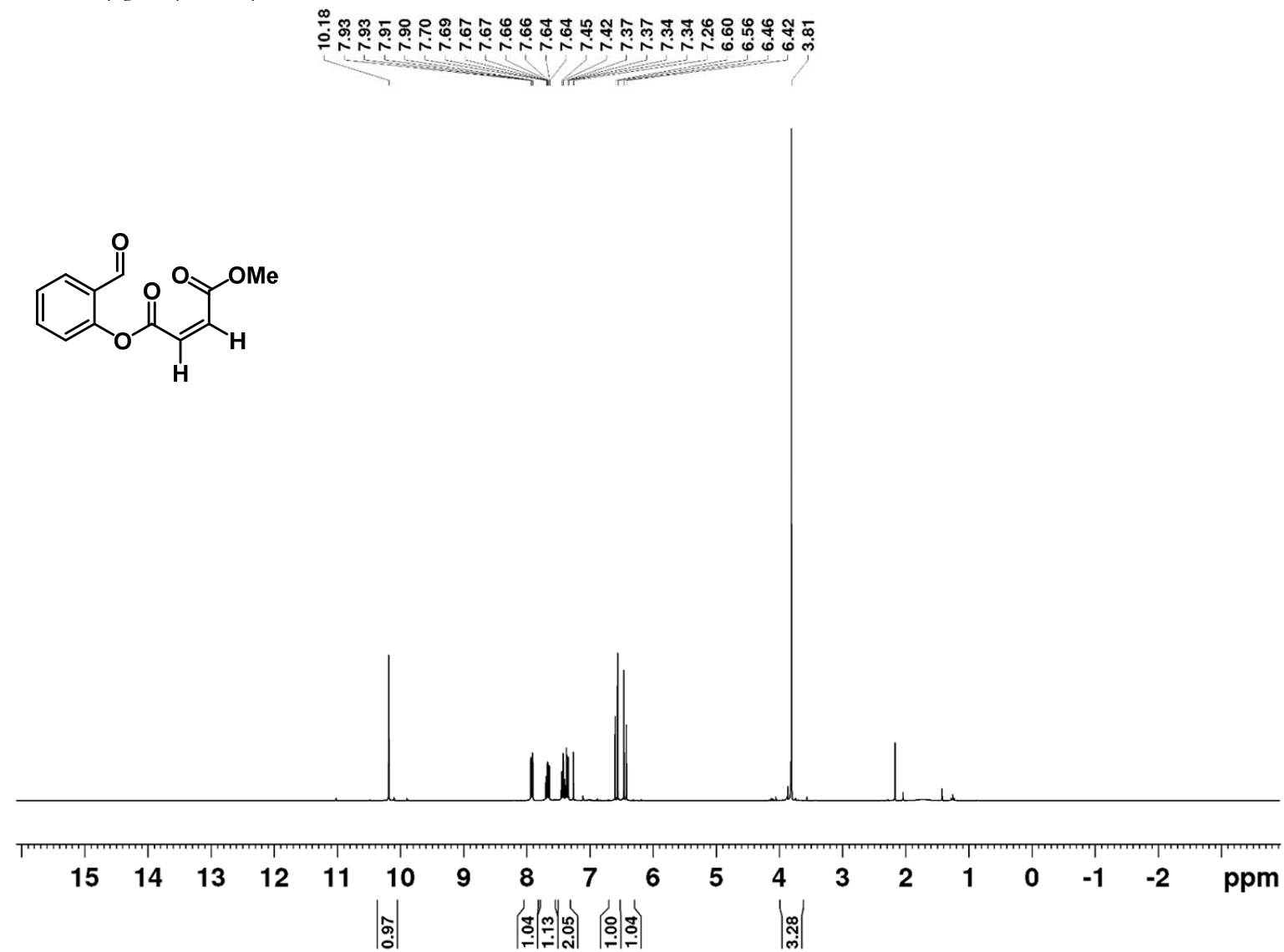
¹H NMR 4-(2-Formylphenyl) 1-methyl 2-methylfumarate (**14**)



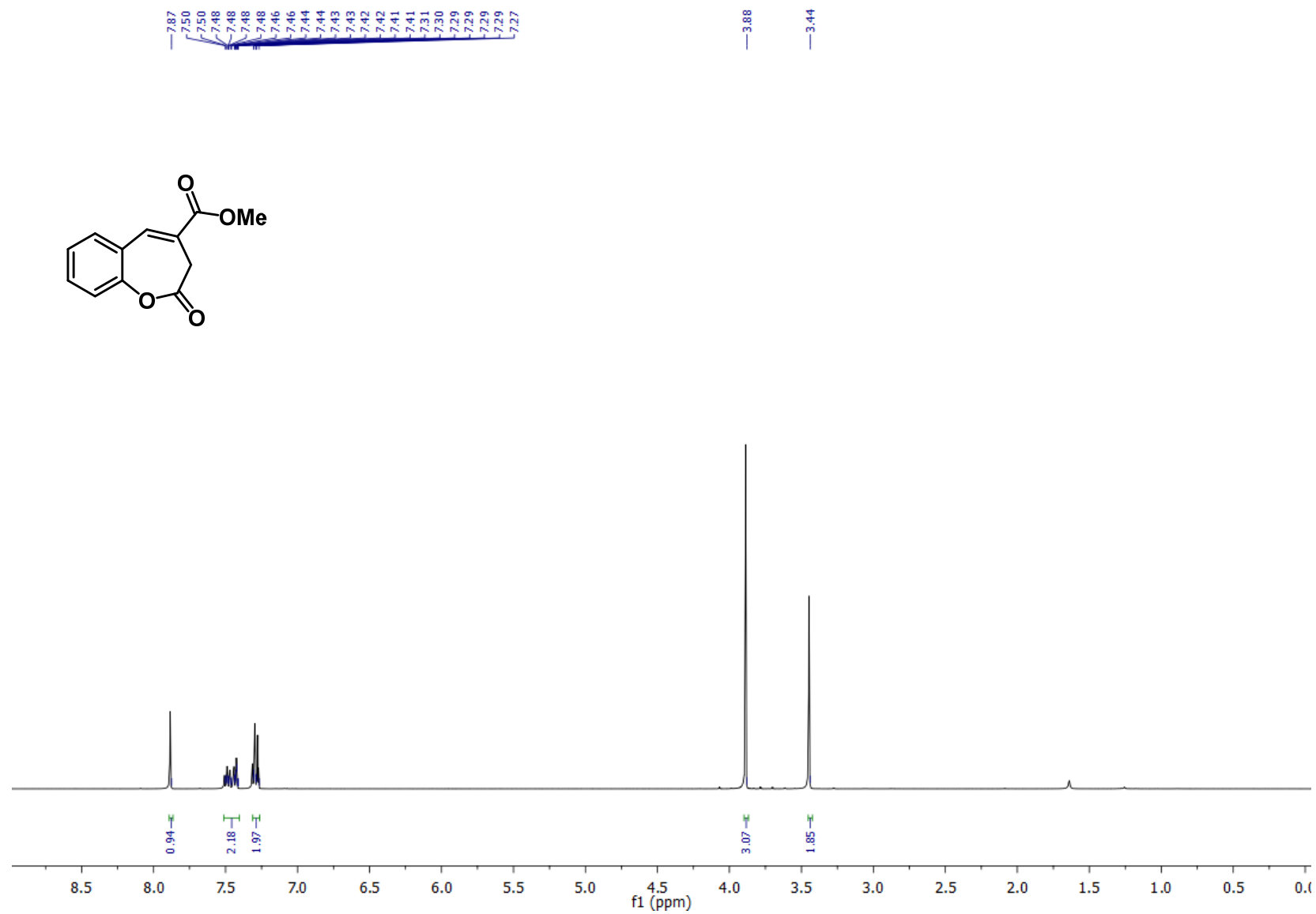
^{13}C NMR 4-(2-Formylphenyl) 1-methyl 2-methylfumarate (**14**)



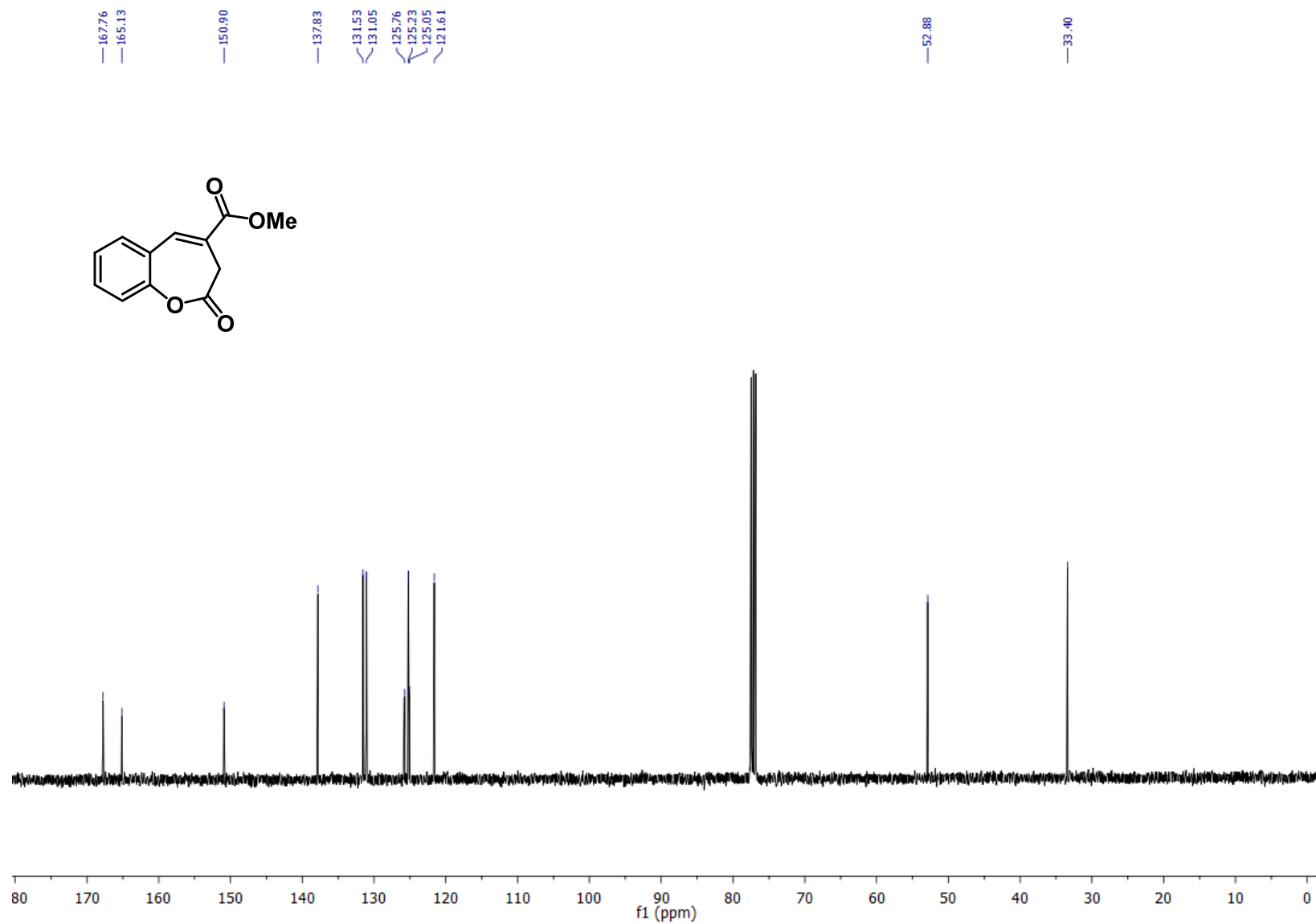
¹H NMR 2-Formylphenyl methyl maleate (**Z-2a**)



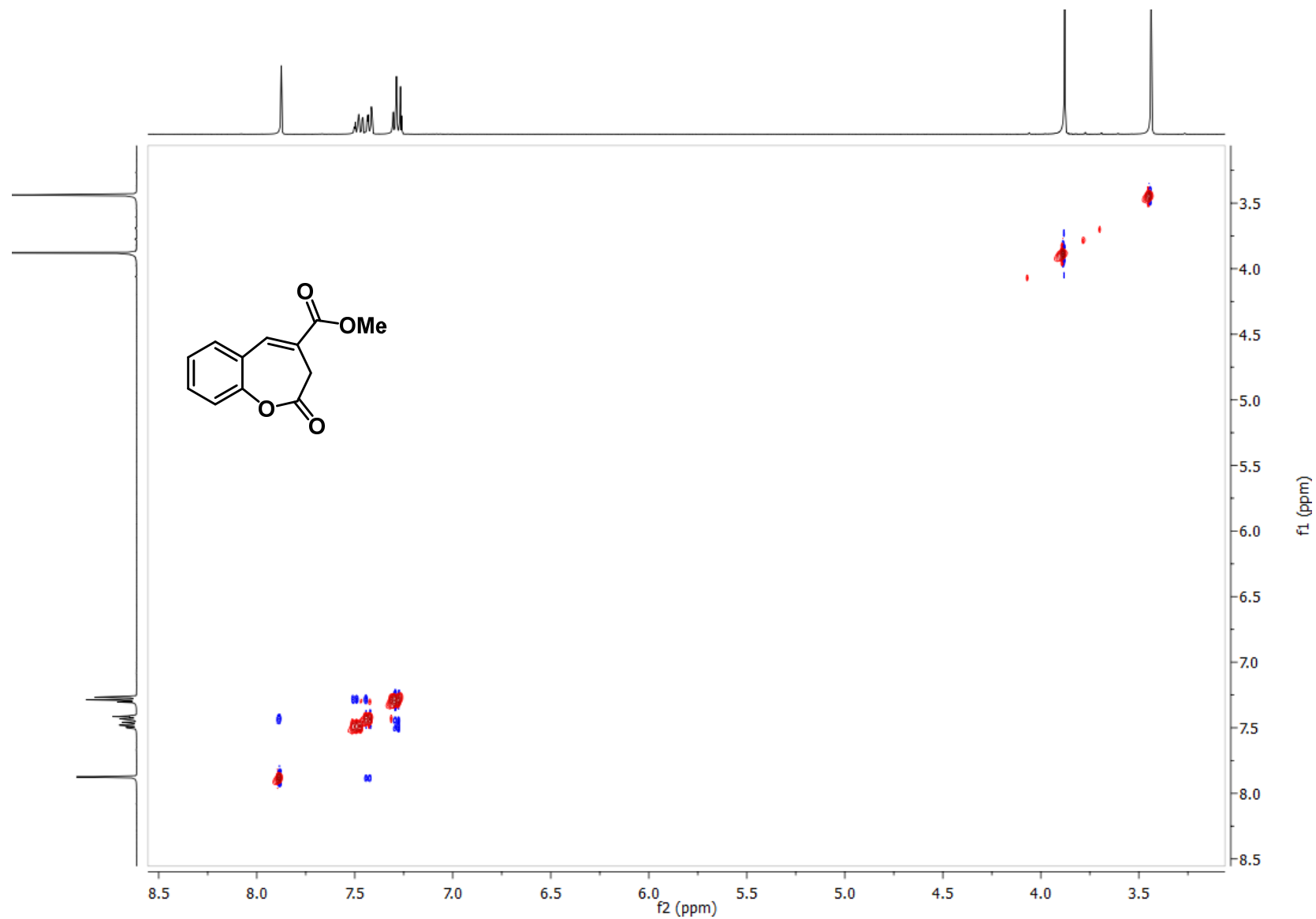
¹H NMR Methyl 2-oxo-2,3-dihydrobenzo[*b*]oxepine-4-carboxylate (**3a**)



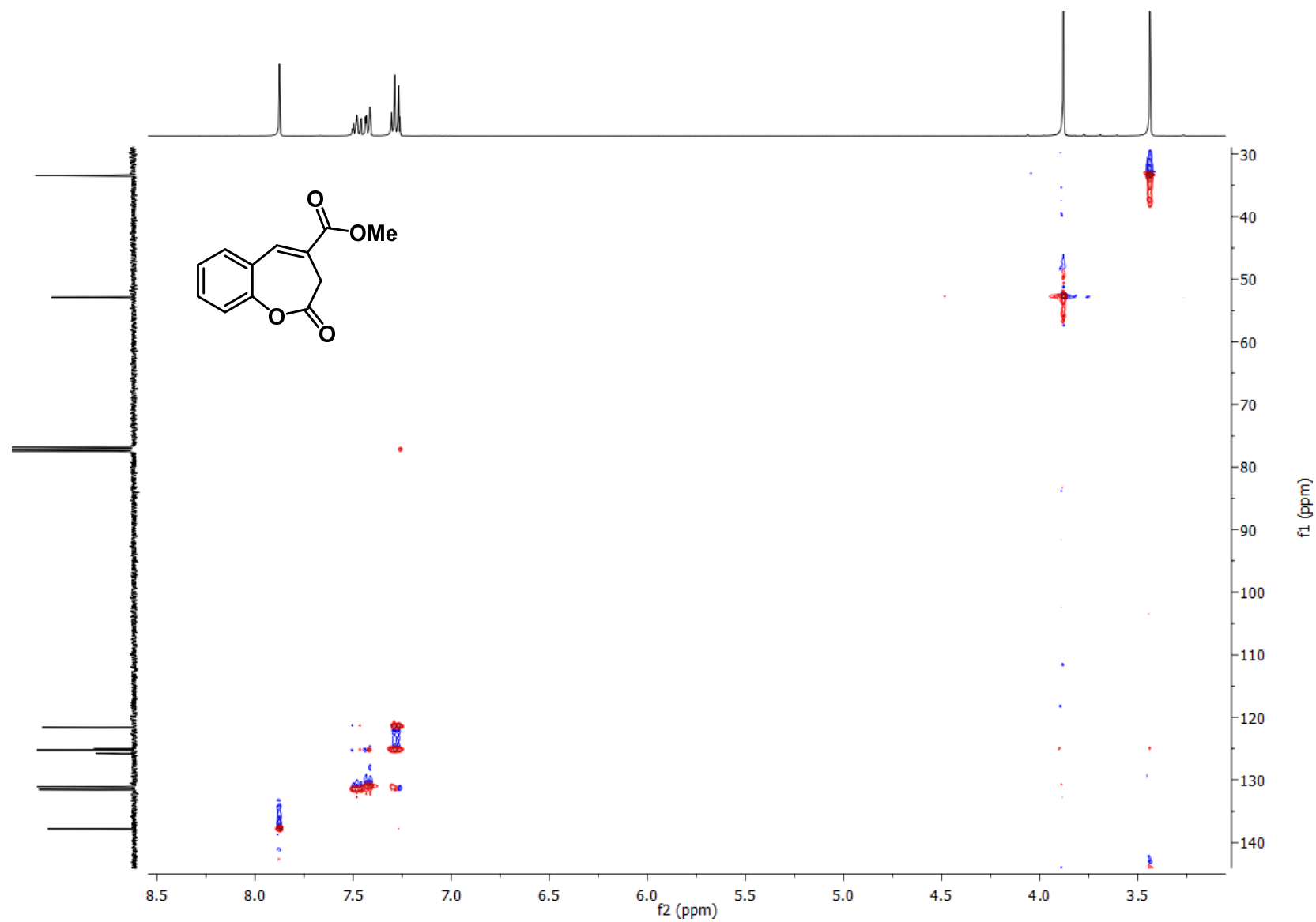
¹³C NMR Methyl 2-oxo-2,3-dihydrobenzo[*b*]oxepine-4-carboxylate (**3a**)



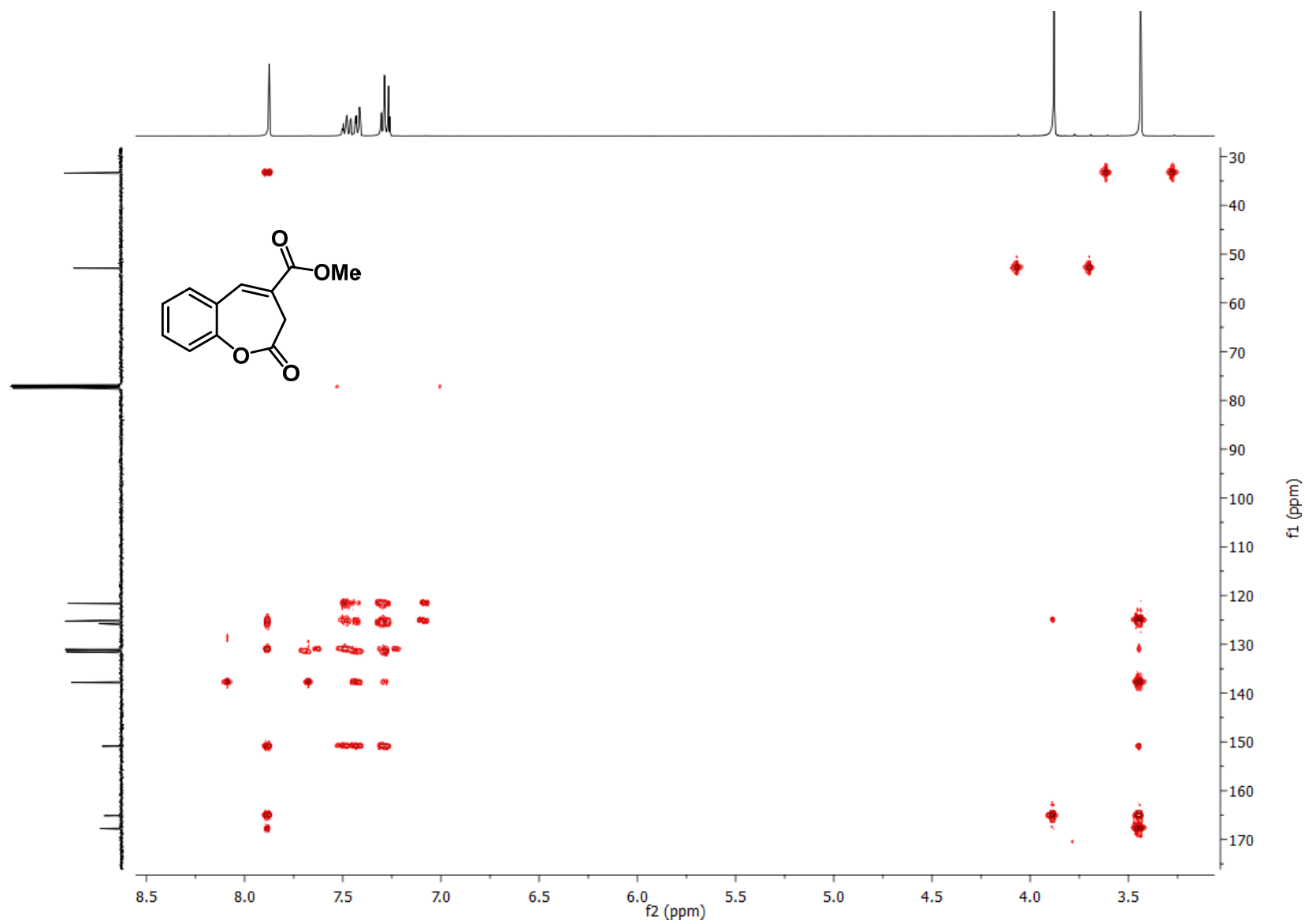
NOESY Methyl 2-oxo-2,3-dihydrobenzo[*b*]oxepine-4-carboxylate (**3a**)



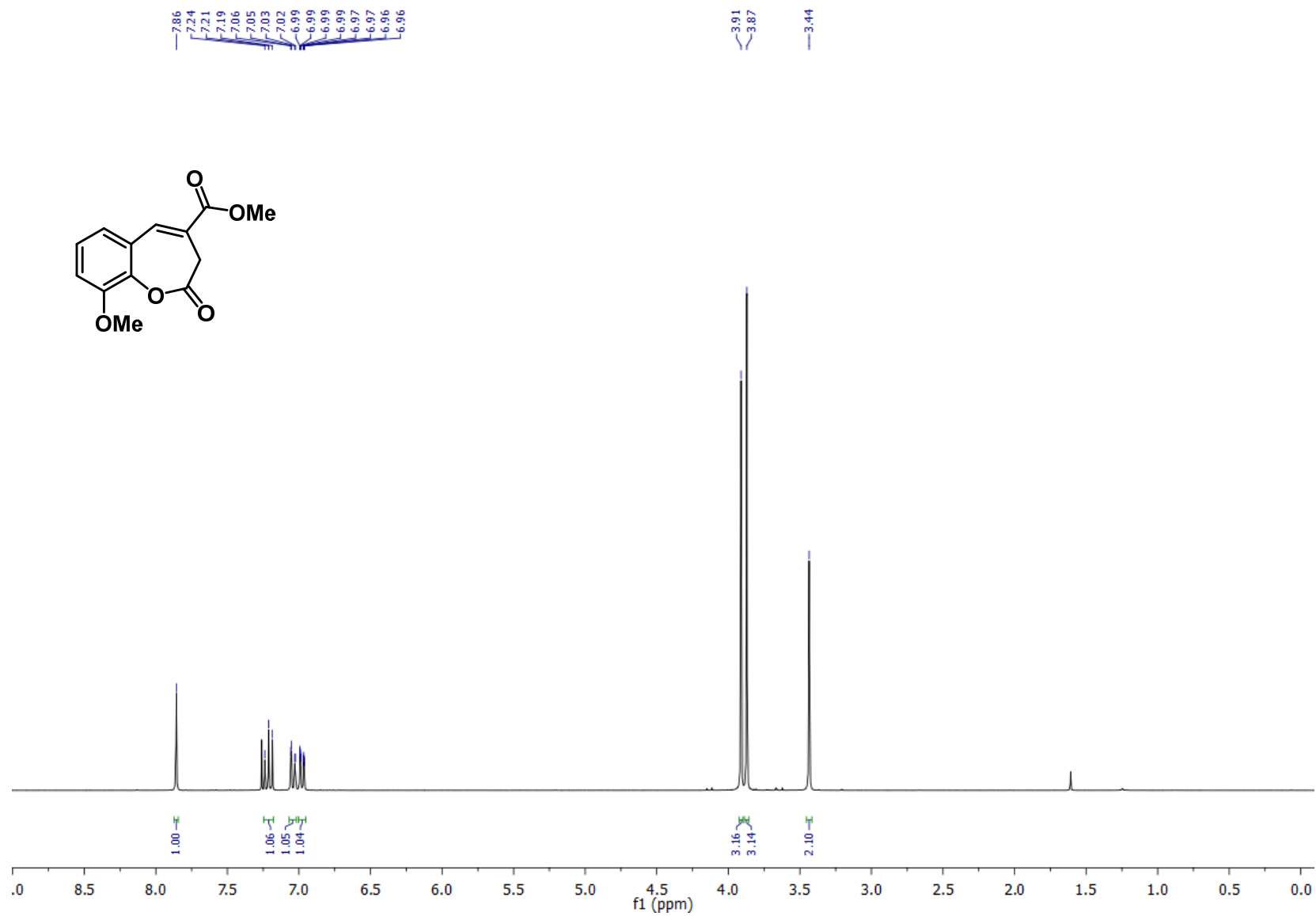
HSQC Methyl 2-oxo-2,3-dihydrobenzo[*b*]oxepine-4-carboxylate (**3a**)



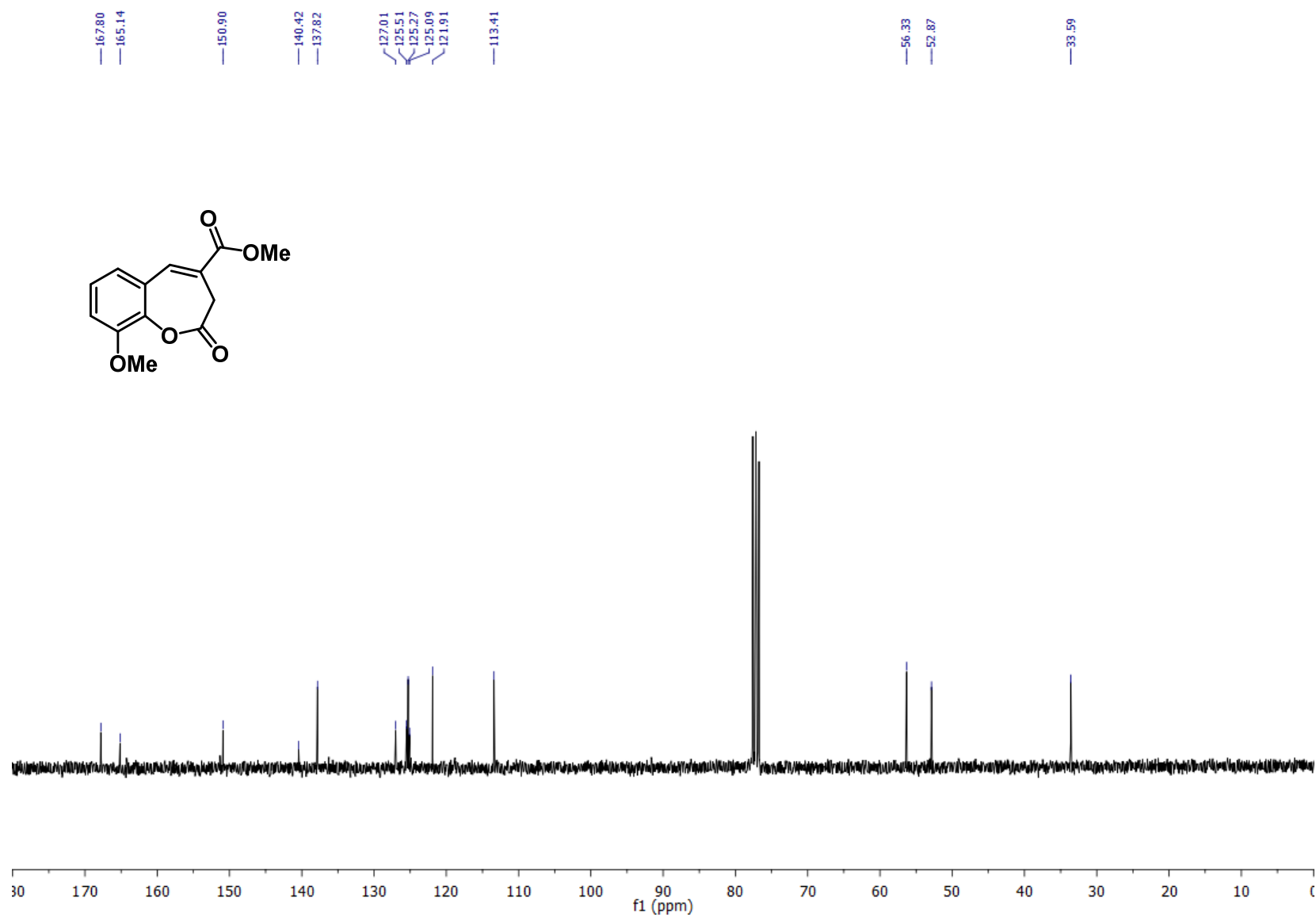
HMBC Methyl 2-oxo-2,3-dihydrobenzo[*b*]oxepine-4-carboxylate (**3a**)



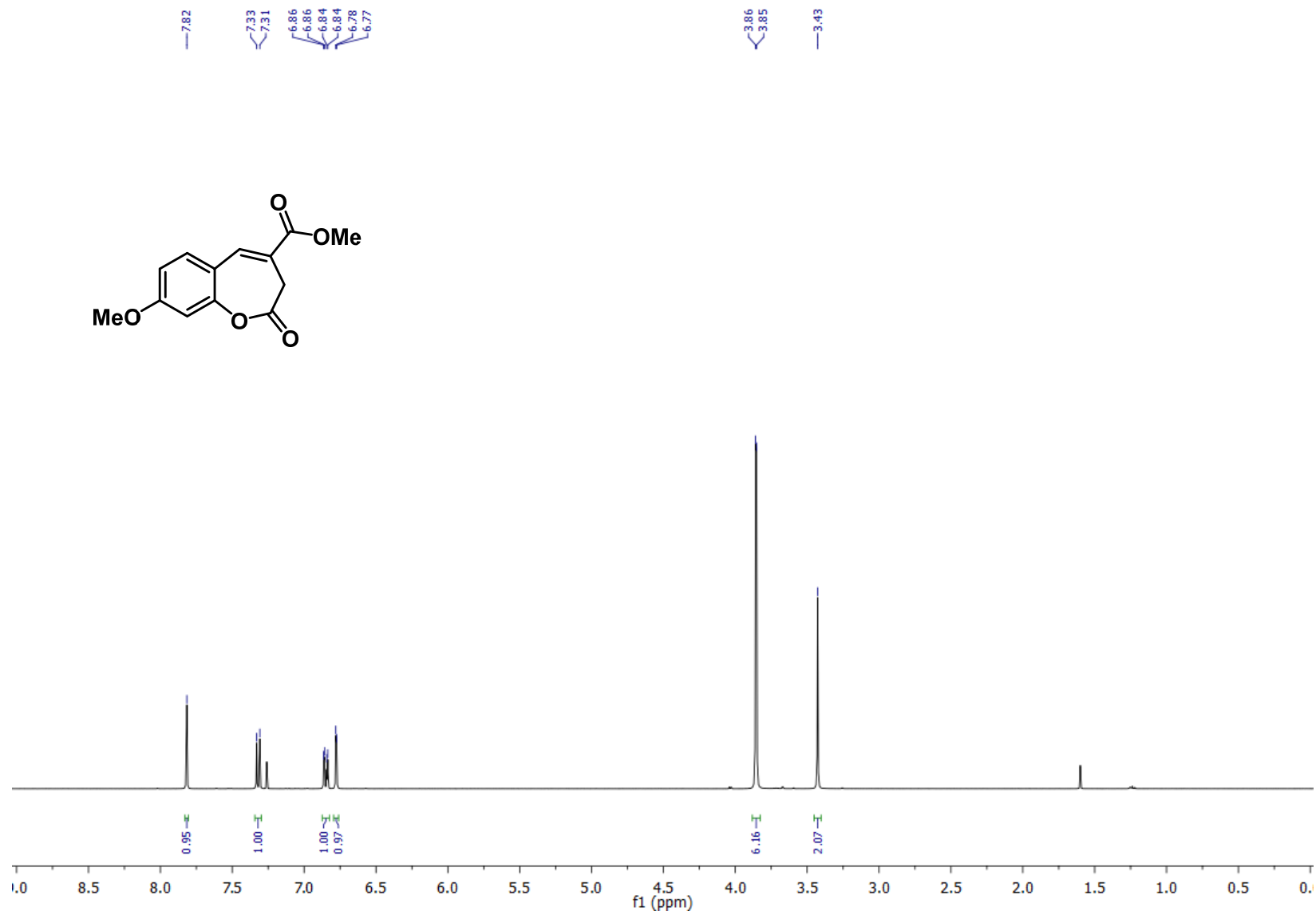
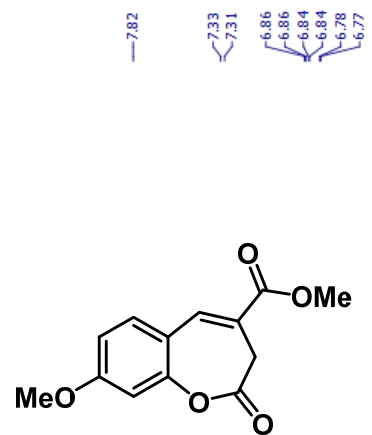
¹H NMR Methyl 9-methoxy-2-oxo-2,3-dihydrobenzo[*b*]oxepine-4-carboxylate (**3b**)



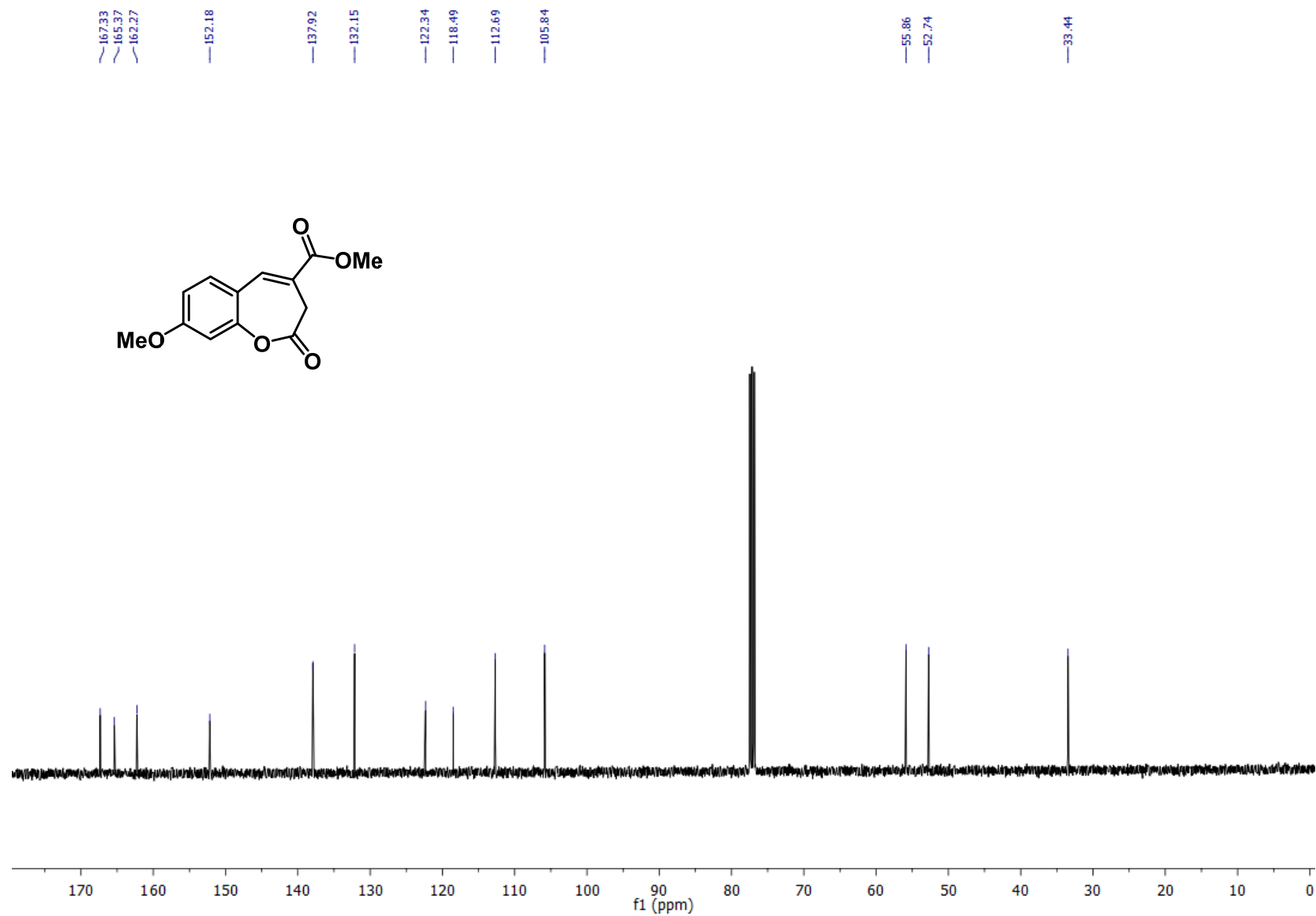
¹³C NMR Methyl 9-methoxy-2-oxo-2,3-dihydrobenzo[*b*]oxepine-4-carboxylate (**3b**)



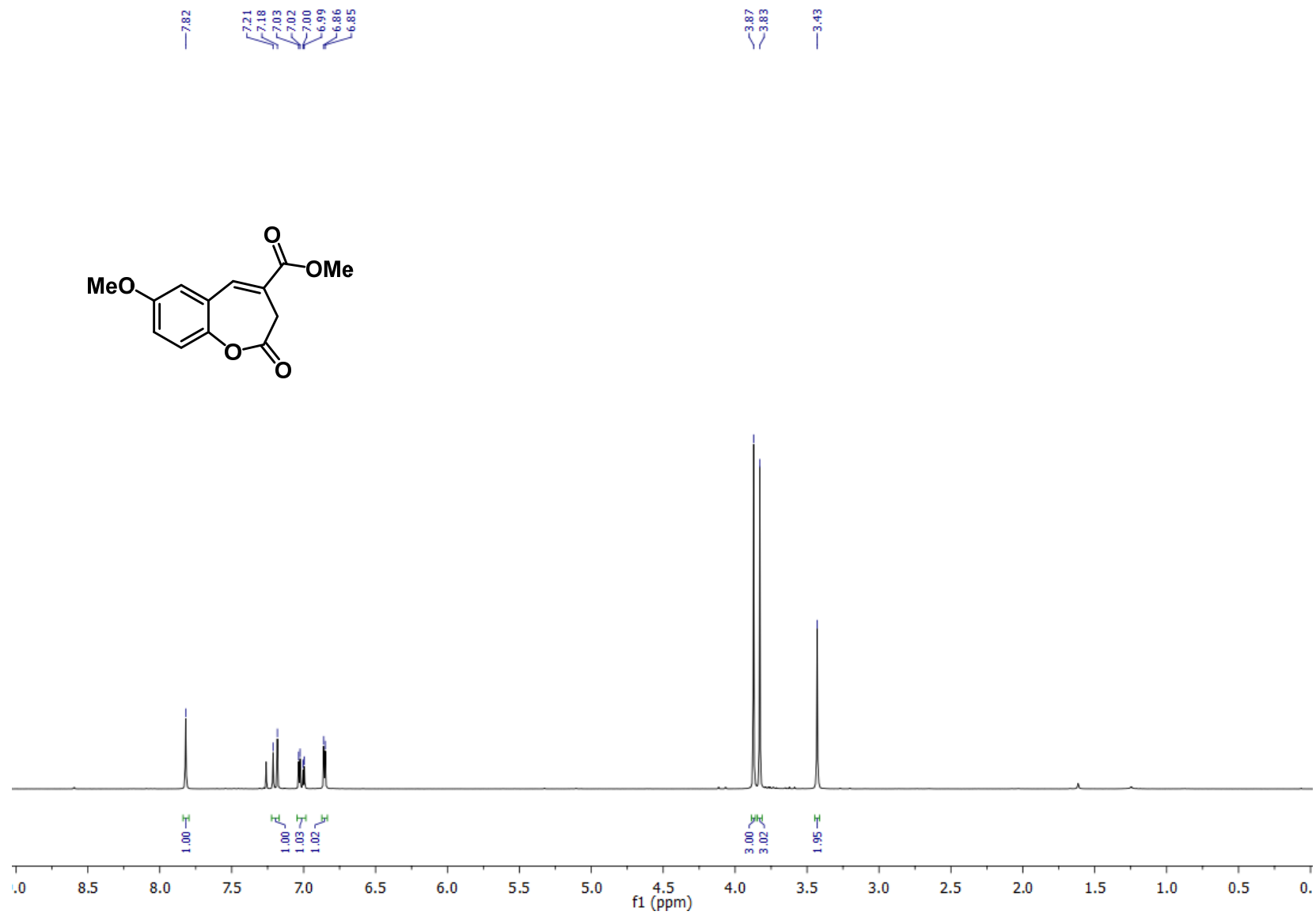
¹H NMR Methyl 8-methoxy-2-oxo-2,3-dihydrobenzo[*b*]oxepine-4-carboxylate (**3d**)



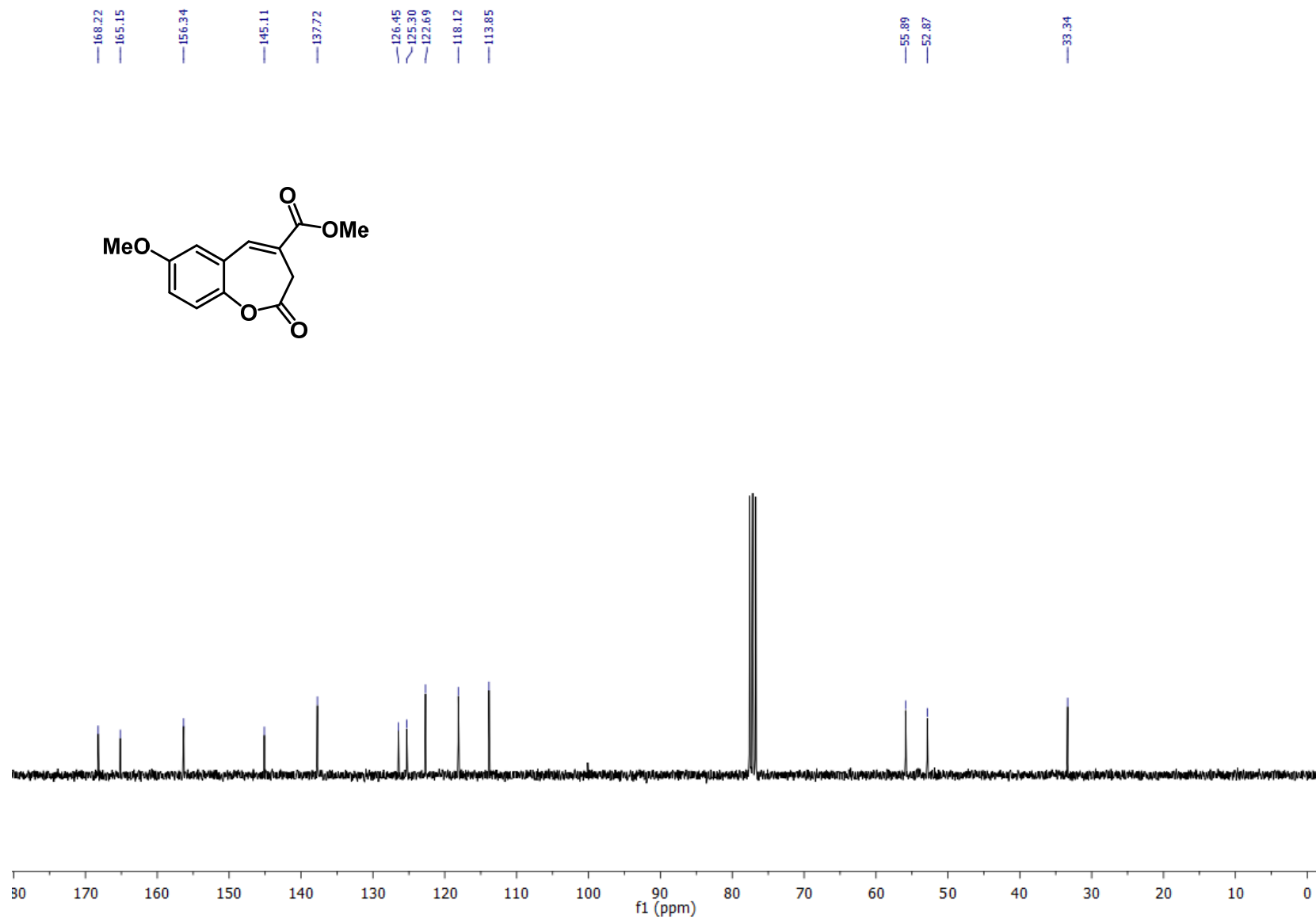
¹³C NMR Methyl 8-methoxy-2-oxo-2,3-dihydrobenzo[*b*]oxepine-4-carboxylate (**3d**)



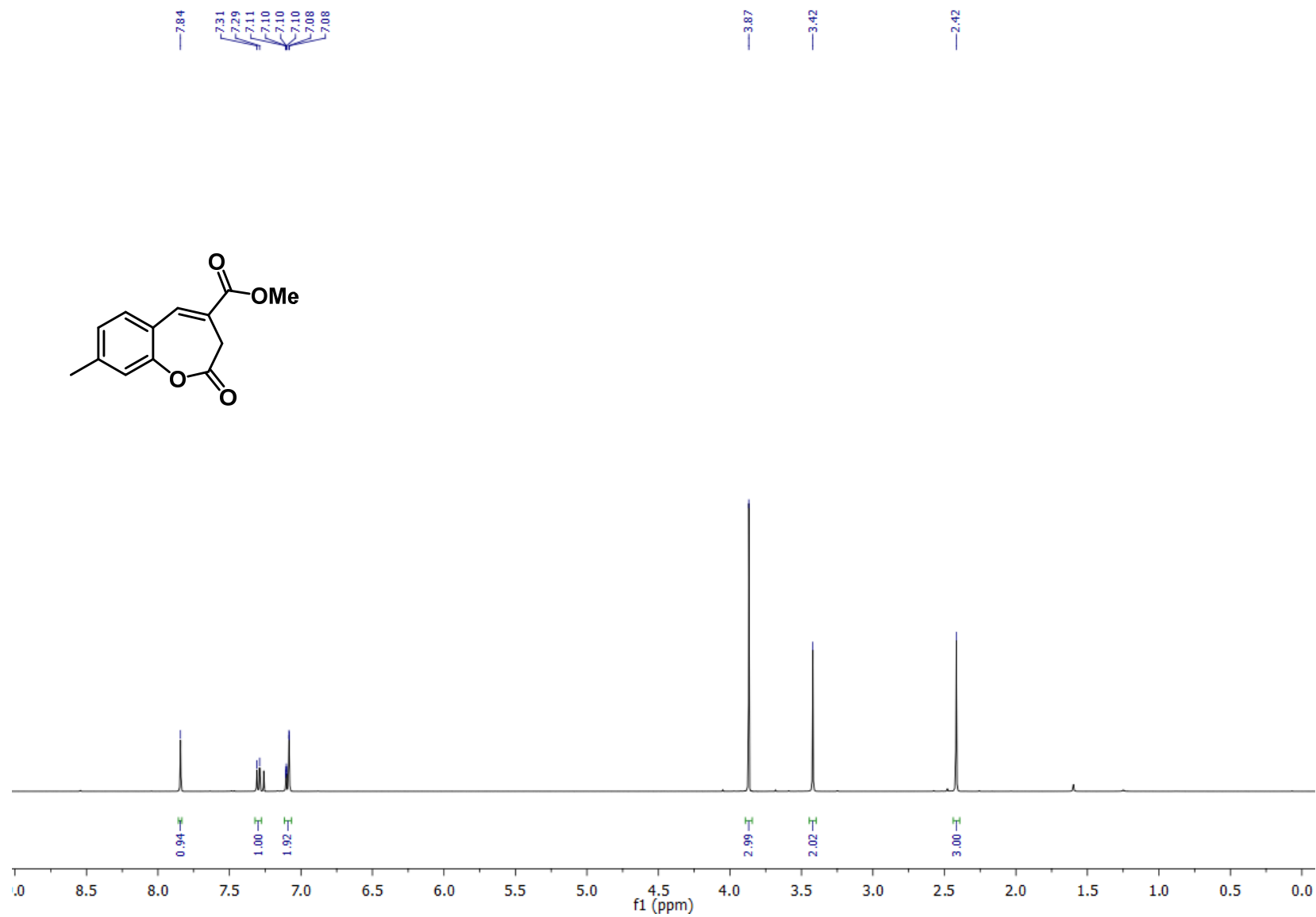
¹H NMR Methyl 7-methoxy-2-oxo-2,3-dihydrobenzo[*b*]oxepine-4-carboxylate (**3e**)



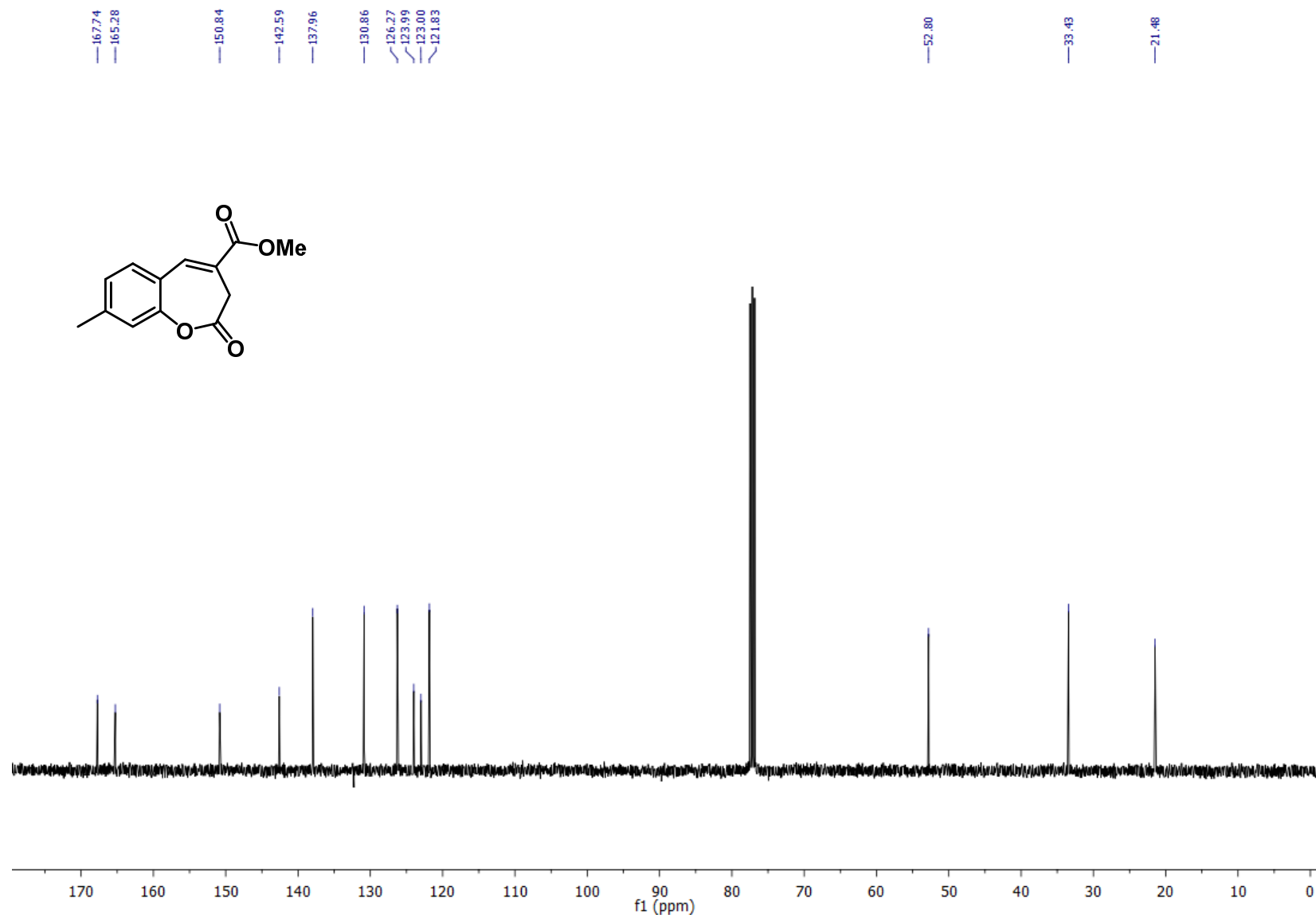
¹³C NMR Methyl 7-methoxy-2-oxo-2,3-dihydrobenzo[*b*]oxepine-4-carboxylate (**3e**)



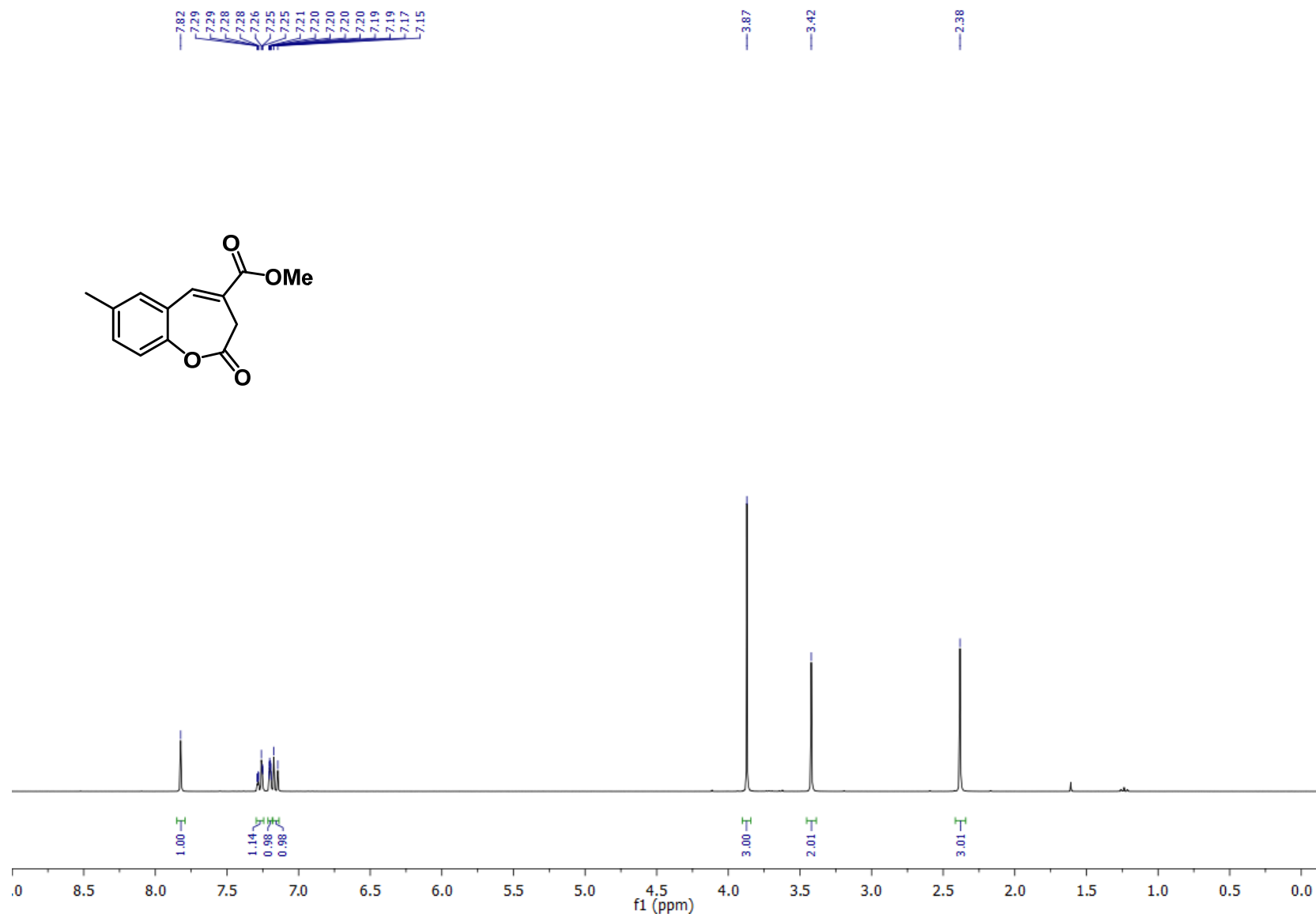
¹H NMR Methyl 8-methyl-2-oxo-2,3-dihydrobenzo[*b*]oxepine-4-carboxylate (**3f**)



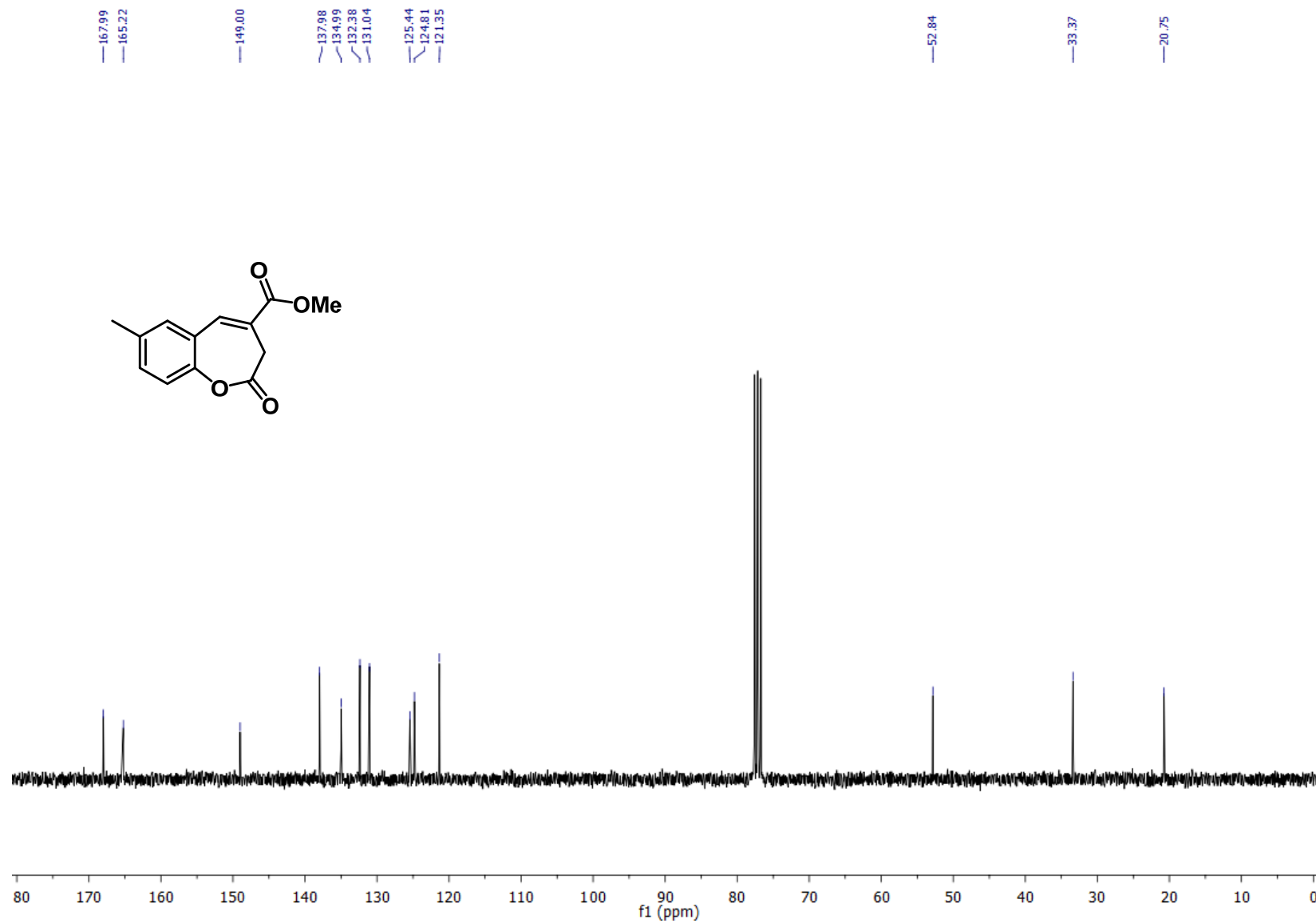
¹³C NMR Methyl 8-methyl-2-oxo-2,3-dihydrobenzo[*b*]oxepine-4-carboxylate (**3f**)



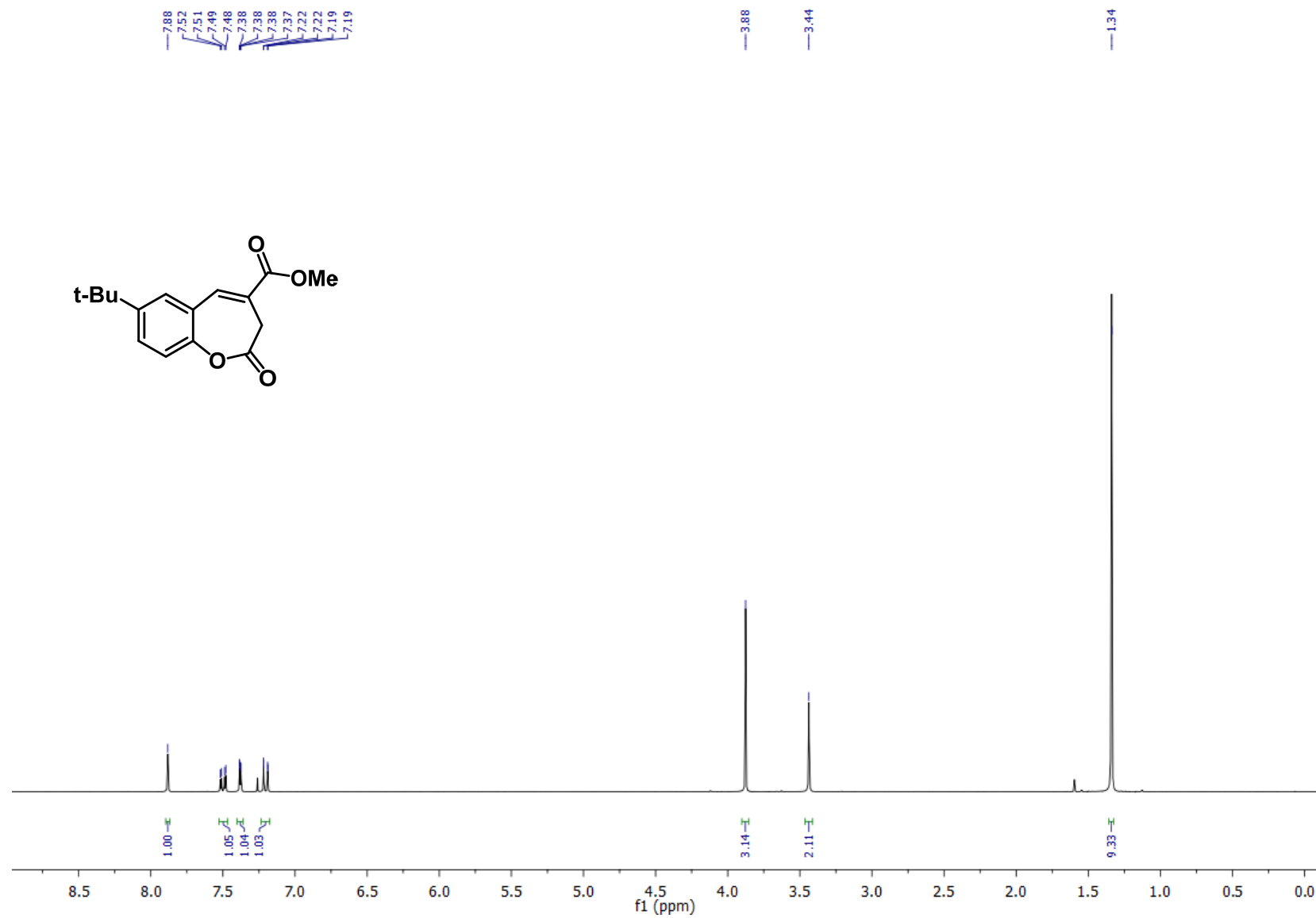
¹H NMR Methyl 7-methyl-2-oxo-2,3-dihydrobenzo[*b*]oxepine-4-carboxylate (**3g**)



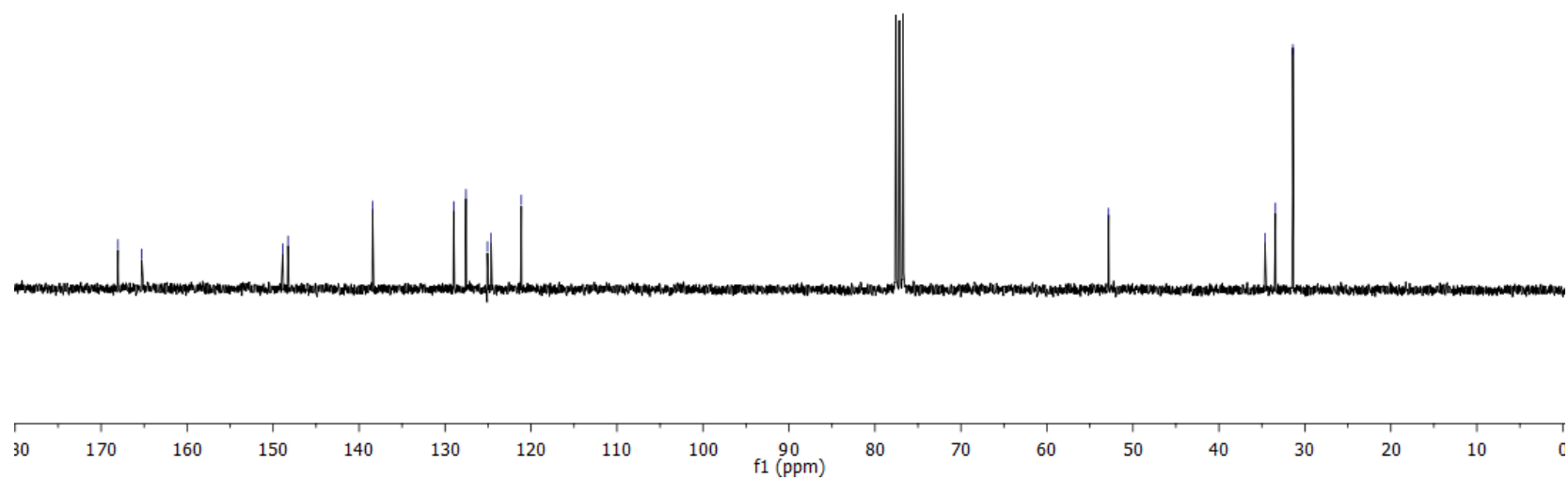
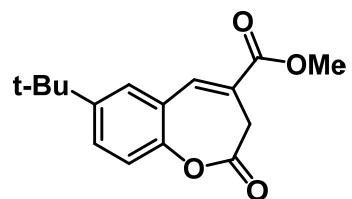
¹³C NMR Methyl 7-methyl-2-oxo-2,3-dihydrobenzo[*b*]oxepine-4-carboxylate (**3g**)



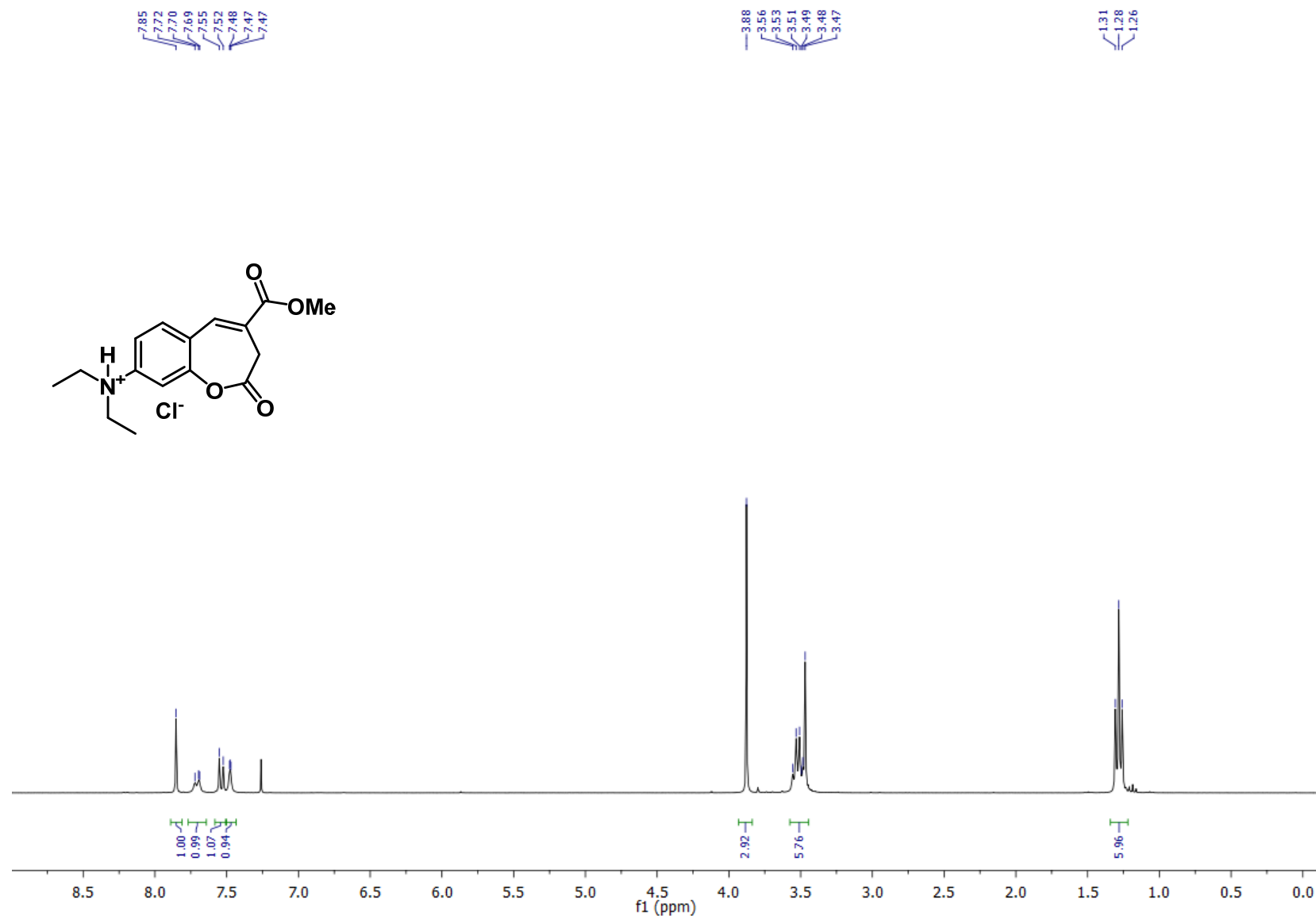
¹H NMR Methyl 7-(*tert*-butyl)-2-oxo-2,3-dihydrobenzo[*b*]oxepine-4-carboxylate (**3h**)



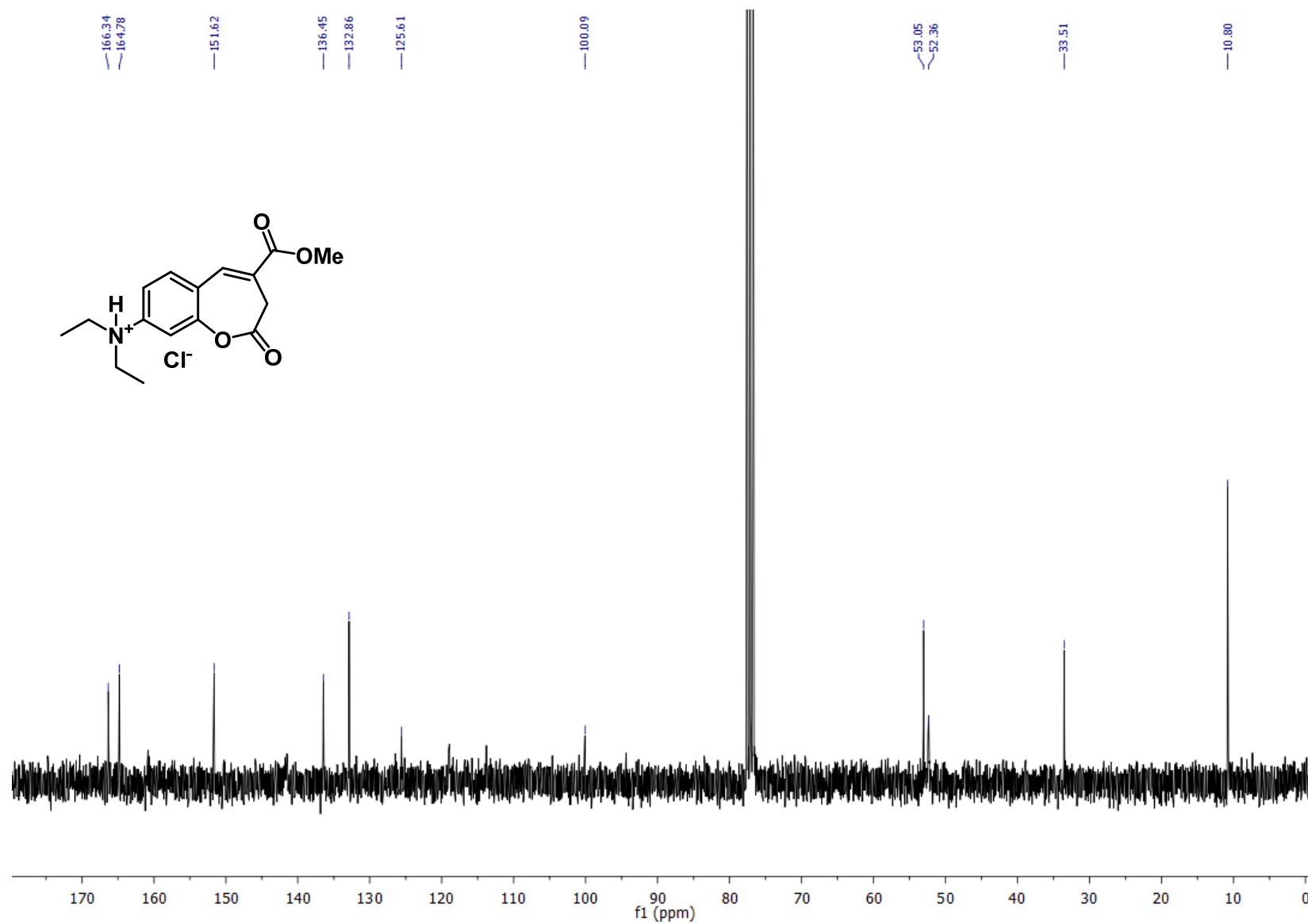
¹³C NMR Methyl 7-(tert-butyl)-2-oxo-2,3-dihydrobenzo[*b*]oxepine-4-carboxylate (**3h**)



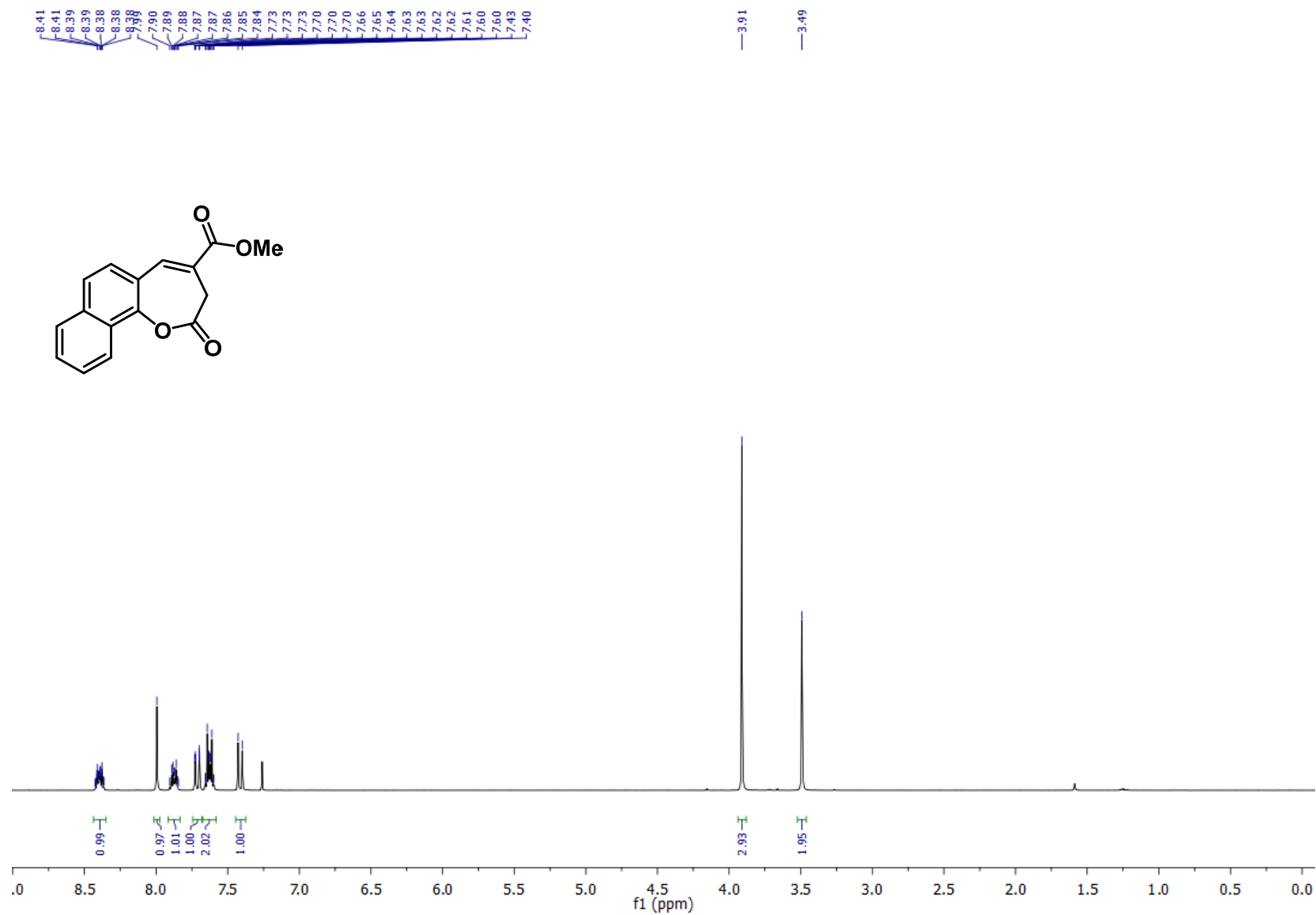
^1H NMR N,N-Diethyl-4-(methoxycarbonyl)-2-oxo-2,3-dihydrobenzo[*b*]oxepin-8-aminium chloride (**3i**)



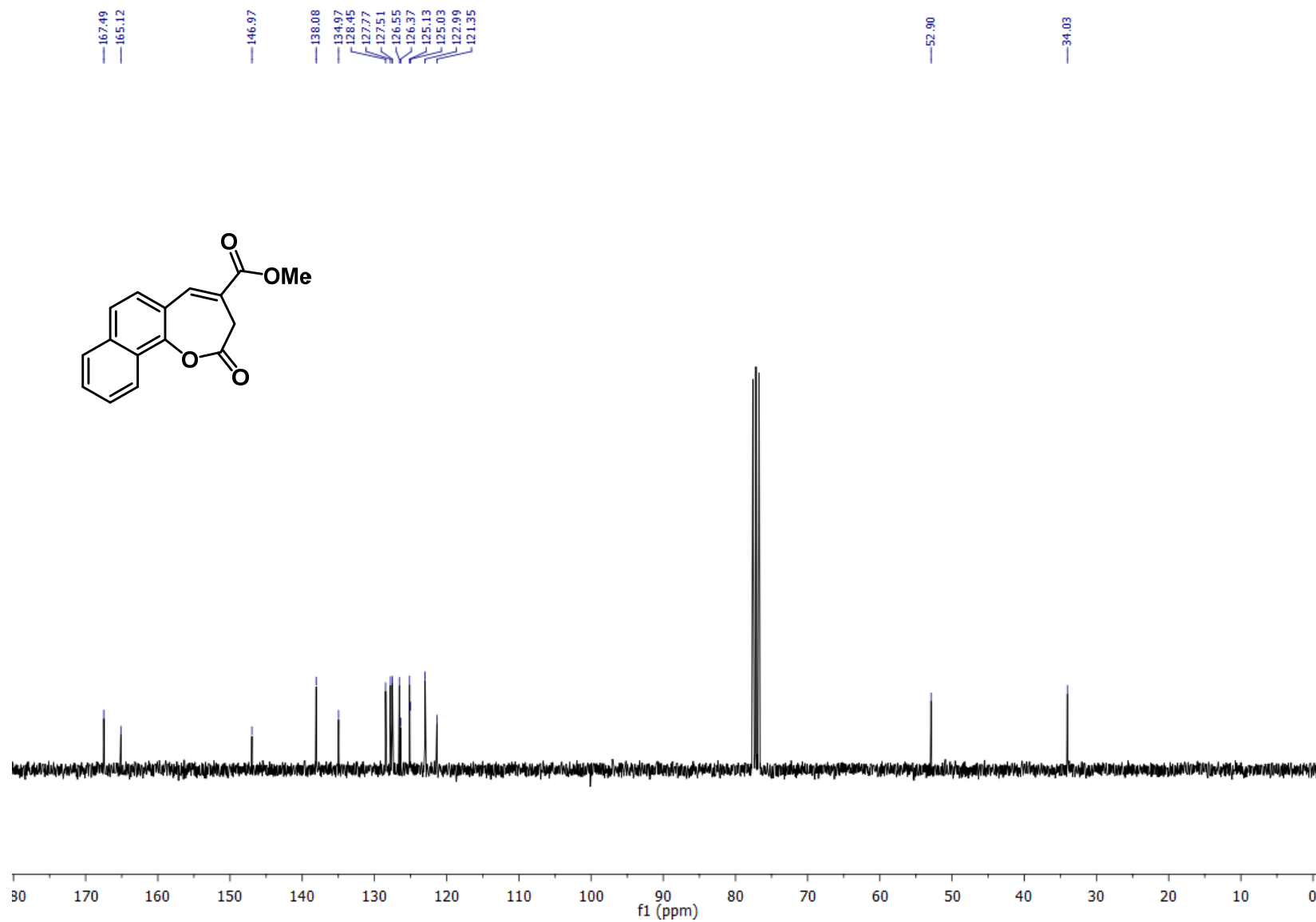
^{13}C NMR *N,N*-Diethyl-4-(methoxycarbonyl)-2-oxo-2,3-dihydrobenzo[*b*]oxepin-8-aminium chloride (**3i**).



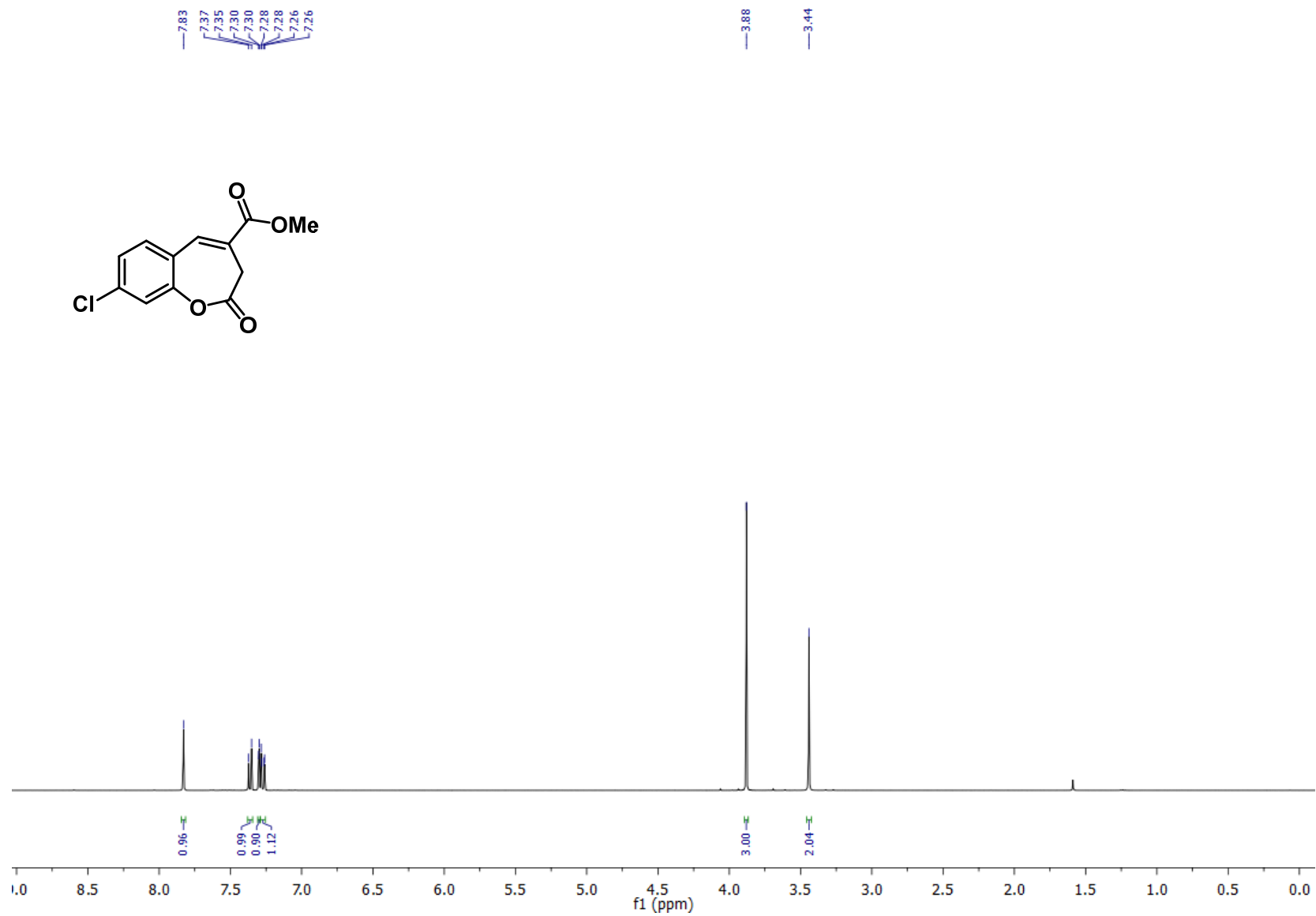
¹H NMR Methyl 2-oxo-2,3-dihydro[1,2-*b*]oxepine-4-carboxylate (**3j**)



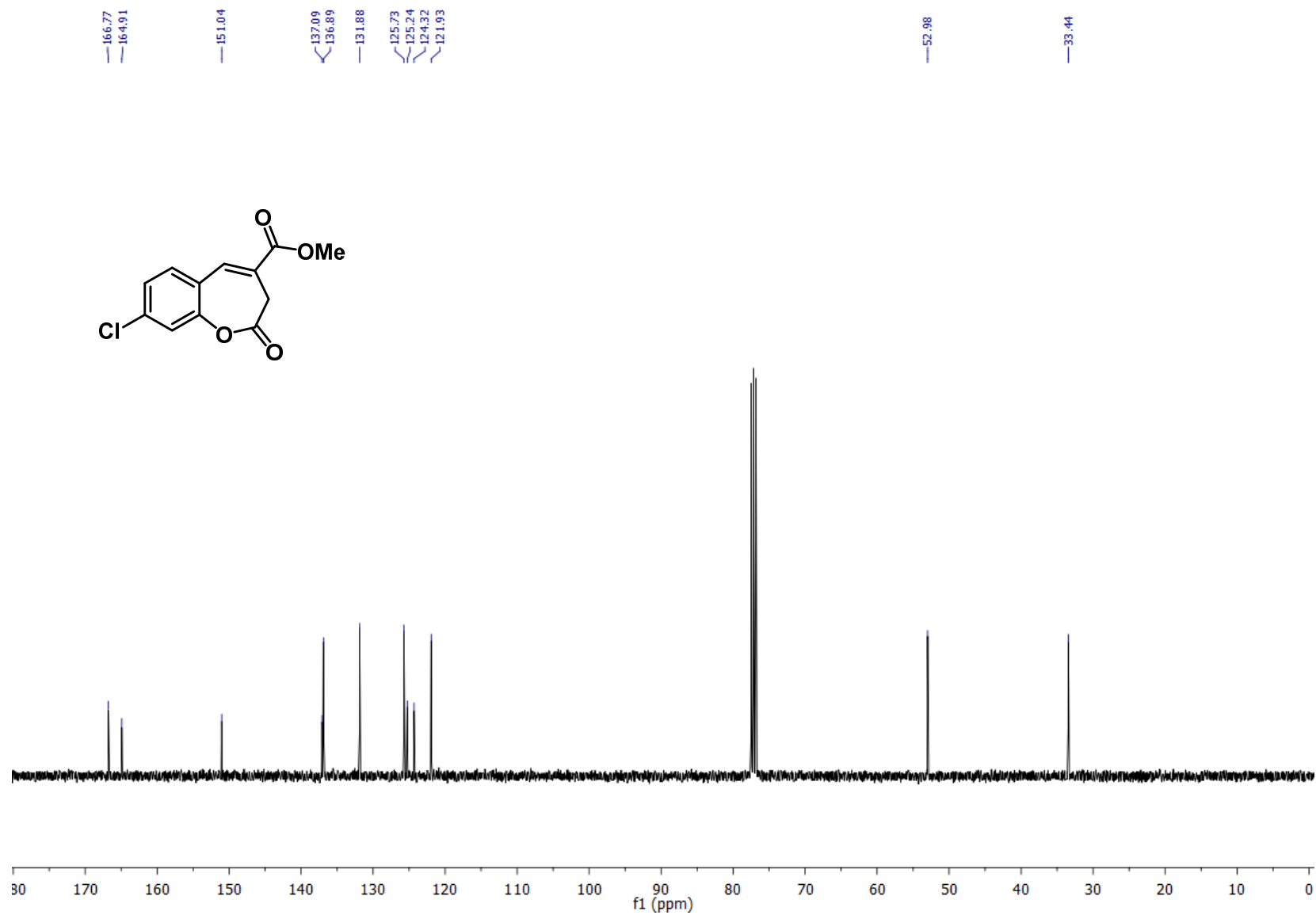
^{13}C NMR Methyl 2-oxo-2,3-dihydronaphtho[1,2-*b*]oxepine-4-carboxylate (**3j**).



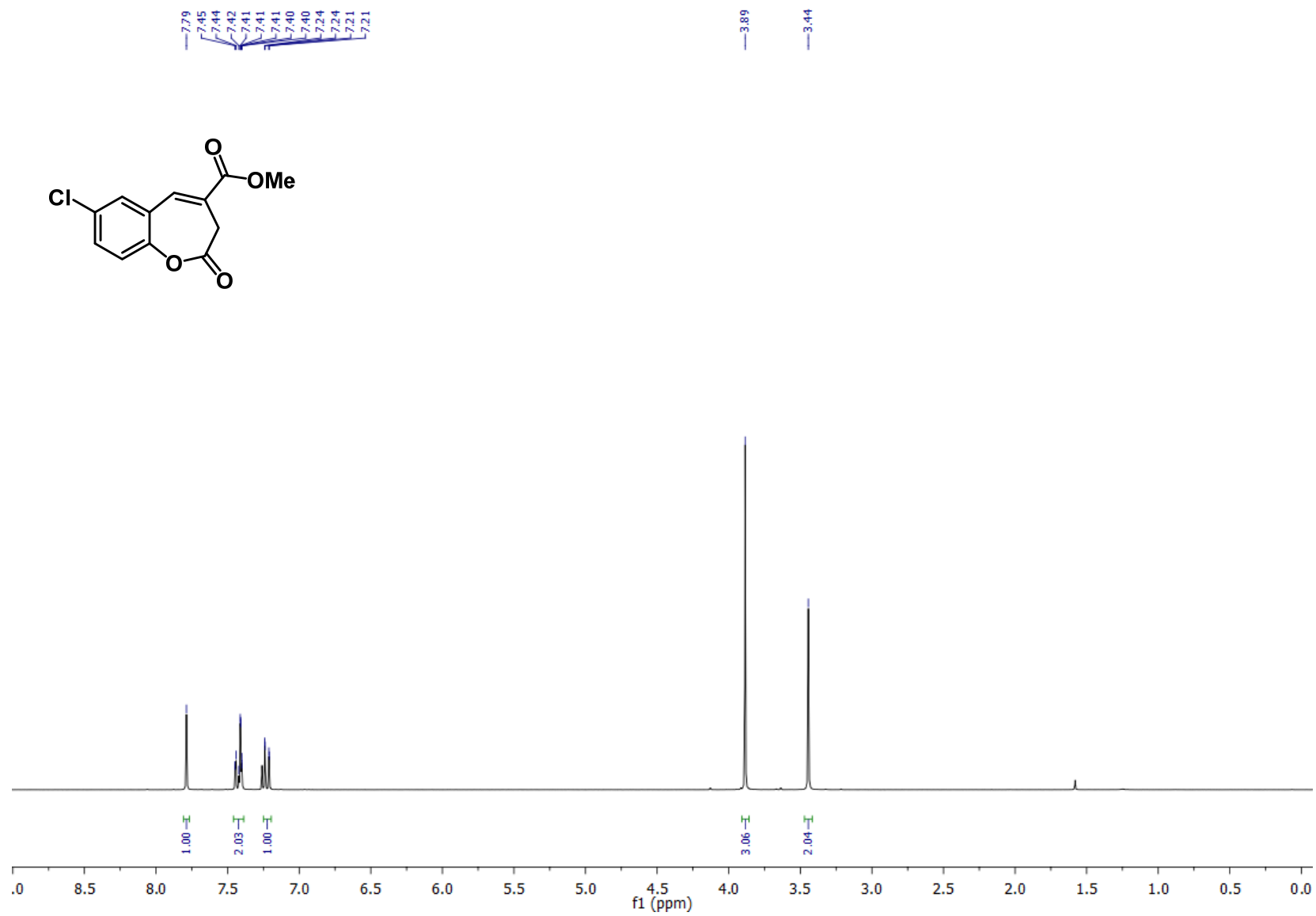
^1H NMR Methyl 8-chloro-2-oxo-2,3-dihydrobenzo[*b*]oxepine-4-carboxylate (**3k**).



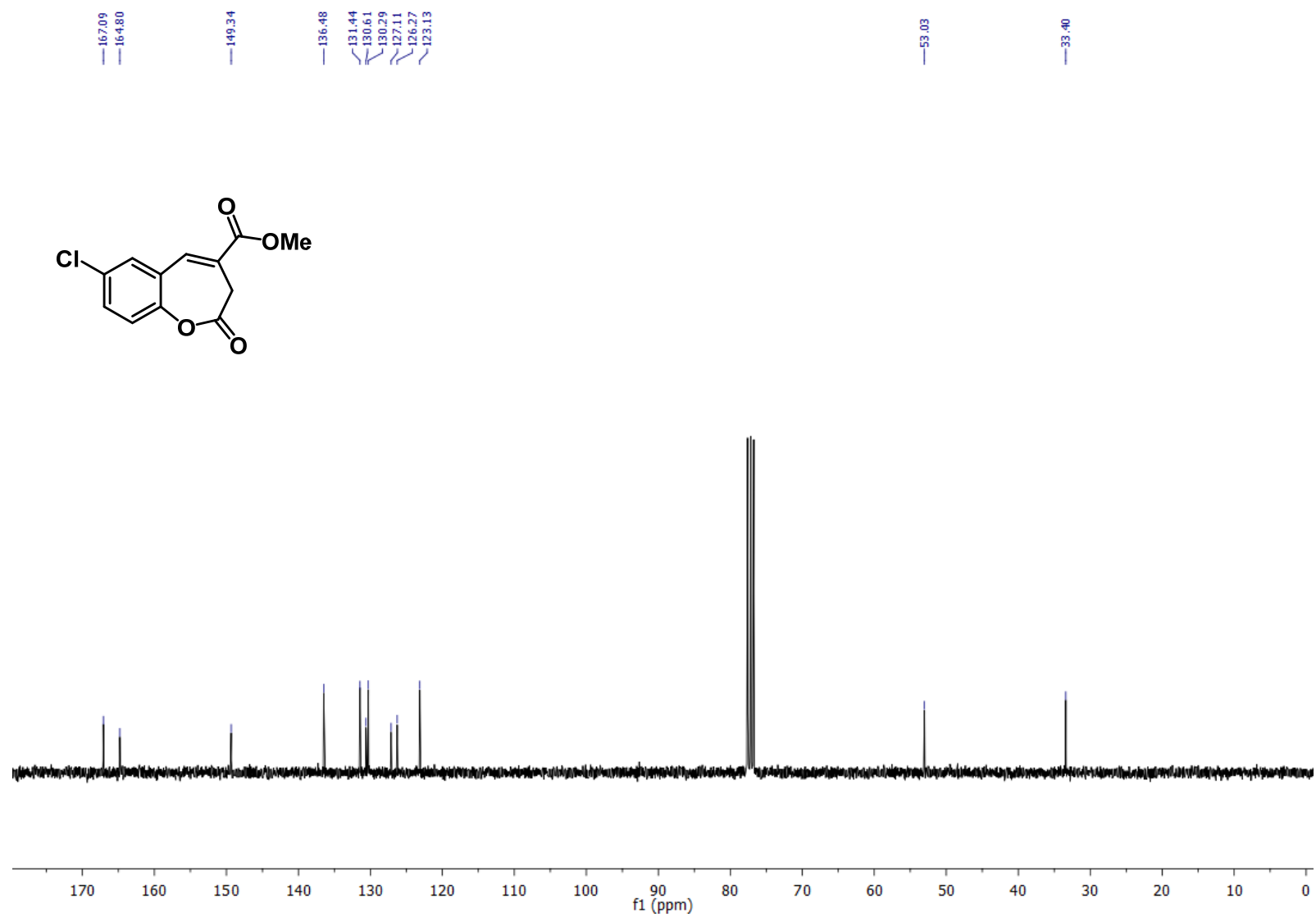
^{13}C NMR Methyl 8-chloro-2-oxo-2,3-dihydrobenzo[*b*]oxepine-4-carboxylate (**3k**).



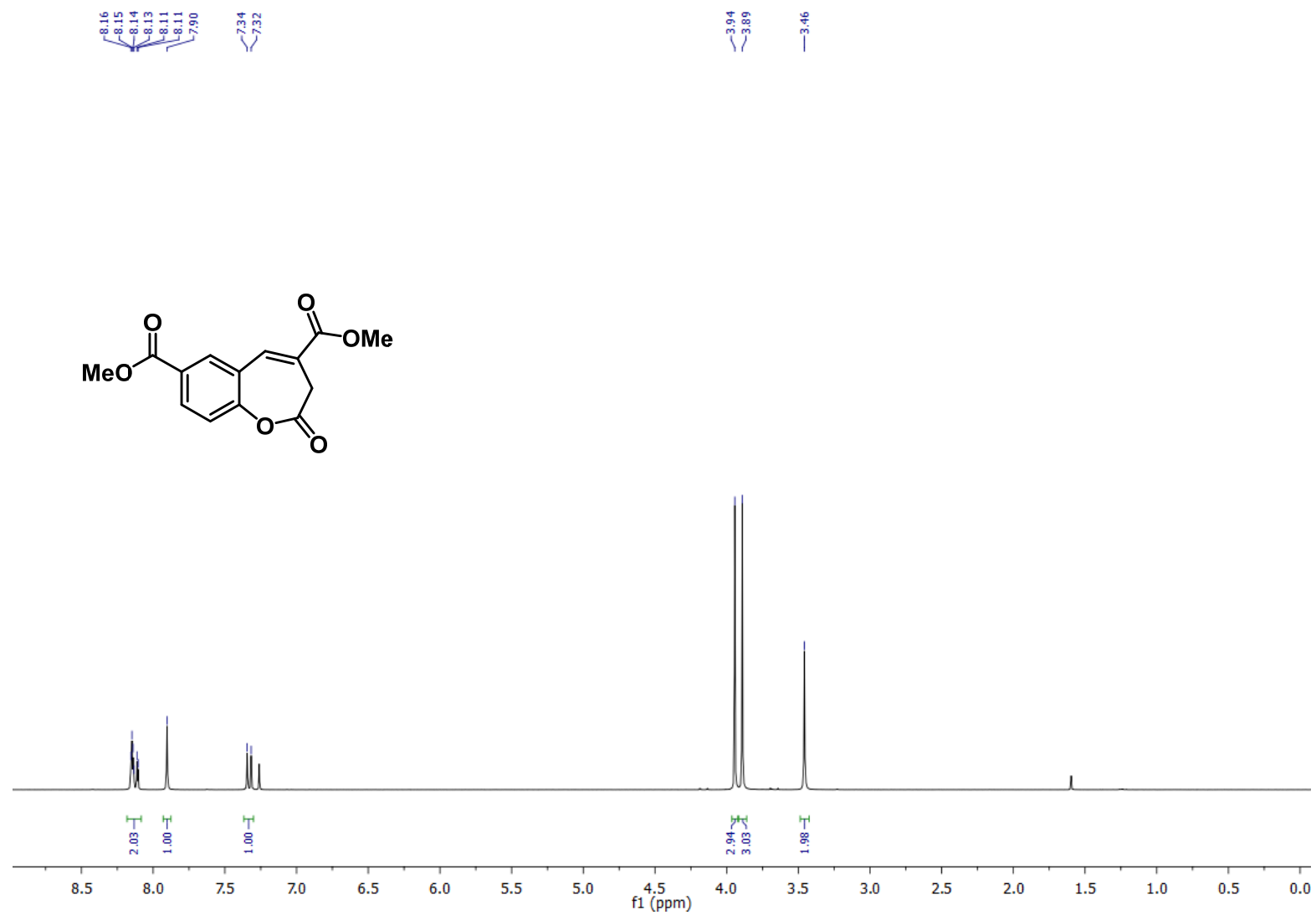
^1H NMR Methyl 7-chloro-2-oxo-2,3-dihydrobenzo[*b*]oxepine-4-carboxylate (**31**).



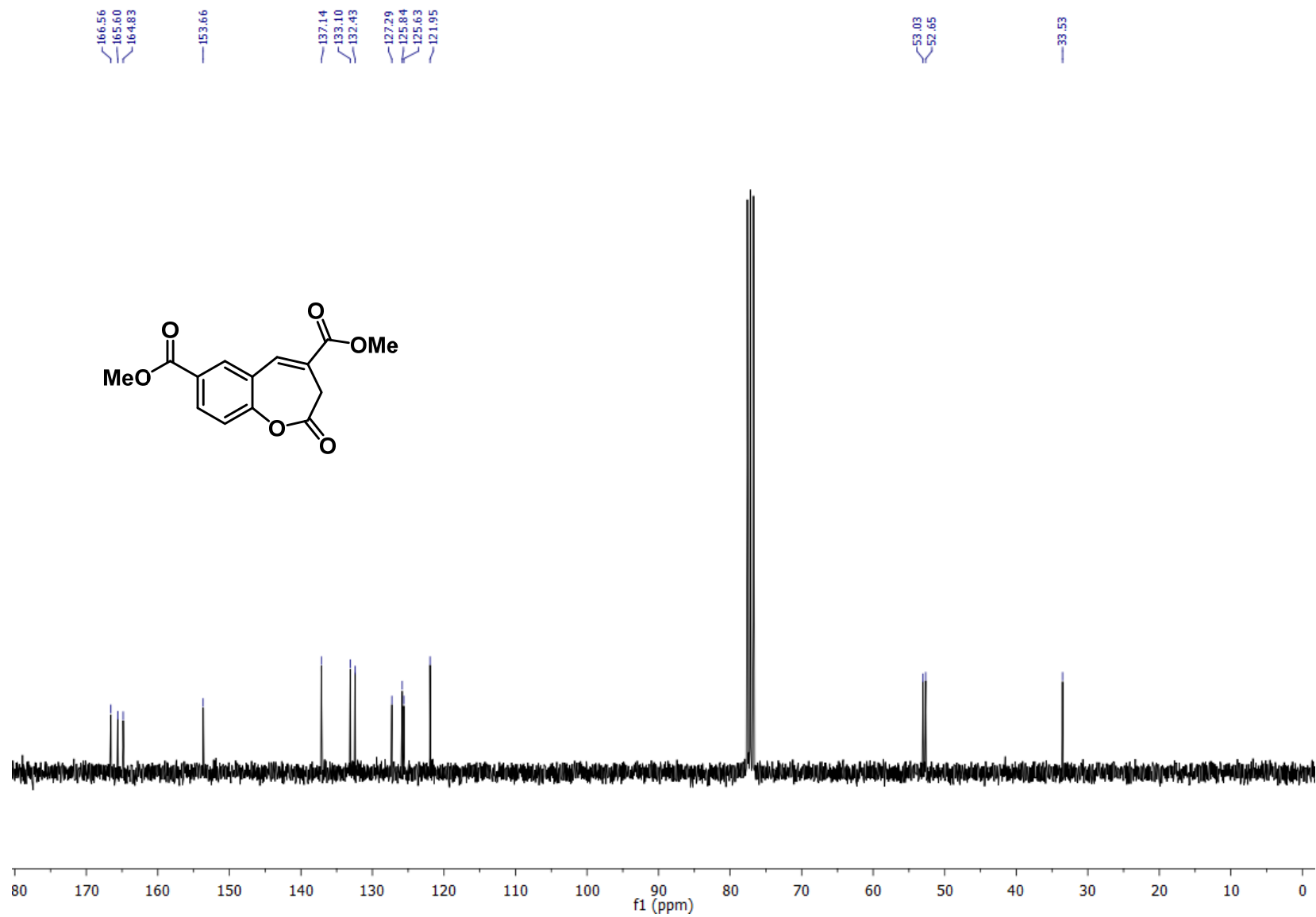
^{13}C NMR Methyl 7-chloro-2-oxo-2,3-dihydrobenzo[*b*]oxepine-4-carboxylate (**31**).



^1H NMR Dimethyl 2-oxo-2,3-dihydrobenzo[*b*]oxepine-4,7-dicarboxylate (**3m**).



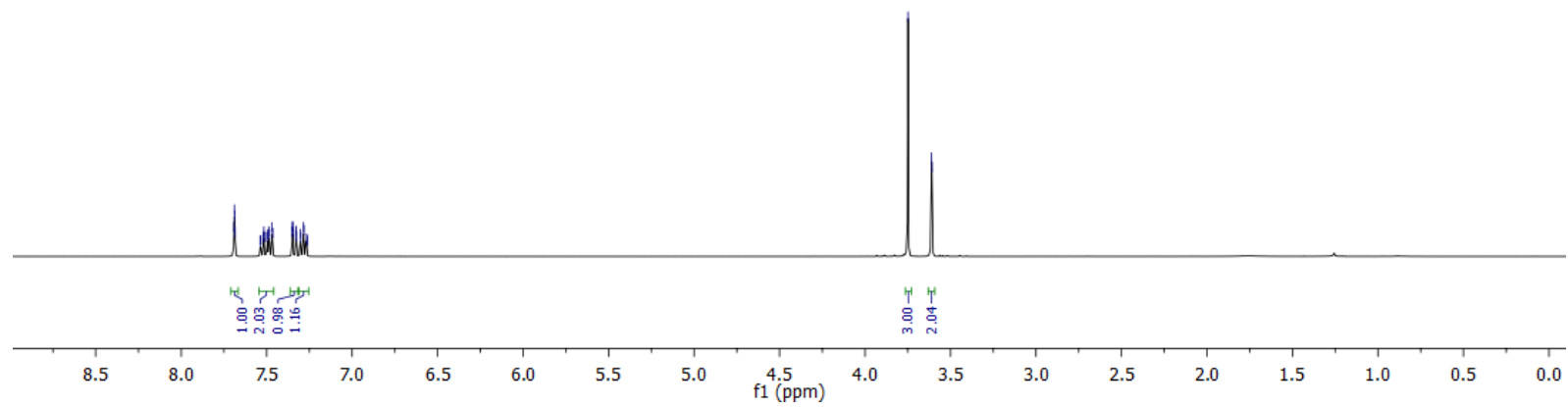
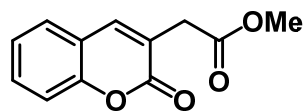
¹³C NMR Dimethyl 2-oxo-2,3-dihydrobenzo[*b*]oxepine-4,7-dicarboxylate (**3m**).



^1H NMR Methyl 2-(2-oxo-2H-chromen-3-yl)acetate (**4**).

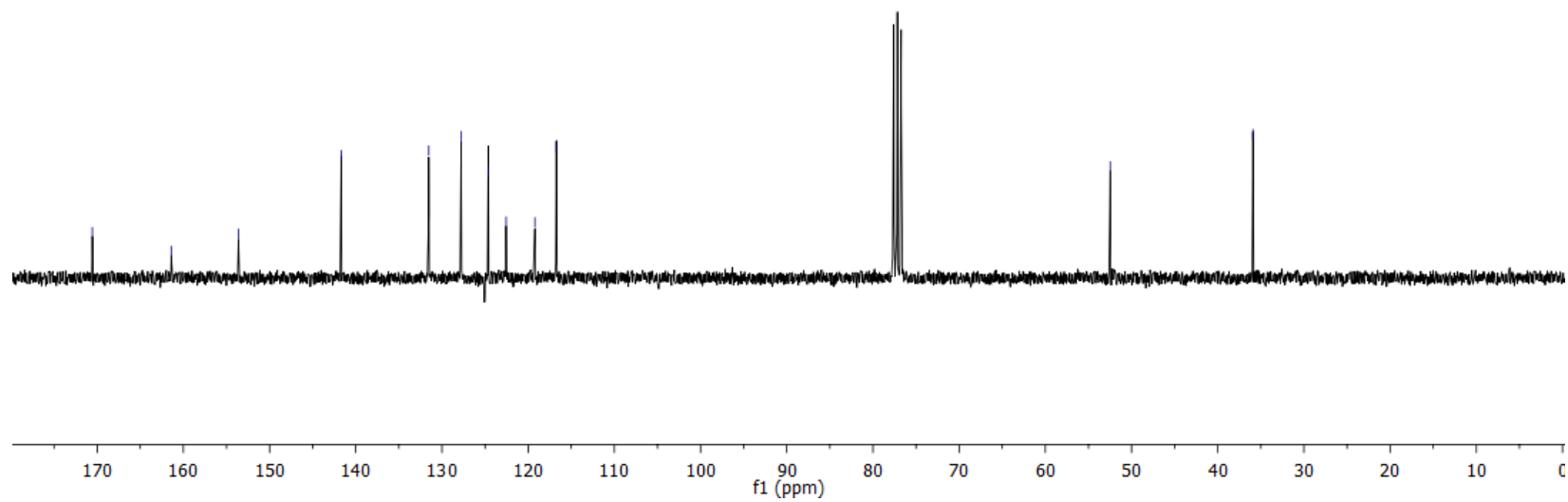
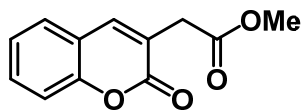
7.69
7.69
7.68
7.54
7.53
7.52
7.51
7.50
7.49
7.48
7.47
7.46
7.35
7.35
7.33
7.33
7.33
7.32
7.30
7.30
7.28
7.28
7.27
7.26

3.75
3.61
3.61

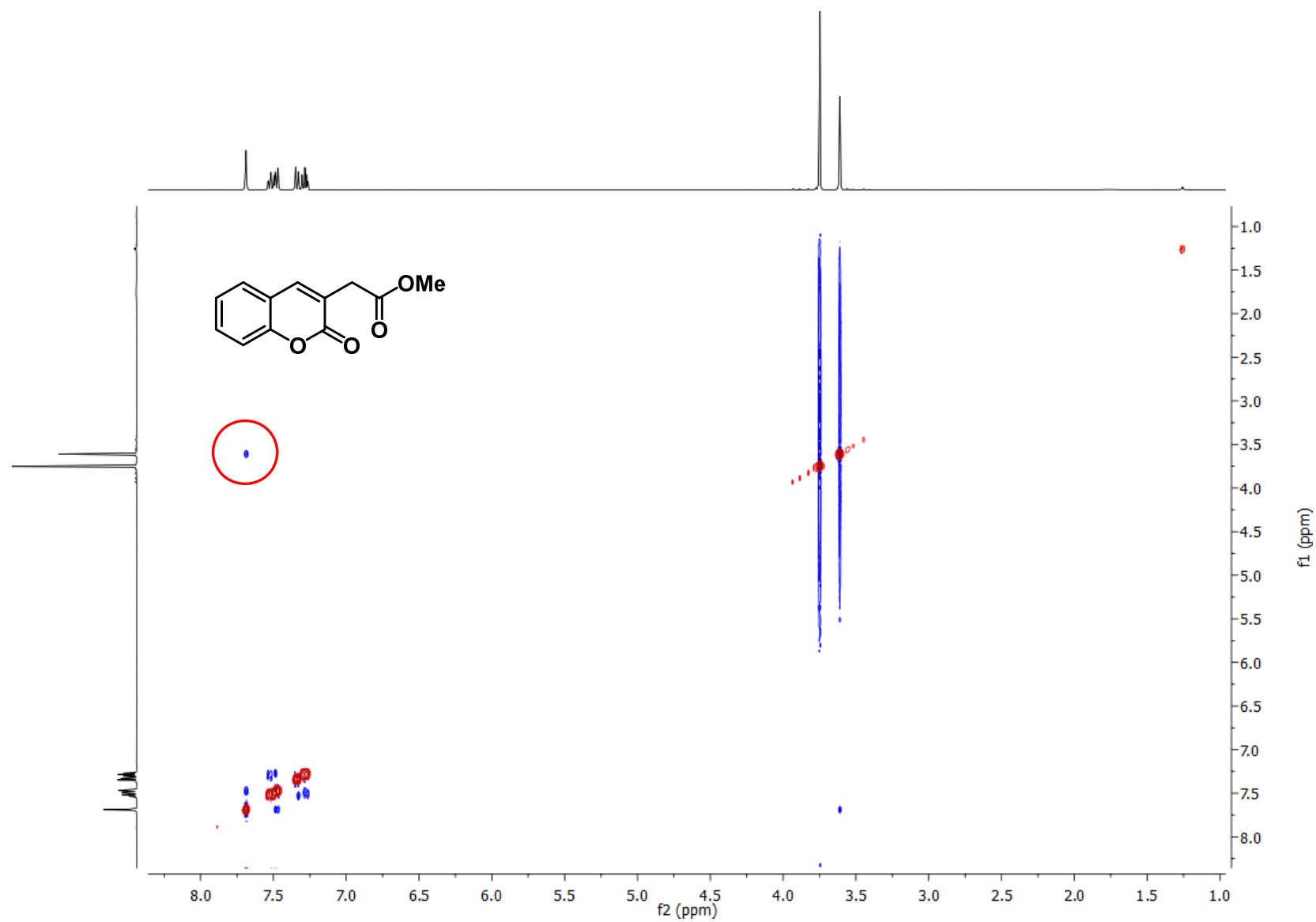


^{13}C NMR Methyl 2-(2-oxo-2H-chromen-3-yl)acetate (**4**).

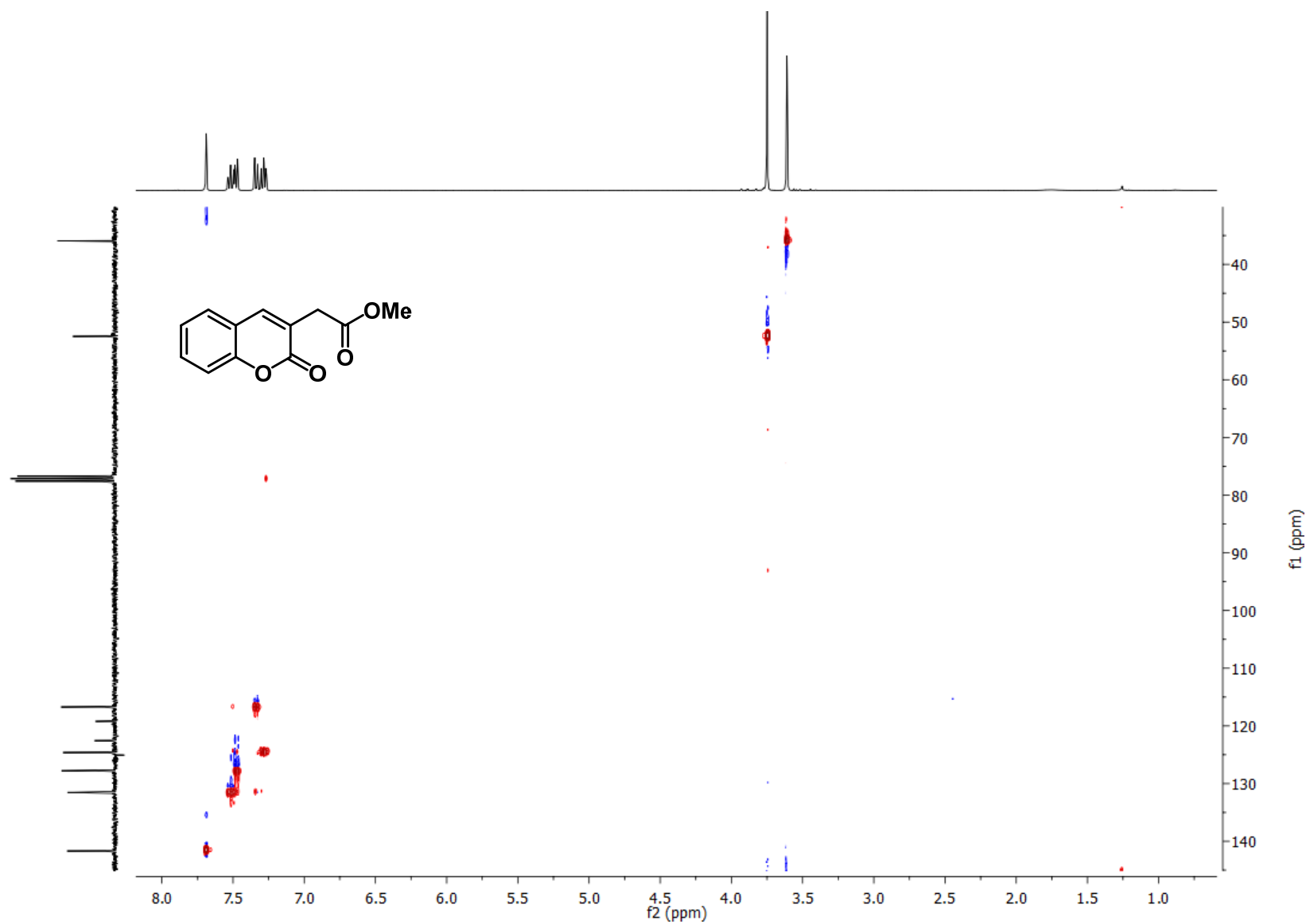
—170.56 —161.41 —153.61 —141.88 —131.53 —127.77 —124.63 —122.55 —119.21 —116.72 —52.47 —35.92



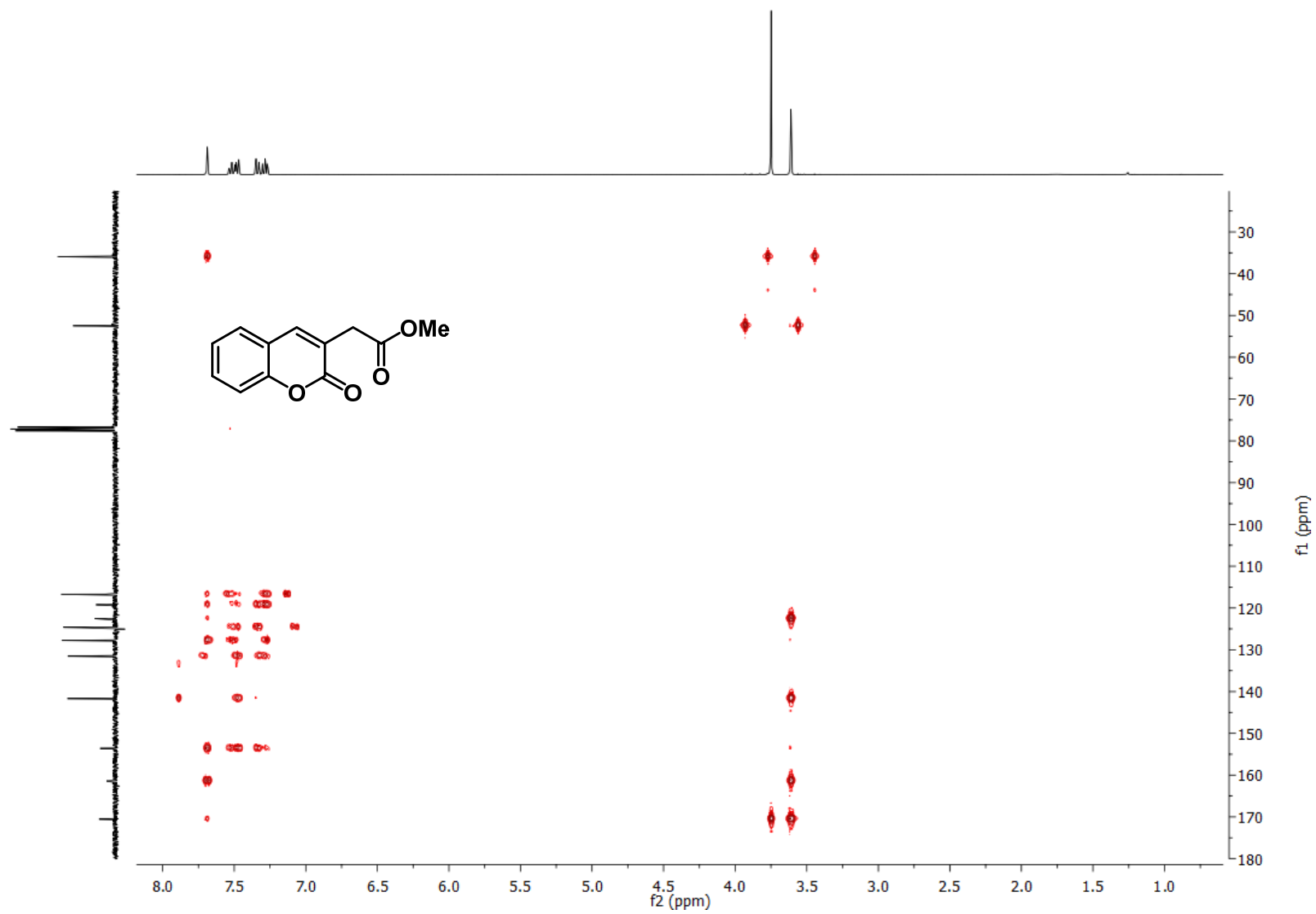
NOESY Methyl 2-(2-oxo-2H-chromen-3-yl)acetate (4).



HSQC Methyl 2-(2-oxo-2H-chromen-3-yl)acetate (4).



HMBC Methyl 2-(2-oxo-2H-chromen-3-yl)acetate (**4**).



References in the Supporting Information

1. Kretzschmar, C.; Roof, C.; Langhammer, T.-S.; Sekora, A.; Pews-Davtyan, A.; Beller, M.; Frech, M. J.; Eisenlöffel, C.; Rolfs, A.; Junghanss, C., The novel arylindolylmaleimide PDA-66 displays pronounced antiproliferative effects in acute lymphoblastic leukemia cells. *BMC Cancer* **2014**, *14*, 71.
2. Sheldrick, G. M., A short history of SHELX. *Acta Cryst.* **2008**, *A64*, 112–122.
3. Sheldrick, G. M., Crystal structure refinement with SHELXL. *Acta Cryst.* **2015**, *C71*, 3–8.
4. Matviitsuk, A.; Greenhalgh, M. D.; Antúnez, D. J. B.; Slawin, A. M. Z.; Smith, A. D., Aryloxide-Facilitated Catalyst Turnover in Enantioselective α,β -Unsaturated Acyl Ammonium Catalysis. *Angew. Chem. Int. Ed.* **2017**, *56*, 12282–12287.
5. Amemiya, S.; Kojima, K.; Sakai, K., Base-Catalyzed Reactions of Dihydromethylenomycin A and Its Derivatives. *Chem. Pharm. Bull.* **1984**, *32*, 457–462.
6. Wolff, M.; Seemann, M.; Grosdemange-Billiard, C.; Tritsch, D.; Campos, N.; Rodríguez-Concepción, M.; Boronat, A.; Rohmer, M., Isoprenoid biosynthesis via the methylerythritol phosphate pathway. (E)-4-Hydroxy-3-methylbut-2-enyl diphosphate: chemical synthesis and formation from methylerythritol cyclodiphosphate by a cell-free system from *Escherichia coli*. *Tetrahedron Lett.* **2002**, *43*, 2555–2559.